2023-08-01

The eighteenth data release of the Sloan Digital Sky Surveys: targeting and first spectra f...

Version	Published version
Citation (published version):	A. Almeida, S.F. Anderson, M. Argudo-Fernández, C. Badenes, K. Barger, J.K. Barrera-Ballesteros, C.F. Bender, E. Benitez, F. Besser, J.C. Bird, D. Bizyaev, M.R. Blanton, J. Bochanski, J. Bovy, W.N. Brandt, J.R. Brownstein, J. Buchner, E. Bulbul, J.N. Burchett, M.C. Díaz, J.K. Carlberg, A.R. Casey, V. Chandra, B. Cherinka, C. Chiappini, A.A. Coker, J. Comparat, C. Conroy, G. Contardo, A. Cortes, K. Covey, J.D. Crane, K. Cunha, C. Dabbieri, J.W. Davidson, M.C. Davis, A.B. de Andrade Queiroz, N. De Lee, J.E. Méndez Delgado, S. Demasi, F. Di Mille, J. Donor, P. Dow, T. Dwelly, M. Eracleous, J. Eriksen, X. Fan, E. Farr, S. Frederick, L. Fries, P. Frinchaboy, B.T. Gänsicke, J. Ge, C. González Ávila, K. Grabowski, C. Grier, G. Guiglion, P. Gupta, P. Hall, K. Hawkins, C.R. Hayes, J.J. Hermes, L. Hernández-García, D.W. Hogg, J.A. Holtzman, H.J. Ibarra-Medel, A. Ji, P. Jofre, J.A. Johnson, A.M. Jones, K. Kinemuchi, M. Kluge, A. Koekemoer, J.A. Kollmeier, M. Kounkel, D. Krishnarao, M. Krumpe, I. Lacerna, P.J.A. Lago, C. Laporte, C. Liu, A. Liu, X. Liu, A.R. Lopes, M. Macktoobian, S.R. Majewski, V. Malanushenko, D. Maoz, T. Masseron, K.L. Masters, G. Matijevic, A. McBride, I. Medan, A. Merloni, S. Morrison, N. Myers, S. Mészáros, C.A. Negrete, D.L. Nidever, C. Nitschelm, D. Oravetz, A. Oravetz, K. Pan, Y. Peng, M.H. Pinsonneault, R. Pogge, D. Qiu, S.V. Ramirez, H.-W. Rix, D.F. Rosso, J. Runnoe, M. Salvato, S.F. Sanchez, F.A. Santana, A. Saydjari, C. Sayres, K.C. Schlaufman, D.P. Schneider, A. Schwope, J. Serna, Y. Shen, J. Sobeck, Y.-Y. Song, D. Souto, T. Spoo, K.G. Stassun, M. Steinmetz, I. Straumit, G. Stringfellow, J. Sánchez-Gallego, M. Taghizadeh-Popp, J. Tayar, A. Thakar, P.B. Tissera, A. Tkachenko, H.H.

The Astrophysical Journal Supplement Series, 267:44 (38pp), 2023 August https://doi.org/10.3847/1538-4365/acda98

The Eighteenth Data Release of the Sloan Digital Sky Surveys: Targeting and First Spectra from SDSS-V

Andrés Almeida[1], Scott F. Anderson[2], Maria Argudo-Fernández[3,4,5], Carles Badenes[6], Kat Barger[7], Jorge K. Barrera-Ballesteros[8], Chad F. Bender[9], Erika Benitez[8], Felipe Besser[10], Jonathan C. Bird[11], Dmitry Bizyaev[12,13], Michael R. Blanton[14], John Bochanski[15], Jo Bovy[16,17], William Nielsen Brandt[18,19,20], Joel R. Brownstein[21], Johannes Buchner[22], Esra Bulbul[22], Joseph N. Burchett[13], Mariana Cano Díaz[8], Joleen K. Carlberg[23], Andrew R. Casey[24,25], Vedant Chandra[26], Brian Cherinka[23], Cristina Chiappini[27], Abigail A. Coker[21], Johan Comparat[22], Charlie Conroy[26], Gabriella Contardo[28], Arlin Cortes[10], Kevin Covey[29], Jeffrey D. Crane[30], Katia Cunha[9], Collin Dabbieri[11], James W. Davidson, Jr[1], Megan C. Davis[31], Anna Barbara de Andrade Queiroz[27], Nathan De Lee[32], José Eduardo Méndez Delgado[33], Sebastian Demasi[2], Francesco Di Mille[10], John Donor[7], Peter Dow[1], Tom Dwelly[22], Mike Eracleous[18,19], Jamey Eriksen[12,13], Xiaohui Fan[9], Emily Farr[34], Sara Frederick[11], Logan Fries[31], Peter Frinchaboy[7], Boris T. Gänsicke[35], Junqiang Ge[36], Consuelo González Ávila[10], Katie Grabowski[12,13], Catherine Grier[37], Guillaume Guiglion[38], Pramod Gupta[2], Patrick Hall[39], Keith Hawkins[40], Christian R. Hayes[41], J. J. Hermes[42], Lorena Hernández-García[43,44], David W. Hogg[14], Jon A. Holtzman[13], Hector Javier Ibarra-Medel[45,46], Alexander Ji[47,48], Paula Jofre[49,50], Jennifer A. Johnson[51,52], Amy M. Jones[23], Karen Kinemuchi[12,13], Matthias Kluge[22], Anton Koekemoer[23], Juna A. Kollmeier[30,53], Marina Kounkel[11], Dhanesh Krishnarao[54], Mirko Krumpe[27], Ivan Lacerna[43,46], Paulo Jakson Assuncao Lago[10], Chervin Laporte[55], Chao Liu[36], Ang Liu[22], Xin Liu[45,56], Alexandre Roman Lopes[57], Matin Macktoobian[58], Steven R. Majewski[1], Viktor Malanushenko[12,13], Dan Maoz[59], Thomas Masseron[60,61], Karen L. Masters[62], Gal Matijevic[27], Aidan McBride[21], Ilija Medan[63], Andrea Merloni[22], Sean Morrison[45], Natalie Myers[7], Szabolcs Mészáros[64,65], C. Alenka Negrete[8], David L. Nidever[66], Christian Nitschelm[67], Daniel Oravetz[12,13], Audrey Oravetz[12,13], Kaike Pan[12,13], Yingjie Peng[68,69], Marc H. Pinsonneault[51], Rick Pogge[70], Dan Qiu[36], Solange V. Ramirez[30], Hans-Walter Rix[38], Daniela Fernández Rosso[10], Jessie Runnoe[11], Mara Salvato[22], Sebastian F. Sanchez[8], Felipe A. Santana[71], Andrew Saydjari[26], Conor Sayres[2], Kevin C. Schlaufman[72], Donald P. Schneider[18,19], Axel Schwope[27], Javier Serna[73], Yue Shen[45], Jennifer Sobeck[74], Ying-Yi Song[16,17], Diogo Souto[75], Taylor Spoo[7], Keivan G. Stassun[11], Matthias Steinmetz[27], Ilya Straumit[51,59,76], Guy Stringfellow[77], José Sánchez-Gallego[2], Manuchehr Taghizadeh-Popp[72], Jamie Tayar[78], Ani Thakar[72], Patricia B. Tissera[79], Andrew Tkachenko[76], Hector Hernandez Toledo[8], Benny Trakhtenbrot[59], José G. Fernández-Trincado[80], Nicholas Troup[81], Jonathan R. Trump[31], Sarah Tuttle[2], Natalie Ulloa[10], Jose Antonio Vazquez-Mata[8,82], Pablo Vera Alfaro[10], Sandro Villanova[83], Stefanie Wachter[30], Anne-Marie Weijmans[84], Adam Wheeler[51], John Wilson[1], Leigh Wojno[38], Julien Wolf[22,85], Xiang-Xiang Xue[36], Jason E. Ybarra[86,87], Eleonora Zari[38], and Gail Zasowski[21]

[1] Department of Astronomy, University of Virginia, Charlottesville, VA 22904-4325, USA
[2] Department of Astronomy, University of Washington, Box 351580, Seattle, WA 98195, USA
[3] Instituto de Física, Pontificia Universidad Católica de Valparaíso, Valparaíso, Chile
[4] Universidad de Granada (UGR), Departamento de Física Teórica y del Cosmos, E-18071, Granada, Spain
[5] Instituto Universitario Carlos I de Física Teórica y Computacional, Universidad de Granada, E-18071, Granada, Spain
[6] PITT PACC, Department of Physics and Astronomy, University of Pittsburgh, Pittsburgh, PA 15260, USA
[7] Department of Physics & Astronomy, Texas Christian University, Fort Worth, TX 76129, USA
[8] Instituto de Astronomía, Universidad Nacional Autónoma de México, A.P. 70-264, 04510, México, D.F., Mexico
[9] Steward Observatory, University of Arizona, 933 North Cherry Avenue, Tucson, AZ 85721-0065, USA
[10] Las Campanas Observatory, Raúl Bitrán 1200, La Serena, Chile
[11] Department of Physics and Astronomy, Vanderbilt University, VU Station 1807, Nashville, TN 37235, USA
[12] Apache Point Observatory, P.O. Box 59, Sunspot, NM 88349, USA
[13] Department of Astronomy, New Mexico State University, Las Cruces, NM 88003, USA
[14] Center for Cosmology and Particle Physics, Department of Physics, 726 Broadway, Room 1005, New York University, New York, NY 10003, USA
[15] Rider University, 2083 Lawrenceville Road, Lawrenceville, NJ 08648, USA
[16] David A. Dunlap Department of Astronomy & Astrophysics, University of Toronto, 50 St. George Street, Toronto, Ontario, M5S 3H4, Canada
[17] Dunlap Institute for Astronomy & Astrophysics, University of Toronto, 50 St. George Street, Toronto, Ontario, M5S 3H4, Canada
[18] Department of Astronomy & Astrophysics, The Pennsylvania State University, University Park, PA 16802, USA
[19] Institute for Gravitation and the Cosmos, The Pennsylvania State University, University Park, PA 16802, USA
[20] Department of Physics, The Pennsylvania State University, University Park, PA 16802, USA
[21] Department of Physics and Astronomy, University of Utah, 115 S. 1400 E., Salt Lake City, UT 84112, USA; gail.zasowski@gmail.com
[22] Max-Planck-Institut für extraterrestrische Physik, Giessenbachstraße 1, D-85748 Garching, Germany
[23] Space Telescope Science Institute, 3700 San Martin Drive, Baltimore, MD 21218, USA
[24] School of Physics & Astronomy, Monash University, Wellington Road, Clayton, Victoria 3800, Australia
[25] Center of Excellence for Astrophysics in Three Dimensions (ASTRO-3D), Australia
[26] Center for Astrophysics | Harvard & Smithsonian, 60 Garden St, Cambridge, MA 02138, USA
[27] Leibniz-Institut für Astrophysik Potsdam (AIP), An der Sternwarte 16, D-14482 Potsdam, Germany
[28] SISSA, Scuola Internazionale Superiore di Studi Avanzati, Italy
[29] Department of Physics and Astronomy, Western Washington University, 516 High Street, Bellingham, WA 98225, USA
[30] The Observatories of the Carnegie Institution for Science, 813 Santa Barbara Street, Pasadena, CA 91101, USA
[31] Department of Physics, University of Connecticut, 2152 Hillside Road, Unit 3046, Storrs, CT 06269, USA

[32] Department of Physics, Geology, and Engineering Technology, Northern Kentucky University, Highland Heights, KY 41099, USA
[33] Astronomisches Rechen-Institut, Zentrum für Astronomie der Universität Heidelberg, Mönchhofstr. 12-14, D-69120 Heidelberg, Germany
[34] Laboratory for Atmospheric and Space Physics, University of Colorado, 1234 Innovation Drive, Boulder, CO 80303, USA
[35] Department of Physics, University of Warwick, Coventry, CV4 7AL, UK
[36] National Astronomical Observatories, Chinese Academy of Sciences, 20A Datun Road, Chaoyang, Beijing 100101, People's Republic of China
[37] Department of Astronomy, University of Wisconsin-Madison, 475 N. Charter Street, Madison WI 53703, USA
[38] Max-Planck-Institut für Astronomie, Konigstuhl 17, D-69117 Heidelberg, Germany
[39] Department of Physics and Astronomy, York University, 4700 Keele Street, Toronto, Ontario, M3J 1P3, Canada
[40] Department of Astronomy, University of Texas at Austin, Austin, TX 78712, USA
[41] NRC Herzberg Astronomy and Astrophysics Research Centre, 5071 West Saanich Road, Victoria, BC, Canada, V9E 2E7, Canada
[42] Astronomy Department, Boston University, 725 Commonwealth Ave, Boston, MA 02215, USA
[43] Millennium Institute of Astrophysics (MAS), Nuncio Monseñor Sótero Sanz 100, Providencia, Santiago, Chile
[44] Instituto de Física y Astronomía, Universidad de Valparaíso, Av. Gran Bretaña 1111, Playa Ancha, Casilla 5030, Chile
[45] Department of Astronomy, University of Illinois at Urbana-Champaign, Urbana, IL 61801, USA
[46] Instituto de Astronomía y Ciencias Planetarias, Universidad de Atacama, Copayapu 485, Copiapó, Chile
[47] Department of Astronomy and Astrophysics, University of Chicago, Chicago, IL 60637, USA
[48] Kavli Institute for Cosmological Physics, University of Chicago, Chicago, IL 60637, USA
[49] Núcleo de Astronomía de la Facultad de Ingeniería y Ciencias, Universidad Diego Portales, Av. Ejército Libertador 441, Santiago, Chile
[50] Millenium Nucleus ERIS, Chile
[51] Department of Astronomy, The Ohio State University, 140 W. 18th Avenue, Columbus, OH 43210, USA
[52] Center for Cosmology and AstroParticle Physics, Ohio State University, 191 West Woodruff Avenue, Columbus, OH 43210, USA
[53] Canadian Institute for Theoretical Astrophysics, University of Toronto, Toronto, ON, M5S-98H, Canada
[54] Department of Physics, Colorado College, 14 East Cache la Poudre Street, Colorado Springs, CO 80903, USA
[55] Institut de Ciències del Cosmos, Universitat de Barcelona, Martí Franquès 1, E-08028 Barcelona, Spain
[56] National Center for Supercomputing Applications, University of Illinois at Urbana-Champaign, Urbana, IL 61801, USA
[57] Departamento de Física, Facultad de Ciencias, Universidad de La Serena, Cisternas 1200, La Serena, Chile
[58] Electrical and Computer Engineering Department, University of Alberta, Edmonton, AB, Canada
[59] School of Physics and Astronomy, Tel Aviv University, Tel Aviv 69978, Israel
[60] Instituto de Astrofísica de Canarias, E-38205 La Laguna, Tenerife, Spain
[61] Departamento de Astrofísica, Universidad de La Laguna, E-38206 La Laguna, Tenerife, Spain
[62] Departments of Physics and Astronomy, Haverford College, 370 Lancaster Avenue, Haverford, PA 19041, USA
[63] Department of Physics and Astronomy, Georgia State University, Atlanta, GA 30302, USA
[64] ELTE Gothard Astrophysical Observatory, H-9704 Szombathely, Szent Imre herceg st. 112, Hungary
[65] MTA-ELTE Lendület "Momentum" Milky Way Research Group, Hungary
[66] Department of Physics, Montana State University, P.O. Box 173840, Bozeman, MT 59717, USA
[67] Centro de Astronomía (CITEVA), Universidad de Antofagasta, Avenida Angamos 601, Antofagasta 1270300, Chile
[68] Department of Astronomy, School of Physics, Peking University, Beijing 100871, People's Republic of China
[69] Kavli Institute for Astronomy and Astrophysics, Peking University, Beijing 100871, People's Republic of China
[70] Department of Astronomy and Center for Cosmology and AstroParticle Physics, The Ohio State University, 140 W. 18th Avenue, Columbus, OH 43210, USA
[71] Departamento de Astronomía, Universidad de Chile, Av. Libertador Bernardo O'Higgins 1058, Santiago, Chile
[72] William H. Miller III Department of Physics and Astronomy, Johns Hopkins University, 3400 N. Charles Street, Baltimore, MD 21218, USA
[73] Instituto de Astronomía, Universidad Nacional Autónoma de México, Ensenada, Baja California, México
[74] Maunakea Spectroscopic Explorer, CFHT, 65-1238 Mamalahoa Highway, Kamuela, HI 96743, USA
[75] Departamento de Física, Universidade Federal de Sergipe, Av. Marechal Rondon, S/N, 49000-000 São Cristóvão, SE, Brazil
[76] Institute of Astronomy, KU Leuven, Celestijnenlaan 200D, B-3001 Leuven, Belgium
[77] Center for Astrophysics and Space Astronomy, Department of Astrophysical and Planetary Sciences, University of Colorado, 389 UCB, Boulder, CO 80309-0389, USA
[78] Department of Astronomy, University of Florida, Bryant Space Science Center, Stadium Road, Gainesville, FL 32611, USA
[79] Instituto de Astrofísica, Pontificia Universidad Católica de Chile, Av. Vicuña Mackenna 4860, 782-0436 Macul, Santiago, Chile
[80] Instituto de Astronomía, Universidad Católica del Norte, Av. Angamos 0610, Antofagasta, Chile
[81] Department of Physics, Salisbury University, Salisbury, MD 21801, USA
[82] Departamento de Física, Facultad de Ciencias, Universidad Nacional Autónoma de México, Ciudad Universitaria, CDMX, 04510, México
[83] Departamento de Astronomía, Universidad de Concepción, Casilla 160-C, Concepción, Chile
[84] School of Physics and Astronomy, University of St Andrews, North Haugh, St Andrews, KY16 9SS, UK
[85] Exzellenzcluster ORIGINS, Boltzmannstr. 2, D-85748 Garching, Germany
[86] Department of Physics and Astronomy, West Virginia University, 135 Willey Street, Morgantown, WV 26506, USA
[87] Center for Gravitational Waves and Cosmology, West Virginia University, Chestnut Ridge Research Building, Morgantown, WV 26505, USA
Received 2023 January 25; revised 2023 May 18; accepted 2023 May 30; published 2023 August 8

Abstract

The eighteenth data release (DR18) of the Sloan Digital Sky Survey (SDSS) is the first one for SDSS-V, the fifth generation of the survey. SDSS-V comprises three primary scientific programs or "Mappers": the Milky Way Mapper (MWM), the Black Hole Mapper (BHM), and the Local Volume Mapper. This data release contains extensive targeting information for the two multiobject spectroscopy programs (MWM and BHM), including input catalogs and selection functions for their numerous scientific objectives. We describe the production of the targeting databases and their calibration and scientifically focused components. DR18 also includes ∼25,000 new SDSS spectra and supplemental information for X-ray sources identified by eROSITA in its eFEDS field. We present updates to some of the SDSS software pipelines and preview changes anticipated for DR19. We also describe three value-added catalogs (VACs) based on SDSS-IV data that have been published since DR17, and one VAC based on the SDSS-V data in the eFEDS field.

Unified Astronomy Thesaurus concepts: Surveys (1671); Astronomy databases (83); Astronomy data acquisition (1860); Astronomy software (1855)

1. The First Two Decades of the Sloan Digital Sky Surveys

This paper describes the eighteenth data release (DR18) of the Sloan Digital Sky Survey (SDSS) and the first data release of SDSS-V.

Since its operations began in 1998, SDSS has been taking near-continuous observations of stars, galaxies, quasars, and other objects, spanning from our solar system to the early days of the Universe. The first phase, SDSS-I (York et al. 2000), imaged over 8000 $\deg^2$ of the sky in the *ugriz* filters and collected optical spectra of more than 700,000 objects. SDSS-II completed the legacy imaging survey and added a dedicated supernova imaging survey (Frieman et al. 2008) and a spectroscopic survey of ∼230,000 Milky Way stars (SEGUE; Yanny et al. 2009).

SDSS-III (Eisenstein et al. 2011) focused entirely on spectroscopy and comprised an extension of SEGUE (SEGUE-2; Rockosi et al. 2022); a radial velocity exoplanet survey (MARVELS; Ge et al. 2008); a clustering survey of galaxies and intergalactic gas in the distant universe (BOSS; Dawson et al. 2013), which required an upgrade to the optical spectrographs (Smee et al. 2013); and an IR survey of Milky Way and Local Group stars (APOGEE-1; Majewski et al. 2017), which introduced IR spectrographs to the suite of SDSS instrumentation (Wilson et al. 2019). SDSS-IV (Blanton et al. 2017) included a significant expansion of the APOGEE survey (APOGEE-2; S. R. Majewski et al. 2023, in preparation), including the deployment of a new APOGEE-S spectrograph for observations with the 2.5 m du Pont telescope at Las Campanas Observatory (LCO), as well as an extension of BOSS observations to previously understudied redshifts (eBOSS; Dawson et al. 2016), and an optical integral field unit (IFU) survey of the gas and stellar properties of low-redshift galaxies (MaNGA; Bundy et al. 2015).

Continuing in this tradition, SDSS-V (Kollmeier et al. 2017; J. A. Kollmeier et al. 2023, in preparation) constitutes a major innovation step in science scope and hardware. It comprises three primary scientific surveys, called "mappers": the Milky Way Mapper (MWM; J. A. Johnson et al. 2023, in preparation), the Black Hole Mapper (BHM; S. F. Anderson et al. 2023, in preparation), and the Local Volume Mapper (LVM; N. Drory et al. 2023, in preparation). See Section 2, Section 6, and Section 7 for more details.

A hallmark of the SDSS family of surveys is the regular release of high-quality, well-documented, and readily usable data to the entire world. Beginning with the Early Data Release (Stoughton et al. 2002), SDSS helped usher in the era of "open science" through its regular data releases. This practice has proven fruitful for the astronomical community, enabling a very broad scientific reach and impact. The final data release of SDSS-IV was DR17, in 2021 December (Abdurro'uf et al. 2022). As of 2022 November, SDSS data (across all survey phases) have been cited in more than 11,000 refereed papers, with over 650,000 citations. Stalzer & Mentzel (2016) named SDSS as one of the most influential data sets, even beyond astronomy and physics. SDSS data are also used in numerous educational contexts, from young schoolchildren to undergraduate and graduate students, especially through the Voyages and SciServer platforms.[88]

[88] https://voyages.sdss.org/ and https://www.sciserver.org/outreach/.

One of the primary reasons for the widespread use of SDSS data is the collaboration's commitment to high-quality, user-friendly documentation to accompany each data release (e.g., Weijmans et al. 2019). SDSS-V continues that core practice with DR18, as summarized in this paper. In Section 2, we briefly summarize SDSS-V's scientific and hardware components. In Sections 3–4, we outline the scope of DR18 and how to access the information. Section 5 describes the multiobject spectroscopic (MOS) databases and targeting software, while Section 6, Section 7, and Section 8 detail the MOS MWM, BHM, and "open-fiber" programs, respectively. Section 9 describes the spectra that are released in DR18, and Section 10 focuses on new and modified software. Section 11 contains the value-added catalogs (VACs) released since DR17. Finally, Section 12 summarizes all of this information and looks forward to the anticipated contents of DR19.

2. SDSS-V: Status and Science Objectives

In this section, we provide a brief summary of the SDSS-V program at the time of this data release. Many of these elements have been described elsewhere (e.g., Kollmeier et al. 2017) and will be described in greater detail in companion papers, including J. A. Kollmeier et al. (2023, in preparation). We provide this information here as a standalone snapshot at this important survey milestone.

SDSS-V sets out to be the first astronomical survey to provide all-sky, multi-epoch spectroscopy in the optical and IR. Its scientific goals and targets are grouped into three top-level "Mapper" programs. MWM (Section 6) is mapping the stellar populations and chemodynamics of the Milky Way to understand its evolution, and is probing stellar physics and stellar system architectures by collecting optical and IR spectra of stars in the Milky Way and the Magellanic Clouds. BHM (Section 7) is studying the physics of black hole growth through time-domain spectroscopy and is providing spectra for extragalactic X-ray-luminous sources from eROSITA (Merloni et al. 2012; Predehl et al. 2021), using optical spectra across the sky. LVM is examining gas emission, star formation, and stellar/interstellar energy exchange processes in the Milky Way and beyond, at unprecedented scales, using ultra-wide-field optical IFU spectroscopy.

MWM and BHM are designed to use the MOS infrastructure of SDSS-V, which includes the Sloan 2.5 m telescope at Apache Point Observatory (APO) in New Mexico, USA (Gunn et al. 2006) and the du Pont 2.5 m telescope at LCO in Chile (Bowen & Vaughan 1973). Obtaining homogeneous, all-sky spectral survey data at both optical and IR wavelengths requires near-identical sets of optical and near-IR fiber spectrographs in both hemispheres. For SDSS-V, one of the optical BOSS spectrographs was moved from APO to LCO, so that each site is now equipped with a pair of APOGEE and BOSS instruments.[89] The central new hardware component for

[89] Details of APOGEE spectrographs are at https://www.sdss.org/instruments/apogee-spectrographs/ and details of BOSS spectrographs are at https://www.sdss.org/instruments/boss-spectrographs/. Within SDSS-V, one will frequently encounter references to "BOSS spectra." This term always means "spectra obtained with one of the two BOSS spectrographs," rather than "spectra obtained as part of the SDSS-III BOSS (or SDSS-IV eBOSS) project."

Table 1
Summary of DR18 Contents

Item	Description	Data Access
Targeting Information[a]		
`mos_catalog`	Crossmatch of input catalogs (Section 5.1)	https://skyserver.sdss.org/dr18
`mos_X` catalogs	Input catalogs (Section 5.1, Table 2 for core catalogs)	https://skyserver.sdss.org/dr18
`mos_target`	Objects meeting the selection criteria of one or more cartons (Section 5.2)	https://skyserver.sdss.org/dr18
`mos_carton_to_target`	Table linking targets, cartons, and observational requirements (Section 5.2)	https://skyserver.sdss.org/dr18
`mos_carton`	Table of SDSS-V cartons (Sections 5.1, 5.3, 6, 7, 8)	https://skyserver.sdss.org/dr18
Spectra		
eFEDS Spectra	Optical spectra of eROSITA-selected sources (Section 7.3 and Section 9.1)	Directories and data models are in Section 9.1.2
VACs		
SDSS-IV VACs	Based on SDSS-IV data (Section 11.1, Table 6)	https://www.sdss.org/dr18/data_access/value-added-catalogs/
SDSS-V VAC	Based on SDSS-V (eFEDS) data (Section 11.2, Table 6)	https://www.sdss.org/dr18/data_access/value-added-catalogs/

Note.
[a] These are a subset of the total individual targeting tables available from the CAS. The full list can be seen in the CAS Schema Browser at https://skyserver.sdss.org/dr18/MoreTools/browser.

MOS observations in SDSS-V is the implementation of a focal plane system (FPS) with robotic fiber positioners (Pogge et al. 2020), which replaces the plug plate system and enables efficient, single-epoch pointings with ∼15 minute exposure times. The adoption of the FPS, in turn, required a new three-element corrector for the Sloan telescope (Barkhouser et al. 2022).

For LVM, SDSS-V is building an entirely new facility at LCO to enable ultra-wide-field IFU observations across ∼1000 deg^2. The Local Volume Mapper Instrument (LVM-i) builds upon replicated instrument concepts from DESI (Perruchot et al. 2018) and the successful IFU technology developed as part of SDSS-IV/MaNGA. To meet the survey science requirements, LVM-i will comprise a set of four 160 mm telescopes coupled via fiber IFUs to three spectrographs providing full coverage of the optical band, all housed in a new dedicated enclosure (Herbst et al. 2020).

3. Scope of DR18

The main focus of DR18 is to lay the groundwork for future SDSS-V releases by presenting the updated access paths, data models, new targeting strategies, and other structures that will be used in DR19 and beyond (Table 1).

DR18 consists primarily of targeting information (algorithms and databases) for the MWM and BHM programs (Section 5). These catalogs comprise 269.5 GB of data in `MOS_TARGET_DIR` (Table 2). They also introduce the concept of a "carton," a new organizational unit for SDSS observations. A carton is a set of targets that results from a specific target selection algorithm, designed to advance certain science goals. Examples of cartons include white dwarfs (WDs) selected from Gaia–SDSS catalogs for MWM and reverberation mapping (RM) targets for BHM. Cartons will play a large role in understanding the SDSS-V targeting strategy, target selection algorithms, and eventual full sample. They are discussed in more detail in Section 5.2, and lists of MWM and BHM cartons are given in Tables 3 and 4, respectively. Cartons are grouped into "programs," which are also columns in the `target` tables that refer to broader science cases whose goals will be met by targets from one or more cartons.

A small number of new BOSS spectra are being made available as part of the eROSITA Final Equatorial Depth Survey (eFEDS; Brunner et al. 2022), an eROSITA follow-up program (Section 9.1). These add a volume of 301.9 GB to `BOSS_SPECTRO_REDUX`, including the ∼25,000 spectra. Accompanying these spectra is a new VAC, which contains updated redshifts and classifications (see Section 11.2). DR18 also contains new software routines and updates to existing SDSS software (Section 10), particularly the BOSS spectral reduction package (Section 10.1).

Finally, all previous SDSS data are also available through the SDSS portals without any changes or additional processing, essentially summarized in DR17 (Abdurro'uf et al. 2022). Newly available as part of DR17, coincident with DR18, are two new VACs based on DR17 data, as well as an earlier DR15-based VAC that has been updated with data from DR17. These VACs are described in greater detail in Section 11.1.

4. Accessing the Data

There are numerous ways to access the SDSS DR18 data products, summarized on the SDSS website[90] and on the data release website.[91] As in previous phases of SDSS, SDSS-V provides a searchable database for the Catalog Archive Server (CAS), using SkyServer,[92] with both Structured Query Language and Jupyter notebook interfaces. The Science Archive Server (SAS) is well suited for directly downloading flat files, including spectra. Both the CAS and SAS are cumulative systems, with some data products replacing or extending data from previous releases, generally speaking. Examples of data products that can be replacements (not in

[90] https://www.sdss.org/dr18/data_access/
[91] https://dr18.sdss.org
[92] http://skyserver.sdss.org

Table 2
Crossmatched Input Catalogs for the Catalog Database (Section 5.1)

Table Name[a]	Catalog Description	Primary Key[a]
mos_allwise	AllWISE (Cutri et al. 2013)	cntr
mos_bhm_efeds_veto	eFEDS-related veto catalog	pk
mos_bhm_rm_v0_2	RM-related targeting catalog	pk
mos_catwise2020	CatWISE2020 (Marocco et al. 2021)	source_id
mos_glimpse	GLIMPSE I, II, 3D (Churchwell et al. 2009)	pk
mos_guvcat	GALEX UV Unique Source Catalog (Bianchi et al. 2017)	objid
mos_legacy_survey_dr8	DESI Legacy Surveys DR8 (Dey et al. 2019)	ls_id
mos_panstarrs1	Pan-STARRS1 (Flewelling et al. 2020; Magnier et al. 2020)	catid_objid
mos_sdss_dr13_photoobj_primary	SDSS DR13 Imaging Catalog (Albareti et al. 2017)	objid
mos_sdss_dr16_specobj	SDSS DR16 Optical Spectra (Ahumada et al. 2020)	specobjid
mos_skies_v2	Sky location catalog (Section 5.4)	pix_32768
mos_skymapper_dr2	SkyMapper DR2 (Onken et al. 2019)	object_id
mos_supercosmos	SuperCOSMOS Sky Survey (Hambly et al. 2001)	objid
mos_tic_v8	TESS Input Catalog v8 (Stassun et al. 2019)	id
mos_tycho2	Tycho-2 (Høg et al. 2000)	designation
mos_uvotssc1	Swift UVOT Serendipitous Source Catalog (Yershov 2014)	id
mos_xmm_om_suss_4_1	XMM OM Serendipitous Ultraviolet Source Survey (Page et al. 2012)	pk

Note.
[a] The Table Name and Primary Key are denoted as mos_X and id_X, respectively, in Figure 2.

DR18) include spectroscopic reductions and their associated parameters and VACs. In these cases, only the latest version is included in the data release, but all previously released versions are available at their original locations. Examples of data products that are cumulative are the raw data transferred from the observatories for each night of observations.

The best way to access a particular data product will depend on the data product itself and the anticipated use case. We recommend using the CAS when accessing the MOS targeting data described in Section 5.1, since this product was originally created as a relational database. The corresponding fits files on the SAS are primarily for archival purposes. Access to the eFEDS spectra is described in Section 9.1.3; these spectra are also available for visual inspection in the Science Archive Webapp at https://dr18.sdss.org/optical/.

Each type of data file on the SAS has an associated data model, which describes its format and content. SDSS-V is developing extensions to the existing data model products to include better accessibility in formats other than the current static html, such as yaml, json, and backward compatibility with classic html. For DR18, all data models can be found at https://data.sdss.org/datamodel/.

The SDSS DR18 website has numerous tutorials and examples available to access and interact with both the MOS targeting data and the eFEDS spectra released in DR18. See https://www.sdss.org/dr18/tutorials/ for more information.

5. MOS Targeting

The primary data products in DR18 are the underlying, crossmatched catalog of objects targeted by SDSS-V and the list of targets. In this section, we describe how these data are organized into crossmatched catalog database tables and target tables. Throughout DR18, we use 0.5 to indicate the version of the catalog crossmatching process (Section 5.1). Variants of the target selection of individual cartons (Section 5.2) using this crossmatch are versioned as 0.5.X, where "X" varies between cartons. A set of cartons and carton targeting versions is referred to as a "targeting generation," which is tracked similarly as 0.5.X. Targeting generation 0.5.3 is the one released in DR18.

5.1. Catalog Database Tables and Crossmatching

Previous generations of SDSS relied almost exclusively on a single imaging catalog for targeting. In the optical, the SDSS imaging survey (Padmanabhan et al. 2008; Abazajian et al. 2009) formed the basis for targeting, while in the *H* band, the Two Micron All Sky Survey (2MASS) was used (Skrutskie et al. 2006). For SDSS-V, this approach is no longer practical, because of the need for all-sky, deep optical imaging and the desire to observe stars in both the optical and the IR. Gaia imaging does not go deep enough in the extragalactic sky, while even the union of SDSS imaging, Pan-STARRS imaging, and other wide-field imaging does not cover the full sky at the necessary wavelengths.

Therefore, to ensure that each object in the sky of relevance to SDSS-V has a unique identifier, regardless of how many imaging catalogs it appears in, we created our own targeting database. All SDSS-V MOS targets (i.e., all targets for MWM and BHM) are stored in a suite of database tables, which contains both a unified list of all sources within a set of crossmatched input catalogs and the targeting classifications of those sources. This section describes how the catalogs are stored; Section 5.2 describes how the targeting classifications are stored.

Figure 1 shows a cartoon representation of the primary database tables and workflows presented in this section. The mos_catalog table is the central unified list of sources. It was created from the set of spatially crossmatched core input catalogs, which are listed in Table 2 and shown in yellow in Figures 1 and 3. We have a set of additional catalogs used in targeting whose entries are associated with entries in the spatially crossmatched catalogs; these are the tables highlighted in blue in Figures 1 and 3. The database in DR18 stores this set of catalogs and the associations between objects within them.

The mos_catalog table contains only a minimum of information for each object: only the positional information and

Table 3
MWM Cartons

Carton Name	Selection Summary[a]	Instrument	Available Targets[b]
manual_mwm_tess_ob	OB(AF)-type pulsating stars in eclipsing binaries	APOGEE	364
manual_nsbh_apogee	Compact NS/BH binaries APOGEE	APOGEE	75
manual_nsbh_boss	Compact NS/BH binaries BOSS	BOSS	249
mwm_cb_300pc_apogee	Compact binaries within 300pc from Gaia+GALEX $G < 16$	APOGEE	17,382
mwm_cb_300pc_boss	Compact binaries within 300pc from Gaia+GALEX $G >= 16$	BOSS	52,267
mwm_cb_cvcandidates_apogee	Compact binaries from literature $G < 16$	APOGEE	61
mwm_cb_cvcandidates_boss	Compact binaries from literature $G >= 16$	BOSS	5167
mwm_cb_gaiagalex_apogee	Compact binaries from Gaia+GALEX $G < 16$	APOGEE	16,287
mwm_cb_gaiagalex_boss	Compact binaries from Gaia+GALEX $G >= 16$	BOSS	261,570
mwm_cb_uvex1	Compact binaries from Gaia+GALEX FUV+NUV for BOSS identification	BOSS	110,447
mwm_cb_uvex2	Compact binaries from Gaia+GALEX NUV only for BOSS identification	BOSS	278,961
mwm_cb_uvex3	Compact binaries from Gaia+XMM-Newton OM for BOSS identification	BOSS	25,032
mwm_cb_uvex4	Compact binaries from Gaia+Swift UVOT for BOSS identification	BOSS	21,036
mwm_cb_uvex5	Compact binaries from Gaia+GALEX RV targets for APOGEE	APOGEE	8641
mwm_dust_core	Sample of bright, nearby, midplane giants complementary with Galactic Genesis	APOGEE	61,926
mwm_erosita_compact_gen	eROSITA/Gaia compact binary candidates for BOSS spectroscopy	BOSS	77,038
mwm_erosita_compact_var	eROSITA/Gaia compact binary candidates, Gaia variability, BOSS identifiation	BOSS	16,835
mwm_erosita_stars	eROSITA/Gaia coronal emitters	BOSS	89,994
mwm_galactic_core	Luminous giants across the sky based on $G - H$ color cuts	APOGEE	5,459,267
mwm_legacy_ir2opt	Follow-up of APOGEE-1/2 targets with BOSS—filler carton	BOSS	209,893
mwm_ob_cepheids	Cepheids from Inno et al. (2021) with BOSS	BOSS	2357
mwm_ob_core	OB(A) stars in the Milky Way and Magellanic Clouds with BOSS	BOSS	603,854
mwm_rv_long_fps	FPS radial velocity monitoring—long temporal baseline	APOGEE	111,233
mwm_rv_short_fps	FPS radial velocity monitoring—short temporal baseline	APOGEE	6,283,604
mwm_snc_100pc_apogee	Volume-limited census of the solar neighborhood $G < 16$	APOGEE	114,173
mwm_snc_100pc_boss	Volume-limited census of the solar neighborhood $G >= 16$	BOSS	322,222
mwm_snc_250pc_apogee	Volume-limited census of the solar neighborhood, extension to earlier types $G < 16$	APOGEE	404,618
mwm_snc_250pc_boss	Volume-limited census of the solar neighborhood, extension to earlier types $G >= 16$	BOSS	417,431
mwm_tess_planet	TESS TOI and 2 minute cadence follow-up	APOGEE	223,764
mwm_tessrgb_core	TESS observed red giant astroseismology follow-up	APOGEE	1,004,714
mwm_wd_core	WDs selected from Gaia + SDSS-V (Gentile Fusillo et al. 2019)	BOSS	192,534
mwm_yso_cluster_apogee	Candidates identified through phase-space clustering	APOGEE	45,461
mwm_yso_cluster_boss	Candidates identified through phase-space clustering	BOSS	59,065
mwm_yso_cmz_apogee	Candidates located in Central Molecular Zone + inner Galactic disk	APOGEE	13,170
mwm_yso_disk_apogee	Optically bright candidates identified through IR excess	APOGEE	28,832
mwm_yso_disk_boss	Optically bright candidates identified through IR excess	BOSS	37,478
mwm_yso_embedded_apogee	Optically faint candidates identified through IR excess	APOGEE	11,086
mwm_yso_nebula_apogee	Candidates found toward areas of high nebulosity	APOGEE	1112
mwm_yso_pms_apogee	Low-mass candidates located above main sequence on H-R diagram	APOGEE	76,361
mwm_yso_pms_boss	Low-mass candidates located above main sequence on H-R diagram	BOSS	73,214
mwm_yso_variable_apogee	Low-mass candidates identified through Gaia variability	APOGEE	52,691
mwm_yso_variable_boss	Low-mass candidates identified through Gaia variability	BOSS	47,758

Notes.
[a] For more complete selection details, see Appendix A and the online documentation: https://www.sdss.org/dr18/mwm/programs/cartons/.
[b] This column is the number of targets that satisfy the carton selection function in the `target` database. The number of targets ultimately observed for each carton will be smaller than this value.

the `catalogid` identifier, which is an internal ID used by the SDSS-V databases to uniquely identify each source. All other information about the sources is stored in the individual crossmatched and targeting catalogs. Each `catalogid` is associated with one or more entries within these original catalogs. For 17 of the original input catalogs, the association between `mos_catalog` and the original catalog is expressed as shown in Figure 2, using a join table `mos_catalog_to_X` for each input catalog "`mos_X`." As above, the list of all original catalogs crossmatched in this fashion is in Table 2, along with the primary key used for each (i.e., the column labeled "`X_id`" in Figure 2).

The initial basis for `mos_catalog` is the TESS Input Catalog (TIC) v8 (Stassun et al. 2019), which is all-sky and uses both Gaia DR2 and 2MASS to identify objects.[93] Then, crossmatching follows a three-phase procedure for each of the subsequent input catalogs listed in Table 2, which can include both point and extended sources. First, we use existing literature crossmatches included with the catalog information to identify physical targets that already exist in the `mos_catalog` table. For those, a new entry is added to the appropriate

[93] We anticipate including Gaia DR3 data in the future.

Table 4
BHM Core Cartons[1]

Carton Name	Simplified Selection[a]	No. Epochs[b] Anticipated	No. Targets Anticipated
bhm_aqmes_wide2	SDSS DR16Q, $16 < i_{psf} < 19.1$ AB	⩾2	∼20,000
bhm_aqmes_med		⩾10	∼2000
bhm_rm_known_spec		100–174	∼1400
bhm_rm_core	Confirmed and candidate QSOs/AGNs		
bhm_rm_var	$15 < i_{psf} < 21.7$ AB (or $16 < G < 21.7$ Vega)		
bhm_rm_ancillary			
bhm_spiders_agn_lsdr8	eROSITA pointlike; $r_{fiber} < 22.5$ or $z_{fiber} < 21$ AB	1	∼250,000
bhm_spiders_agn_ps1dr2	$F_{0.5-2keV} > 2 \times 10^{-14}$ erg s^{-1} cm^{-2}		
bhm_spiders_clusters_lsdr8	eROSITA + red-sequence finder	1	∼50,000
bhm_spiders_clusters_ps1dr2	$r_{fiber} < 21$ or $z_{fiber} < 20$ AB		

Notes.
[a] For more complete selection details, see Appendix B or the online documentation at https://www.sdss.org/dr18/bhm/programs/cartons/.
[b] Each BHM epoch typically relies on a 1–2 hr BOSS exposure.

mos_catalog_to_X table that references the matched catalogid and the unique identifier in the input catalog.

For targets in the input catalog that do not have an available association with mos_catalog, we perform a cone search around the coordinates of each target and find the associated mos_catalog entries within the search radius. We use a default 1″ search radius, but this value is sometimes modified to match the spatial resolution of the input catalog. All the cone-search-matched catalogid entries are associated with the input catalog target via the corresponding mos_catalog_to_X table. The match with the smallest on-sky separation is marked as the "best" match[94] by setting the best column in the mos_catalog_to_X table to True. Finally, targets in the input catalog that cannot be spatially crossmatched are considered new physical objects and added to mos_catalog and mos_catalog_to_X with a new unique catalogid.

For some of these 17 catalogs, the database contains further associations between them and the additional catalogs used in targeting. Figure 3 shows these other catalogs and how they are associated in the database with the crossmatched catalogs.

DR18 contains the catalog crossmatching version v0.5, which was used for targeting at the beginning of MOS observations in SDSS-V. Due to the size of the databases involved, the tables in the released DR18 version only contain sources that were ultimately identified with potential targets (i.e., are in one or more cartons). DR18 also excludes some X-ray catalogs from eROSITA that were used for targeting in v0.5 but have not yet been made public. Due to an error, DR18 also excludes tables associated with the TESS Objects of Interest (TOIs), the Spitzer/MIPSGAL program (Gutermuth & Heyer 2015), and the Gaia ASAS-SN Classical Cepheid sample (Inno et al. 2021); these tables will be included in DR19.

5.2. Target Database Tables and MOS Cartons

Drawing on the catalog database and the information stored in the linked catalogs described above (Section 5.1), the target selection software determines which objects should be targeted for spectroscopy using the selection criteria and other properties of the target cartons. The target selection criteria are described in later sections, on the website, and in other program papers; here, we only describe how the information is organized.

After the target selection software is run, the targeting database contains a set of targets and a set of cartons. Figure 4 shows how this information is stored for a generalized subset of the database tables. The associations between targets and cartons are stored in the mos_carton_to_target table. Each carton is associated with all of the candidate targets that satisfy the selection criteria for the carton. Each target is associated with one or more cartons.

For example, consider a star that has a detection in Gaia DR2. This star will appear in TIC v8, and thus will have an entry in mos_catalog. If this star satisfies the selection criteria for *any* carton, it will also appear in mos_target, with a corresponding entry in mos_carton_to_target. If this star satisfies the criteria for multiple cartons, then multiple entries in mos_carton_to_target will be associated with the star's single entry in mos_target. Each mos_carton_to_target entry is also associated with an entry in the mos_carton table, which gives the name of the carton and other information.

Each mos_carton_to_target entry has an associated set of entries—*cadence, value*, and *priority*—that are used in the process of determining the survey strategy and the fiber assignment process. The *cadence* describes how the target should be observed (number of epochs, number of observations per epoch, and observing conditions). The cadence_pk values allow a join to a cadence table with the cadence name and other parameters associated with it.

The *value* expresses how important the target is to the overall objectives of the MOS program, which is used in the determination of the overall survey strategy. The priority expresses the order in which targets should be assigned to fibers during fiber assignment in a given pointing. These quantities are more fully explained in the robostrategy paper (M. R. Blanton et al. 2023, in preparation).

[94] This crossmatching approach is sensitive to the order in which the input catalogs are ingested. In general, catalogs were processed in order of higher to lower spatial resolution, which minimizes the problem of misassociations in the spatial crossmatch phase due to mismatching resolutions.

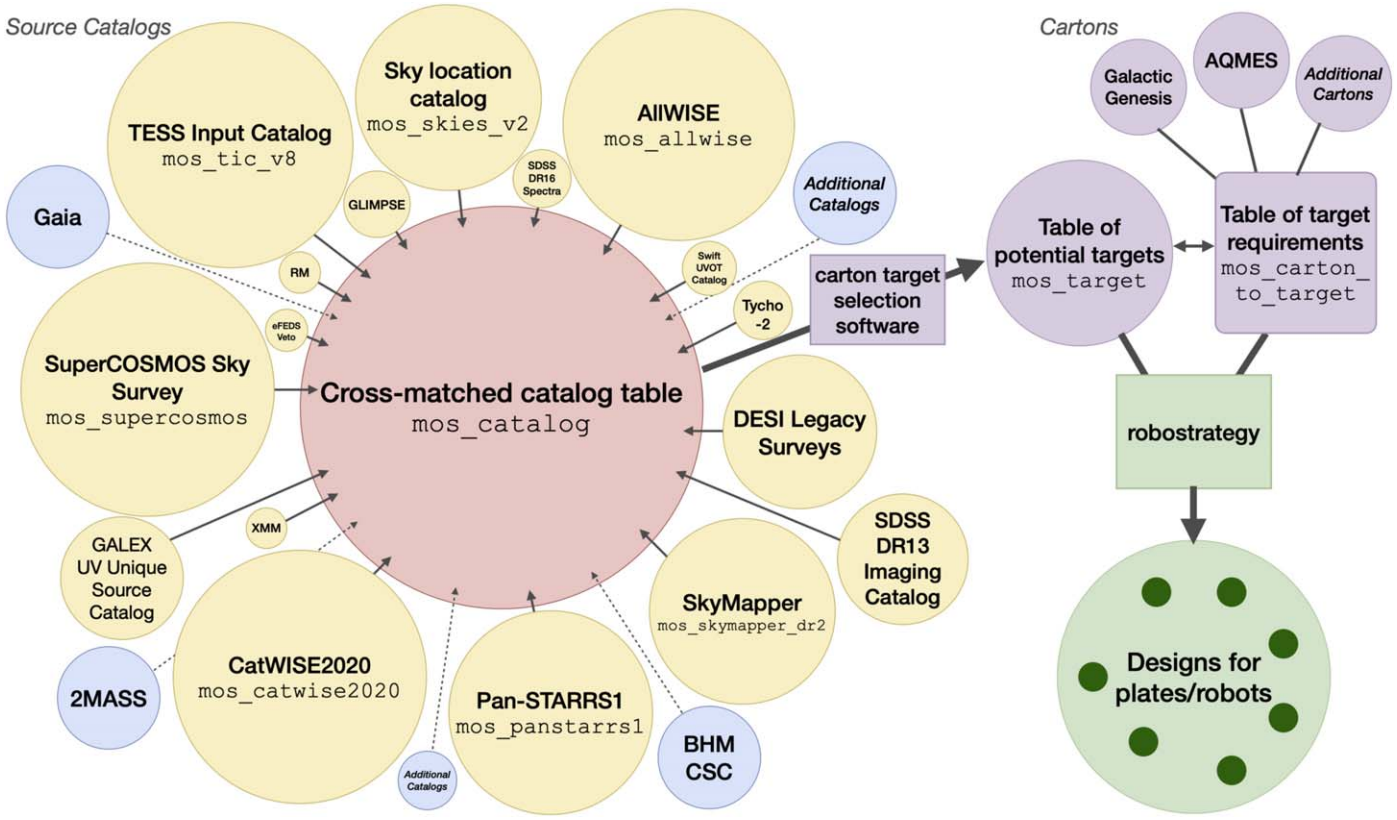

Figure 1. Cartoon diagram of the relationships between several key database tables and of the workflow between sky sources and observed targets (Sections 5.1–5.2). The objects colored yellow, blue, pink, and purple correspond to the same types of tables in Figures 2–4. The green color has been repurposed to highlight the "observational" section of the workflow, where candidate targets are downselected and grouped into observable designs (Section 5.2). Left: the pink `mos_catalog` is built as a superset of the yellow core input catalogs (Section 5.1, Table 2), whose circles are approximately scaled here to the sizes of the catalogs. The blue "additional catalogs" (Section 5.1) provide supplementary information to the sources in `mos_catalog`. Right: the small purple circles represent the many individual cartons (Section 5.2), which specify both target selection criteria and observational requirements. The potential targets satisfying the selection criteria, along with the observational requirements (stored in `mos_carton_to_target`), are used by the robostrategy code (M. R. Blanton et al. 2023, in preparation) to produce observable designs, previously for plates (K. Covey et al. 2023, in preparation) and now for the FPS robots.

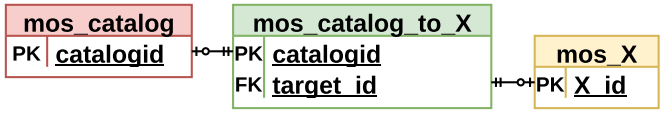

Figure 2. Relationships between the crossmatched `mos_catalog` table and the original source input catalogs (Section 5.1). There are 17 source input catalogs that are linked to `mos_catalog` through the structure shown above, with "X" representing the name of the original catalog (Table 2).

Each carton also has an assigned *category*, which can be one of `science`, `sky_boss`, `standard_boss`, `sky_apogee`, or `standard_apogee`. The first category indicates science targets, and the others are different types of calibration targets (Sections 5.3–5.4).

Among the science target cartons, there are those whose observations are required for the stated success of SDSS-V science, as laid out in the survey's science requirements document (SRD). These cartons tend to have descriptive names. The cartons that arose from an initial call within the SDSS-V collaboration for "open-fiber" targets have carton names starting with `opentargets`. There is also a set of filler targets for spare fibers. The released tables in DR18 do not unambiguously identify which cartons are SRD, open, or filler (although the information can often be approximately guessed from the carton names), because this identification is associated with the fiber assignment results, which will not be released until DR19.

5.3. Standard Star Cartons

5.3.1. APOGEE Standard Stars

The standard stars for APOGEE observations are used primarily to correct telluric absorption by Earth's atmosphere. They are selected in a process very similar to that used for APOGEE-1 and APOGEE-2 observations, which aimed to select hot, blue stars (with few absorption lines of their own) distributed as evenly as possible across the field of view, to allow for spatially dependent telluric corrections (Zasowski et al. 2013, 2017).

The carton `ops_std_apogee` contains these calibration stars, which are drawn from the 2MASS point-source catalog (PSC; Skrutskie et al. 2006). They are restricted to have magnitude $7 < H < 11$, color $-0.25 < (J - K_s) < +0.5$, and magnitude uncertainties (JERR, HERR, KERR) of $\leqslant 0.1$ mag. In addition, we applied the requirements that the 2MASS read flag be equal to "1" or "2," that the quality flag for J, H, and K_s be equal to "A" or "B," that the galaxy contamination flag be equal to "0," that the confusion flag be equal to "000," that the extkey ID (linking to the 2MASS Extended Source Catalog; Jarrett et al. 2000) be `Null`, and that the star lie at least $6''$ from its nearest 2MASS neighbor. From this subset of potential standard stars, the five bluest sources are chosen from each HEALPix NSIDE = 128 pixel (0.21 deg^2 pix^{-1}; Górski et al. 2005) as telluric standard stars.

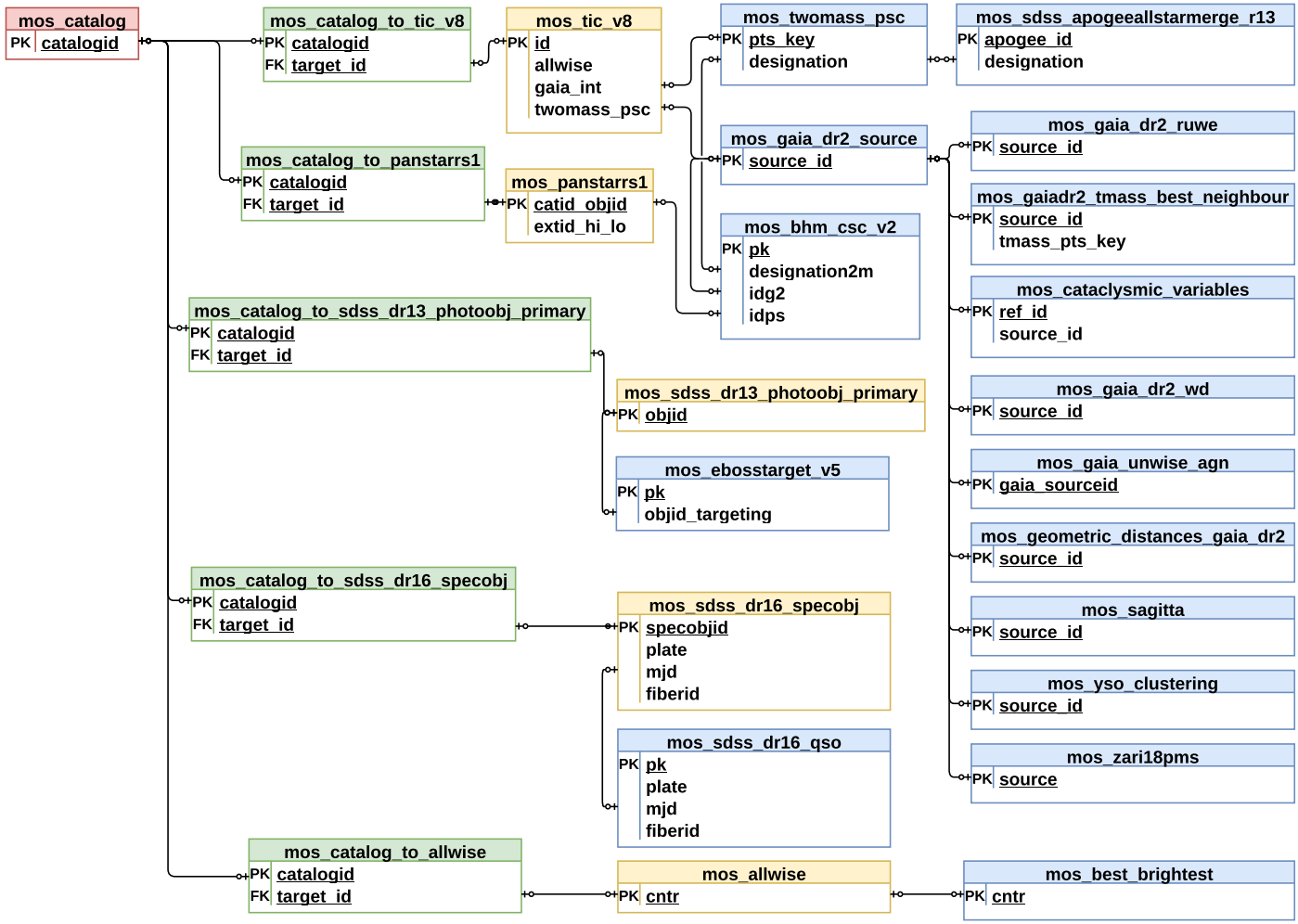

Figure 3. Relationships between crossmatched `mos_catalog` table (pink), original source catalogs (yellow), and additional catalogs used for targeting (blue), for the cases where additional such catalogs exist. `mos_catalog` contains the full crossmatched list of sources, and it is associated with the original source catalogs through join tables (green) in the manner described in Figure 2 and Section 5.1. Additional catalogs can be joined to the original source catalogs, as shown, and thereby to the `mos_catalog` table, as shown. For clarity, only the columns necessary for table joins are shown in this diagram.

5.3.2. *BOSS Spectrophotometric Standard Stars*

Spectrophotometric standard stars are used by the BOSS pipeline to calibrate the absolute and relative throughput of the instrument during science observations. The strategy for selecting BOSS standards in SDSS-V builds upon past experience from the SDSS-III/IV BOSS and eBOSS projects (see, e.g., Dawson et al. 2013, 2016). Selecting standards for the SDSS-V program presents some new challenges: (i) we need to select standard stars outside the footprint of the SDSS photometric imaging catalog; and (ii) we need to reliably select standards along lines of sight that may be heavily reddened by Galactic dust. In order to satisfy the first challenge, we exploited wider area photometric and astrometric information from Pan-STARRS, the DESI Legacy Surveys, and Gaia. To mitigate the complications of extinction, we used the 3D reddening information provided by TIC v8 (Stassun et al. 2019).

Below, we briefly describe the target selection criteria for the various BOSS standard cartons used in early SDSS-V operations, which are released as part of DR18 (targeting generation `v0.5.3`).

The `ops_std_eboss` carton is identical to the spectrophotometric standards used by the eBOSS survey

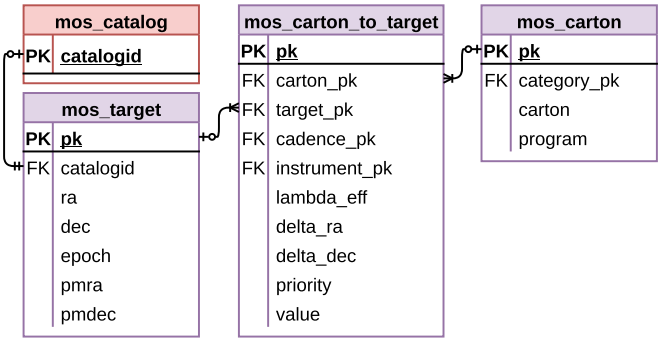

Figure 4. Association of `catalogids` with targeting information. Each `catalogid` that is selected by one or more cartons is given an entry in the `mos_target` table. For each carton that selects it, there is a `mos_carton_to_target` entry. Each entry is associated with one target and one carton, and specifies the cadence, instrument (BOSS or APOGEE), and other observing conditions. Further tables in the database define the properties of the cadences, the names of the instruments, and the names of the categories (`science`, `sky_boss`, `standard_boss`, `sky_apogee`, and `standard_apogee`).

(Dawson et al. 2016). These standards lie in the magnitude range $16 < r_{\rm psf} < 18$ AB and so are most suitable for use in dark time. The use of these standards maintains an important continuity with archival SDSS spectroscopy, which is

especially important when investigating the long-term variations of QSOs (Section 7).

The ops_std_boss_ps1dr2, ops_std_boss_lsdr8, and ops_std_boss_gdr2 standard star cartons are based on Pan-STARRS1 DR2, Legacy Survey DR8, and Gaia DR2 photometry, respectively. For each carton, we use the empirically determined location of eBOSS standards within the dereddened color space of the given photometric system to train our new selection locus. Additional cuts on data quality, and in the parallax versus magnitude plane (via Gaia DR2), are applied to further clean outliers from the sample. Magnitude limits are applied such that these standards are appropriate for BOSS dark-time observations (approximately $16 < r_{\rm psf} < 18$ AB, or $16 < G < 18$ Vega). Additionally, the ops_std_boss_gdr2 carton is limited to Galactic latitudes of $|b| > 10°$. We estimate SDSS $g_{\rm psf}$, $r_{\rm psf}$, $i_{\rm psf}$, $z_{\rm psf}$ magnitudes for each BOSS standard star target, transferring their native multiband photometry into the SDSS system via color transforms derived from the ops_std_eboss sample.

Additional BOSS standard cartons were developed to facilitate all-sky observations during bright time: ops_std_boss_tic, ops_std_boss, and ops_std_boss_red. These cartons fill in the regions of the sky that are not covered by the BOSS standard cartons described above, and they include brighter standards, to mitigate the potential impact of crosstalk from brighter science targets in the design. The ops_std_boss_tic carton consists of likely F stars, selected via $T_{\rm eff}$ and surface gravity cuts applied to TIC v8 stellar parameters (Stassun et al. 2019). To provide uniform coverage over the sky, targets are sorted into an NSIDE = 128 HEALpix grid ($0.21\,{\rm deg}^2\,{\rm pix}^{-1}$), and the 10 highest-gravity stars in each healpix are retained for the final carton. The ops_std_boss carton similarly targets F stars, but selected via cuts on Gaia parallax, color, and absolute magnitude. Finally, the ops_std_boss_red carton is intended to provide standards even in the most heavily extincted sections of the Galactic midplane. This carton uses cuts on observed and dereddened Gaia+2MASS colors, as well as parallax, proper motion, and reduced proper-motion criteria, to reduce contamination from non-F stars whose observed colors can be dereddened into the relevant areas of color–magnitude space.

5.4. Sky Fiber Locations

The data reduction pipelines for BOSS and APOGEE both require a number of fibers to be placed at "sky" locations, which do not contain light from astrophysical sources and thus allow for the correction of the observed spectra for contamination by emission processes in Earth's atmosphere. The number and "quality" of sky fibers per configuration is dependent on the type of observation to be performed. For example, for SDSS-V observations targeting faint extragalactic populations in dark time, we reserve 20% of the BOSS fibers for sky observations, and those locations must be empty of astrophysical sources down to the magnitude limit of the deepest wide-area imaging that we currently have available. In contrast, observations of bright targets in bright time generally require fewer sky fibers, and can sometimes tolerate mild contamination from faint astrophysical sources. However, even with such reduced criteria, suitable sky fiber locations can be challenging to find in the densest Galactic plane fields.

With these constraints in mind, we have designed a hierarchy of sky fiber cartons, which collectively satisfy all SDSS-V FPS observational requirements. BOSS observations use three cartons: ops_sky_boss_best, ops_sky_boss_good, and ops_sky_boss_fallback; and APOGEE observations draw on two cartons: ops_sky_apogee_best and ops_sky_apogee_good.

First, the sky is divided into HEALPix NSIDE = 32 pixel "tiles," comprising roughly $3.4\,{\rm deg}^2\,{\rm pix}^{-1}$, which is approximately the area spanned by a single FPS configuration. Each tile is further divided into HEALpix NSIDE = 32,768 pixels ($41\,{\rm arcsec}^2\,{\rm pix}^{-1}$), the centers of which are considered candidate sky locations.[95] Each candidate sky location is then compared to a set of input catalogs (given below) and labeled valid (with respect to each comparison catalog, separately) if (i) their NSIDE = 32,768 HEALpixel contains no astrophysical objects in that catalog, and (ii) they lie farther than a magnitude-dependent separation from the nearest potentially contaminating astrophysical source. This minimum separation is computed as $s^* = s + \frac{(m_{\rm thr} - m)^\beta}{a}$, where $s = 5''$ is a minimum radius floor and $m_{\rm thr}$ is a fixed brightness threshold (14 mag). The $a = 0.15$ and $\beta = 1.5$ parameters control the scaling of the exclusion radius with brightness and are set to conservative values. We consider the H, G, $V_{\rm total}$, $r_{\rm psf}$, and $r_{\rm model}$ magnitudes for objects from the 2MASS PSC, Gaia DR2, Tycho2, Pan-STARRS1 DR2, and Legacy Survey DR8 catalogs, respectively (Høg et al. 2000; Skrutskie et al. 2006; Gaia Collaboration et al. 2018; Dey et al. 2019; Flewelling et al. 2020). Candidate sky locations lying near 2MASS extended sources (Jarrett et al. 2000) are considered to be valid if they lie outside the "extrapolation/total radius" of the source. All of these candidate locations that are valid in one or more catalogs are stored in the catalogdb table skies_v2 and serve as inputs for the cartons below.

The highest-quality sky carton for BOSS (i.e., suitable for darkest observations) is ops_sky_boss_best. For this carton, we require locations to be valid in each of the 2MASS (point and extended sources), Tycho2, and Gaia DR2 catalogs. Furthermore, selected sky locations must be within the Pan-STARRS1 or Legacy Survey DR8 survey footprints, and must not be contaminated by sources from either catalog. Somewhat less restrictive is the ops_sky_boss_good carton, which drops the requirement to avoid Pan-STARRS1 and Legacy Survey DR8 sources, and so extends the list of available sky locations to the entire sphere, excepting an area of the Galactic bulge and the inner parts of the Magellanic Clouds. In order to provide sky fiber locations in those remaining regions, the ops_sky_boss_fallback carton loosens the radial exclusion criteria, preferring locations that lie farthest from Gaia DR2 sources, but requiring only that the sky location lies more than $3''$ from a Gaia DR2 or Pan-STARRS1 source, more than $5''$ from any 2MASS source, and more than $15''$ from any Tycho2 star.

For APOGEE observations, the highest-quality ops_sky_apogee_best carton requires sky locations to be valid in each of the 2MASS (point and extended sources), Tycho2, and Gaia DR2 catalogs. The lower-priority ops_sky_apogee_good carton is dedicated to finding the remaining least-bad sky locations in dense regions. These positions have a maximum nearest neighbor brightness of $H = 10$, and candidates lying farthest from 2MASS contaminants are preferred.

[95] For comparison, BOSS and APOGEE-N fibers cover ∼3.14 arcsec^2 on the sky, and APOGEE-S fibers ∼1.32 arcsec^2.

6. MWM: Science Programs and Target Selection

The Milky Way can serve as a "model organism" for understanding the physical processes that shape galaxies over an enormous range of temporal and physical scales in the context of hierarchical cosmogony. MWM takes advantage of our unique perspective within the Milky Way to create an unprecedented high-resolution map of our galaxy's stellar populations. MWM is observing stars formed in the dawn of the galaxy through the present day, thoroughly sampling the H-R diagram and chemical abundance space. Through multi-epoch, multiwavelength observations of single stars and stellar systems, MWM seeks to understand the evolution of the luminous constituents of the galaxy and detect unseen compact objects and substellar objects.

MWM focuses on four connected themes:

1. *Galactic Archeology.* We can reconstruct the deep history of the Milky Way through observing the number, masses, composition, ages, and motions of its stars and the structures that they create. Luminous red giants cover a large range of ages, from ∼1 Gyr and older. However, samples of red giants are insensitive to the history of intermediate-mass stars older than ∼1 Gyr. Such stars have turned into stellar remnants, mostly WDs. Other sites of Galactic archeology studied in open-fiber programs (Section 8) in targeting generation `v0.5.3` include the Galactic halo and the Magellanic Clouds.
2. *The Young Galaxy.* The programs under Galactic Archeology investigate the cumulative history of star formation, chemical enrichment, and radial migration of the Milky Way, as told through evolved stars across a range of masses. Young stars (here, ∼5–100 Myr) fill in the early phases of low-mass stellar evolution and the full life cycles of massive stars. They provide a detailed and complete snapshot of the youngest generation in the Milky Way. In MWM, we systematically target low-mass young stars (young stellar objects, or YSOs) within ∼500 pc and all luminous, hot stars throughout the Galactic disk. Dust is relevant not only to the current structure of the Milky Way, but also to how metals are incorporated into the interstellar medium (ISM) and thence into the next generation of stars. MWM takes advantage of dust and extinction indicators along lines of sight to its observed stars to map the dust and its properties in the disk.
3. *The High-energy Galaxy.* Galactic sources of X-ray emission include compact object accretors, young stellar objects, and flaring stars, all objects of intense interest for the other themes here as well. The eROSITA mission is measuring X-ray fluxes for millions of point sources in the galaxy. However, to identify and explore the physical nature of such objects, optical and/or IR spectra rich in absorption and emission features are critical.
4. *Stellar Physics and Stellar Systems.* Undergirding all of MWM's Galactic explorations are the properties of stars and stellar systems. We begin these investigations close to home—in the solar neighborhood, the only place in the universe where it is practicable to obtain a spectroscopic census of stars down to the hydrogen burning limit.

   To reliably predict the age, evolutionary state, nucleosynthesis, internal mixing, and end state of stars, we need to understand their structure. Astereoseismology —the study of how waves propagate through stellar interiors—provides a powerful tool for this work, especially when combined with stellar and dynamical parameters from spectra. MWM is targeting oscillating red giant and hot stars. In the latter case, we are focusing on OBA stars in massive eclipsing binaries (EBs).

   Most stars orbit other stars. MWM is unique among current large spectroscopic surveys in targeting a vast range of stellar types for time-domain radial velocity observations, including YSOs, OB stars, WDs, and red giants. Particular attention is also paid to compact binaries, which are binary systems where at least one component is a WD, neutron star (NS), or black hole (BH), and to stars observed at high cadence for planet transits. By increasing the number of epochs, MWM is increasing the probability of orbit reconstruction, with the goal of probing long baselines (>8 yr) and the brown dwarf desert.

These top-level science goals are achieved by observing an anticipated ∼5 million stars, with the different target categories structured in a set of target cartons. Each carton has a well-defined selection function to enable subsequent population modeling (Rix et al. 2021). These cartons are summarized in Table 3, with complete selection functions provided in Appendix A and on the DR18 website.[96] It is important to note that these target selections are the inputs into the observational design code (Section 10). The final targets that will actually be observed are an as yet unknown subset of these selections. See J. A. Johnson et al. 2023 (in preparation) for a complete description of MWM's goals and targeting.

DR18 contains substantial targeting information for MWM, including the input catalogs used to generate potential target lists, the selection functions for the numerous cartons, and the data models for the anticipated output files. Users anticipating the first spectroscopic data release in DR19 can use this information to prepare for analysis of the DR19 data. We confine our discussion here to the `v0.5.3` targeting scheme, deferring the presentation of cartons added in subsequent targeting schemes (e.g., for validating stellar parameters, observing Gaia binaries, and other expansions and improvements) to the future MWM overview and DR19 papers. Thus, the subsections below enumerate the specific programs, and their constituent cartons, designed under the `v0.5.3` targeting strategy to address the scientific goals above.

6.1. Galactic Genesis

Galactic Genesis (GG) is the flagship program of MWM, with near-IR (APOGEE) observations of over four million stars planned. GG's central science goal is to obtain a fine sampling of the chemo-orbital distribution of stars across the entire radial extent of the Milky Way, probing the Galactic plane, the central regions of our galaxy, and the far side of the disk. To do this, GG targets luminous red giants, above the red clump, where the multimillion sample size with dust-penetrating APOGEE observations provides a decisive advantage over other surveys.

All of the GG targets are contained in the `mwm_galactic_core` carton.

[96] https://www.sdss.org/dr18/mwm/programs/cartons/

6.2. WDs

WDs are tracers of Galactic star formation, progenitors of type Ia supernovae, important end products of both single- and binary star evolution, and important cosmic physics laboratories (e.g., for the formation of strong magnetic fields). Gaia has recently produced enormous, well-defined samples of WDs (∼250,000 objects). SDSS-V is enlarging the subset of these WDs that have complementary spectroscopy (especially in the southern hemisphere) and also providing multi-epoch observations for empirical input on the binary WD merging channels toward type Ia supernovae and other remnant products (e.g., Chandra et al. 2021).

All of the MWM WDs targeted for this program are contained in the `mwm_wd_core` carton.

6.3. Solar Neighborhood Census

MWM's Solar Neighborhood Census (SNC) program targets a volume-limited sample of stars with the goal of cataloging low-luminosity stellar populations. While not technically "complete," the SNC will provide high-quality, two-epoch BOSS or APOGEE spectra of $>10^5$ stars within 100 pc and within 250 pc. The most complete census will be within 100 pc. However, there are few stars hotter than K types that close to the Sun, so a sample of stars out to 250 pc away is also targeted to enable a reliable match to higher-luminosity populations.

The SNC targets span four cartons, all beginning with `mwm_snc`: `mwm_snc_100pc_apogee`, `mwm_snc_100pc_boss`, `mwm_snc_250pc_apogee`, and `mwm_snc_250pc_boss`, where the latter part of the carton names indicate the volume size and instrument.

6.4. YSOs

The MWM YSO program targets the pre-main-sequence phase of low-mass stars. These objects are key to understanding the early phases of low-mass stellar evolution, on what orbits stars are born, and how they disperse from their clustered birth sites to become field stars. The YSO program selects objects via their position in the color–magnitude diagram (CMD), optical/IR spectral energy distribution, or variability. APOGEE spectra then provide stellar parameters and velocities, while BOSS spectra provide indicators of youth, such as Li absorption and Hα emission. Kounkel et al. (submitted) present a complete discussion of the target selection rationale and on-sky validation.

Cartons that fall under the YSO program have names beginning with `mwm_yso`, a third label indicating their selection method, and a fourth label indicating the instrument used (either `apogee` or `boss`). The shorthand labels for the selection methods are `cluster`, `cmz`, `disk`, `embedded`, `nebula`, `pms`, and `variable`. For example, YSO targets selected based on their variability and observed with the APOGEE instrument are contained in the `mwm_yso_variable_apogee` carton. The full selection functions for these methods are detailed in Appendix A.

6.5. OB Stars

Massive stars on the main sequence are unambiguously young because of their short hydrogen burning lifetimes. They are excellent tracers of the recent star formation throughout the disk (e.g., Zari et al. 2021) and they are most likely luminous companions to BHs and NSs, objects that were once even more massive stars. These hot stars are also the dominant ionizers of the ISM. The MWM OB program targets all stars brighter than $G = 16$ that are also likely to be hotter than ∼8000 K.

The massive stars in this program fall into two cartons: `mwm_ob_cepheids`, targeting known Cepheid stars (Inno et al. 2021), and `mwm_ob_core`, targeting a larger sample of OBA stars across the Milky Way and Magellanic Clouds.

6.6. Galactic eROSITA Sources

In addition to the spectroscopic follow-up of high-redshift X-ray sources from eROSITA (Section 7.2), the Galactic eROSITA sources program in MWM is targeting likely Milky Way X-ray sources, including accreting compact objects, YSOs, and flare stars. The optical and IR counterparts of these sources were identified by the eROSITA Stars and Compact Objects working groups and are being observed with the APOGEE and/or BOSS instrument(s), depending on the *H*-band or *G*-band magnitude, for source characterization.

The Galactic eROSITA program targets comprise three cartons: `mwm_erosita_stars`, for likely stellar coronal emitters, and `mwm_erosita_compact_gen` and `mwm_erosita_compact_var` for likely compact object accretors, using two different methods for finding the likeliest optical counterpart.

6.7. Massive EBs

The main-sequence structure of massive stars, including the size of their convective cores, is intimately linked to their (eventual) remnant mass and other properties. The Massive Eclipsing Binaries program uses asteroseismic and photometric data to identify the likeliest double-lined spectroscopic EBs with pulsational variability, among OBA stellar types.

These targets are contained in the `manual_mwm_tess_ob` carton.

6.8. Binary Systems

The APOGEE-1 and APOGEE-2 surveys contributed to binary studies both through statistical studies of large samples (e.g., Mazzola et al. 2020; Price-Whelan et al. 2020) and through reconstructing orbits (e.g., Washington et al. 2021). In MWM, the orbital size and mass range spanned by targets in the OB Stars and YSO programs will be increased by serendipitous observations of previously observed stars that meet the GG criteria (see above). The Binary Systems program is further enhancing this sample of stellar and substellar companions of stars across the H-R diagram by investing fibers to extend the time baselines of red giants, subgiants, and M dwarfs. This program exclusively uses the APOGEE spectrograph because of its superior spectral resolution and improved radial velocity precision.

Targets in this program fall into one of two cartons: `mwm_rv_long_fps`, for stars *with* existing multi-epoch observations from APOGEE, and `mwm_rv_short_fps`, for stars without these earlier observations.

6.9. Compact Binaries

Spectra of compact binary systems are frequently marked by nonstellar emission—such as X-ray, UV, or Hα flux—that can probe mass transfer or other nonthermal processes. The

Compact Binaries program is observing a large number of likely compact binary systems, identified through different combinations of CMD position, UV excess, and previous association with a cataclysmic variable (from the AAVSO).[97]

These different combinations of selections are reflected in the many cartons contained in the Compact Binaries program. All of the carton names begin with `mwm_cb` or `manual_nsbh`, followed by additional labels indicating the selection method and (in some cases) the instrument used for the MWM observations. The shorthand labels for the selection methods are `300pc`, `cvcandidates`, `gaiagalex`, and `uvex[1-5]`. The full selection functions for these methods are detailed in Appendix A.

6.10. Planet Hosts

Understanding the conditions that impact a star's likelihood of hosting planets, and the properties of the planetary orbits and the planets themselves, is essential for understanding planet formation and solar system evolution. The Planet Hosts program targets TESS stars with and without associated TOIs. These will be observed with the APOGEE instrument to provide stellar parameters and detailed stellar abundances.

The single carton in this program is called `mwm_tess_planet`.

6.11. Asteroseismic Red Giants

For stars on the red giant branch (RGB), asteroseismology arguably provides the gold standard of stellar mass and surface gravity measurements, but maximizing its power requires additional input from spectroscopy (such as stellar metallicity). The goal of the Asteroseismic Red Giants program is to obtain spectra for stars with asteroseismic signals, especially those observed by TESS. The start of SDSS-V overlapped with the nominal mission of the TESS satellite, so this program targets bright RGB stars throughout most of the sky (avoiding the Galactic plane), under the expectation that some large fraction of them would eventually have detectable oscillations. This simple selection function will enhance the legacy value of this program's sample.

The single carton in this program is called `mwm_tessrgb_core`.

6.12. Dust

Interstellar dust presents both a challenge and an opportunity in studying the structure and history of our galaxy. For example, rigorous modeling of the Milky Way's structure, based on stellar observations, requires (approximate) knowledge of the 3D extinction distribution, as seen from the Sun. Such a map then permits dust-corrected estimates of stellar distances for stars with spectroscopic luminosity estimates, but poor parallaxes, as well as valuable information on the 3D structure of the cold ISM. MWM's Dust program is obtaining spectra for mapping distributions of the density and properties of dust (such as R_V; e.g., Schlafly et al. 2016). Those spectra will also provide information on the column density and kinematics of the ISM via the diffuse interstellar bands (e.g., Zasowski et al. 2019). The targets for this program are RGB stars selected to "fill in" the regions of low extinction avoided by the GG program, to achieve an even sampling of the Milky Way's dust with the total MWM sample.

The single carton in this program is called `mwm_dust_core`.

6.13. Science Validation

The only carton in this program in the `v0.5.3` targeting generation is `mwm_legacy_ir2opt`, which is a filler carton to obtain BOSS spectra of stars observed in APOGEE-1 and APOGEE-2. The stellar parameters from the higher-resolution APOGEE spectrum of a given star are used to provide labels for the BOSS spectrum, facilitating data-driven modeling and cross-calibration of the BOSS spectra. Future targeting generations will include additional cartons targeting stars with known fundamental parameters and stars targeted by other large spectroscopic surveys.

7. BHM: Science Programs and Target Selection

BHM sets out to better understand the growth of supermassive black holes (SMBHs) at the centers of galaxies, through both time-domain spectroscopy of quasars and other active galactic nuclei (AGNs), and the first large-area optical spectroscopic follow-up of the newly available eROSITA X-ray survey. In its quasar time-domain program, SDSS-V will provide orders-of-magnitude advances in both time baseline and sample sizes. The BHM time-domain core programs (Section 7.1) will target about $\sim 10^{4.5}$ previously known quasars with multiple additional optical spectral epochs. SDSS-V will also provide optical counterpart spectra for $\sim 10^{5.5}$ X-ray sources (Section 7.2), especially recently discovered X-ray sources from SRG/eROSITA (Predehl et al. 2021).

In DR18, BHM is releasing two categories of data: (i) initial catalogs of candidate targets for its main science programs, which may provide guidance to the community in planning for future SDSS-V data releases; and (ii) optical BOSS spectra for $\sim 10^4$ candidate counterparts to eROSITA X-ray sources from the eFEDS field (Section 7.3; Brunner et al. 2022). In the subsections below, we provide a high-level summary of those BHM science programs that directly flow down from the driving science goals of the project (i.e., the "core" programs); these are summarized in Table 4. Further details of the target selection criteria for the full set of BHM target cartons released in DR18 can be found in Appendix B and on the SDSS DR18 website.[98] As in the MWM section above, these targeting selections provide inputs into the observational design software (Section 10). The actual targets that are finally observed are a subset of these selections, determined by the survey optimization software.

7.1. Spectral Time-domain Programs

The time-domain BHM core programs will target about $\sim 10^{4.5}$ previously known quasars with multiple additional optical spectral epochs. These spectral time-domain programs aim to sample a broad range of timescales and cadences, ranging from days to decades (when all SDSS data are combined), as different aspects of quasar physics result in variability on very different timescales. SDSS-V studies black hole masses via RM, possible SMBH binarity, time-resolved

[97] https://www.aavso.org/cataclysmic-variables

[98] https://www.sdss.org/dr18/bhm/programs/cartons/

accretion events, broad-line region (BLR) dynamics, and broad absorption line quasi-stellar object outflows. The SDSS-V quasar time-domain programs build on the results and experience of earlier generations of SDSS, e.g., the SDSS-III/IV RM project (Shen et al. 2015) and the Time Domain Spectroscopic Survey (MacLeod et al. 2018), to enable long time baselines.

7.1.1. All-quasar Multi-epoch Spectroscopy

The All-quasar Multi-epoch Spectroscopy (AQMES) program is core to the BHM science, with different tiers in survey area and number of epochs. It includes cartons that are aimed at wide areas with low cadence, and cartons aimed at a more modest area with higher cadence (see Table 4). Together, these two tiers add new epochs in SDSS-V for ∼22,000 quasars that already have at least one previous epoch of spectroscopy from SDSS-I–IV. These AQMES targets are selected from the SDSS DR16 quasar catalog (Lyke et al. 2020) and are readily observable from APO.

For ∼20,000 known quasars, the primary associated targeting carton is `bhm_aqmes_wide2`. This carton aims to add ∼two additional epochs of SDSS-V optical spectroscopy for each of these known SDSS quasars. When combined with their archival SDSS optical spectra, these data will sample ∼1–25 yr timescales (observer frame). The primary science goals include probing the BLR dynamics of the most massive black holes, constraining the statistics of changing-look quasars, and charting broad absorption line disappearance/emergence. This is a relatively wide-area but low-cadence time-domain tier, encompassing ∼2000–3000 $\deg^2$ of the sky.

For ∼2000 quasars, the `bhm_aqmes_medium` carton (Table 4) aims to add ∼10 optical spectral epochs in SDSS-V, probing down to 1 month to 1 yr timescales (in addition to the longer-baseline timescales enabled with archival SDSS spectroscopy). The primary science goals of AQMES-Medium are to trace out BLR structural and dynamical changes, including BLR changes in modest-mass SMBHs. This is a medium time-domain tier in area and cadence, encompassing ∼200–300 $\deg^2$.

7.1.2. RM

The RM program is core to the BHM science of measuring black hole masses.

For ∼1000 quasars in four to five dedicated fields to be targeted under the BHM RM program, a set of cartons (with names starting with `bhm_rm`; Table 4) aim to obtain optical repeat spectra with a high cadence of up to ∼174 epochs, which sample down to (observer-frame) timescales of days to weeks. The time lags between the continuum and BLR emission, plus line velocity widths, yield virial estimates of the black hole mass, advancing RM measures yet further to a broad range of luminosities and redshifts. This is a small-area but high-cadence time-domain tier, encompassing a total of ∼30 $\deg^2$.

7.2. Spectroscopic Follow-up of X-Ray Sources

In addition to the time-domain science projects described above, BHM is carrying out a program of spectroscopic characterization of counterparts to an unprecedentedly large sample of X-ray sources. In almost all cases, this will be via optical spectroscopy. The broad science emphasis is to chart the astrophysics, and the growth and evolution, of SMBHs. The X-ray selection provides a probe of accretion onto SMBHs that is significantly less sensitive to intervening absorption, and that generally selects a broader range of AGN luminosities, than purely optical-based selections. BHM features a large core program aimed at eROSITA X-ray sources (Section 7.2.1) and a substantial complementary program following up Chandra archival X-ray source catalogs (Section 7.2.2).

7.2.1. Spectroscopic Identification of eROSITA Sources

The SPectroscopic IDentification of ERosita Sources (SPIDERS) program is core to BHM science and will help reveal the connections between statistical samples of X-ray emitting quasars/AGNs and clusters of galaxies, and the large mass structures that they trace. The BHM SPIDERS program expands greatly on the SDSS-IV SPIDERS program (e.g., Clerc et al. 2016; Dwelly et al. 2017; Comparat et al. 2020).

The main goal of the SPIDERS program (sometimes referred to as the "(Southern) Hemisphere" survey) is to provide complete and homogeneous optical spectroscopic follow-up of $\sim 10^{5.5}$ X-ray sources detected by eROSITA, across ∼10,000 $\deg^2$ at high Galactic latitude (nominally $|b| > 15°$), within the German or "DE" half of the sky. Ultimately, SPIDERS, via its wide-area survey, aims to obtain the optical spectroscopic identifications and redshifts, evolutions, and astrophysics of ∼250,000 counterparts to X-ray pointlike sources. It is anticipated that AGN/quasar identifications will form the large majority of the targets, but with a significant minority of X-ray emitting stars (from compact binaries to coronal emitters). Eventually, SPIDERS will use X-ray sources from eROSITA's first 1.5 yr of survey operation (termed "eRASS:3," because it contains data from three passes over the whole sky), which were completed in 2021 June. The SPIDERS "AGN" project cartons have names that start with `bhm_spiders_agn` (Table 4). However, note that the initial SPIDERS targeting information in `v0.5.3` released in DR18 is derived from the somewhat shallower first six months of eROSITA-DE observations ("eRASS:1").

An additional SPIDERS project is targeting $\sim 10^4$ X-ray emitting clusters of galaxies ($>5 \times 10^4$ galaxy targets), selected from a combination of X-ray imaging and the eROSITA red-sequence Matched-filter Probabilistic Percolation galaxy cluster-finding algorithm (eROMaPPeR; Rykoff et al. 2014; Ider Chitham et al. 2020) applied to multiband wide + deep optical/IR imaging catalogs. For the SPIDERS clusters cartons (with names including `bhm_spiders_clusters`), the new SDSS-V spectroscopy will provide redshifts and confirmations for the candidate clusters, as well as constraints on the velocity dispersion of the member galaxies. See Bulbul et al. (2022) for additional discussion on the complexity of selecting galaxy clusters in X-ray data sets.

A related pilot survey that began in SDSS-IV, and extended into early SDSS-V, has already largely completed BOSS spectroscopy for $\sim 10^4$ candidate counterparts in the eROSITA–eFEDS minisurvey field, a ∼140 $\deg^2$ region of the sky. The optical spectra in eFEDS are a centerpiece of the DR18 data release, and are detailed further in Section 9.1.

7.2.2. Chandra Source Catalog

The Chandra Source Catalog (CSC) program is a more modest, complementary program of mainly optical spectroscopy of X-ray

counterparts (but including some IR APOGEE spectra as well). The SDSS-V/CSC program produces identifications, redshifts, and other properties of tens of thousands of X-ray source counterparts selected from the CSC[99] (Evans et al. 2010); again, many are likely to be verified as AGNs in their SDSS-V spectra. The CSC sample is expected to probe fainter X-ray fluxes than the SPIDERS Hemisphere samples. The CSC target cartons released as part of DR18 are based on CSC2.0. In the future, we plan to switch to the more recent CSC2.1 catalog in order to increase the available pool of targets.

7.3. The SDSS-V/eFEDS Minisurvey

The SDSS-V/eFEDS survey is a pathfinder component of the BHM survey program that exploits early performance validation observations from the SRG/eROSITA X-ray telescope in the eFEDS field (Brunner et al. 2022). The eFEDS X-ray footprint comprises 140 $\deg^2$ centered near $(\alpha, \delta) = (9^h, +1^\circ)$, encapsulating the "GAMA09" Field (Driver et al. 2009). We used plate observations at APO to collect optical BOSS spectroscopy for counterparts to both pointlike and extended X-ray sources (Klein et al. 2022; Salvato et al. 2022). From past experience (e.g., Clerc et al. 2016, 2020; Menzel et al. 2016; LaMassa et al. 2019), one can expect these X-ray populations to be numerically dominated by AGNs and clusters of galaxies, but we also expect a substantial minority to be associated with stellar coronal emitters or accreting compact objects.

Below, we give a summary of the observational goals, target selection, and survey strategy for the SDSS-V/eFEDS observations. Details of the plate design and the scope and quality of the observed data set can be found in Section 9.1.

7.3.1. SDSS-V/eFEDS Observational Goals

The primary observational goal for this program was to achieve near-complete and reliable redshifts and classifications for optical counterparts to X-ray sources that were detected as part of the eROSITA/eFEDS performance verification survey, particularly for counterparts in the magnitude range $16 < r < 22$ AB. On the one hand, this goal was constrained by the number of hours of dark observing time available to the project, a general desire to minimize the total number of drilled plug plates, and the overall capabilities of the plate system to place fibers on naturally clustered targets. On the other hand, this goal of high completeness was assisted by the wealth of previous spectroscopic survey data in the eFEDS field, both from previous SDSS generations and from other telescopes and instruments. Our strategy was therefore to prioritize targets that did not have existing high-quality spectroscopic observations.

7.3.2. Target Selection for SDSS-V/eFEDS Plates

The generation of targeting used for the eFEDS plates, during the 2020 December–2021 May run of plate operations, predates the global `v0.5.3` targeting information that is being released in DR18. The parent catalogs from which the eFEDS targets were selected were derived from early reductions of the eROSITA/eFEDS X-ray data set and are based on early attempts to match those X-ray sources to longer-wavelength counterparts provided by several supporting optical/IR catalogs, including the DESI Legacy Survey (DR8; Dey et al. 2019), SDSS DR13 (Albareti et al. 2017), and the Hyper Suprime-Cam Subaru Strategic Project (HSC-SSP DR2; Aihara et al. 2019). The eFEDS science target selection process concentrates on AGN candidates (one target carton) and galaxy cluster candidates (four cartons):

`bhm_spiders_agn-efeds`. A carton that contains candidate AGN targets found in the eROSITA/eFEDS X-ray survey field. This carton provides optical counterparts to pointlike (unresolved) X-ray sources detected in early reductions (eROSITA Science Analysis Software, or eSASS, version "c940/V2T") of the eROSITA performance validation survey data in the eFEDS field. The sample is expected to contain a mixture of QSOs, AGNs, stars, and compact objects. The X-ray sources have been crossmatched by the eROSITA-DE team to the Legacy Survey[100] optical/IR counterparts (Salvato et al. 2022).

`bhm_spiders_clusters-efeds-ls-redmapper`. A carton that contains galaxy cluster targets found in the eROSITA/eFEDS X-ray survey field. The carton provides a list of galaxies that are candidate members of clusters selected from early reductions (eSASS version "c940") of the eROSITA performance verification survey data. The parent sample of galaxy clusters and their member galaxies has been selected via a joint analysis of X-ray and (multiple) optical/IR data sets using the eROMaPPeR red-sequence finder algorithm (Rykoff et al. 2014; Ider Chitham et al. 2020). This particular carton relies on optical/IR data from the DESI Legacy Surveys (Dey et al. 2019).

`bhm_spiders_clusters-efeds-sdss-redmapper`. Similar to the `bhm_spiders_clusters-efeds-ls-redmapper` carton, except that the red-sequence finder algorithm is run on the SDSS DR13 photometric catalog (Albareti et al. 2017).

`bhm_spiders_clusters-efeds-hsc-redmapper`. Similar to the `bhm_spiders_clusters-efeds-ls-redmapper` carton, except that the red-sequence finder algorithm is run on the HSC-SSP DR2 photometric catalog (Aihara et al. 2019).

`bhm_spiders_clusters-efeds-erosita`. This carton includes manually identified counterparts to X-ray extended sources that were not also selected by the eROMaPPeR algorithm, when applied to any of the DESI Legacy Survey, SDSS DR13, or HSC-SSP data sets.

Additional details on these cartons can be found in Appendix B and at https://www.sdss.org/dr18/bhm/programs/cartons/.

8. MOS Open-fiber Programs

The hardware and the survey strategy for SDSS-V's MOS programs were designed around a set of core science cases that define this part of the survey. The underlying target densities in these science cartons vary dramatically across the sky, from star-rich Baade's Window toward the Galactic bulge to sparse high galactic latitudes. In addition, the FPS is subject to geometric constraints in placing fibers within a pointing's field of view: in a given individual exposure, fibers cannot be placed closer than $\sim 50''$ to each other, and—given the limited patrol radius of each robot—the mean fiber density across the field of

[99] https://cxc.cfa.harvard.edu/csc/

[100] https://legacysurvey.org/dr8

view cannot be changed. These constraints imply that after survey optimization for SDSS-V's core science, many robots with either BOSS or APOGEE fibers remain unallocated. After simulating the entire survey, over three million anticipated fiber exposures remained available.

In light of this, SDSS-V set up an "open-fiber" program, based on multiple collaboration-wide calls for ideas and proposals, which serves three purposes. First, and most immediately, to make sure that as few fibers as possible go scientifically unused. Second, to provide a mechanism to broaden the science case beyond the initial, defining science cases. And third, to provide a mechanism, through repeated open-fiber proposal calls, to incorporate scientifically exciting targets that only become known or available as the survey goes on.

In 2020, SDSS-V issued a first call for open-fiber proposals from the consortium, whose results have entered the targeting documented here in various ways. The boundary conditions for these proposals were that: (i) the science goals could be reached with single 15 minute exposures using either APOGEE or BOSS; (ii) the targeting information was freely available to all consortium members, and a target selection function could be specified; (iii) the existing core science goals were complemented or enhanced; and (iv) the science goals had proponents within the SDSS-V consortium.

The project received nearly 30 proposals in late 2020. Much of the proposed science fell into one of three broad categories: (i) more extensive surveying of AGNs and X-ray sources across the sky; (ii) broader stellar physics, in particular binary star physics, across the CMD; and (iii) studying the Milky Way's stellar halo and metal-poor population, which (intentionally) had not been a focus of the MWM GG program (Section 6). These programs were reviewed in early 2021 by the SDSS-V technical advisory group and the project leadership, who called on three consortium members not involved in the proposals to help with the review. The resulting target cartons are listed in Table 5. For the `v0.5.X` versions of the targeting, including the `v0.5.3` generation released in DR18, we adopted these cartons as they were. In future versions of the target selection, a number of these cartons may be consolidated and incorporated into the versioned science programs of the BHM and MWM surveys.

9. Spectra

This section describes the spectra being released in DR18, particularly the eFEDS survey and its data products.

9.1. The SDSS-V/eFEDS Minisurvey

The scientific objectives and carton design of the eFEDS program can be found in Section 7.3. Below, we describe the observational design details and the final data set.

9.1.1. Tiling and Plate Design

Due to COVID-19-induced delays in the completion of the FPS systems, SDSS-V started observations at APO using the existing fiber plug plate system, including the eFEDS observations. Modifications to the existing system included a new joint BOSS+APOGEE configuration, in which the focal plane was populated with 500 fibers feeding a BOSS optical spectrograph and 300 fibers feeding an APOGEE IR spectrograph. New procedures and software were put in place to manage target selection, fiber assignment, and plate design for the single season of SDSS-V data that were obtained in this mode. These procedures will be described in more detail in a future publication (K. Covey et al. 2023, in preparation). Here, we provide a summary of the special considerations that apply specifically to the SDSS-V/eFEDS plates.

Each plate-based observing run comprises a set of plates created to observe a set of targets from a given field (a region of the sky) and drilled to observe around a specific hour angle (to account for atmospheric refraction effects). The targets on a given plate were assigned using a specific combination of cartons (Section 7.3.2). For each plate, we created a prioritized list of cartons (including cartons associated with calibration targets such as skies and spectrophotometric standards; Section 5.2) to fill the fibers for each spectrograph. Individual fiber-filling rules were shared by multiple plates in the same observing run or even across different runs; different fiber-filling rules are distinguished by a shift in priority of a carton with respect to another or an update to the version of the carton that was used. Each combination of fiber-filling rule and unique set of targets was identified with a `designID`. Figure 5 shows the sky locations of the SDSS-V/eFEDS sources in relation to the other data sets available in the region.

SDSS-V/eFEDS plates were designed within two independent iterations of the tiling and plate design process. The first of these plate runs (`2020.11.a.bhm-mwm`) consisted of 31 initial plates spanning most of the $\sim$140 deg^2 eFEDS field, with an inner region (roughly corresponding to the GAMA09 field) targeted with two plates per sky position. The large fractional overlap between the eFEDS plates required special attention to ensure proper control over which targets were prioritized in which plates, as the standard SDSS `platedesign` software treats all plates independently. This complexity, and constraints on the fiber reach of the plate fibers, resulted in only 20 of the `2020.11.a.bhm-mwm` plates being available for observation. A second eFEDS plate run (`2021.01.a.bhm-mwm`) was designed to recover eFEDS targets from the unobservable plate designs and to take advantage of updated projections of the available observing time and plug plate manufacturing resources. A new heuristic tiling algorithm resulted in all 17 plates from this run being observed.

For each of these 37 SDSS-V/eFEDS plates, we reserved at least 80 BOSS fibers per plate for skies and 20 BOSS fibers for spectrophotometric standard stars, leaving up to 400 BOSS fibers for science targets.[101] We applied a bright limit for science targets of $g_{\rm psf}$, $r_{\rm psf}$, $i_{\rm psf} > 16.5$ AB, and we avoided placing fibers near brighter stars. These bright limits are imposed to allow observation of the faint end of the target population (Figure 6), without significant degradation from on-chip crosstalk between neighboring BOSS fiber traces.

9.1.2. Spectroscopic Observations, Reductions, and Data Quality

The SDSS-V/eFEDS observing strategy prioritized coverage over depth, given the somewhat uncertain amount of good-quality observing time that would be available while the eFEDS field was visible from APO. By the end of the visibility window (2020 December–2021 May), all 37 eFEDS plates had achieved a total fiducial g-band signal-to-noise ratio (S/N)

[101] The SDSS-V/eFEDS plates also included up to 300 APOGEE targets per plate; these will be presented in a future SDSS data release (Section 9.2).

Table 5
Open-fiber Cartons

Carton Name	Selection Summary[a]	Instrument	Available Targets[b]
openfibertargets_nov2020_3	Binaries—Bright Eclipsing Binaries	BOSS	34,689
openfibertargets_nov2020_5	Galactic Halo—[Fe/H] < -3 Candidates	BOSS	39,099
openfibertargets_nov2020_6a	Galactic Halo—SkyMapper BHB	BOSS	50,611
openfibertargets_nov2020_6b	Galactic Halo—SkyMapper RGB Metal-Poor	BOSS	340,436
openfibertargets_nov2020_6c	Galactic Halo—SkyMapper Dwarf Metal-Poor	BOSS	890,043
openfibertargets_nov2020_8	Young/Massive Stars—Young Galactic Disk	BOSS/APOGEE	704,638
openfibertargets_nov2020_9	Young/Massive Stars—F Star Physics	BOSS/APOGEE	1,197,354
openfibertargets_nov2020_10	Binaries—RVs in chemically anomalous stars	BOSS/APOGEE	917
openfibertargets_nov2020_11	All QSOs/AGNs—SDSS-I/II Quasars observed only once	BOSS	39,684
openfibertargets_nov2020_12	Binaries—Close Binary Stars	BOSS/APOGEE	33,577
openfibertargets_nov2020_14	Binaries—MS–WD Binaries	BOSS	10,798
openfibertargets_nov2020_15	Open Cluster Survey	BOSS/APOGEE	177,185
openfibertargets_nov2020_17	Young/Massive Stars—Census of YSOs < 500pc	BOSS	32,891
openfibertargets_nov2020_18	All QSOs/AGNs—Hard X-Ray Sources	BOSS	10,012
openfibertargets_nov2020_19a	TESS 2 minute cadence targets—a	BOSS/APOGEE	224,773
openfibertargets_nov2020_19b	TESS 2 minute cadence targets—b	BOSS/APOGEE	1605
openfibertargets_nov2020_19c	TESS 2 minute cadence targets—c	BOSS/APOGEE	1615
openfibertargets_nov2020_22	Binaries—Ellipsoidal Binaries	APOGEE	28,408
openfibertargets_nov2020_24	Chemodynamics in the Solar Neighborhood	BOSS	1,323,442
openfibertargets_nov2020_25	Galactic Halo—Local Halo	BOSS/APOGEE	293,741
openfibertargets_nov2020_26	All QSOs/AGNs—Quasar Winds	BOSS	2105
openfibertargets_nov2020_27	All QSOs/AGNs—All Bright Quasars	BOSS	814,963
openfibertargets_nov2020_28a	Galactic Halo—Distant K Giants	BOSS	73,627
openfibertargets_nov2020_28b	Galactic Halo—Distant BHBs	BOSS	49,900
openfibertargets_nov2020_28c	Galactic Halo—Distant RRLs	BOSS	51,234
openfibertargets_nov2020_29	Extratidal Globular Cluster Stars	BOSS/APOGEE	107,688
openfibertargets_nov2020_30	All QSOs/AGNs—JWST North Ecliptic Pole Time Domain	BOSS	237
openfibertargets_nov2020_31	RAVE Cross Calibration	APOGEE	62,275
openfibertargets_nov2020_32	Binaries—Wide MS–WD Binaries	BOSS/APOGEE	34,230
openfibertargets_nov2020_33	All QSOs/AGNs—Variability-selected AGNs and Blazars	BOSS	22,250
openfibertargets_nov2020_34a	CMD tiling—nonvariables	BOSS	8,701,166
openfibertargets_nov2020_34b	CMD tiling—variables	BOSS	643,546
openfibertargets_nov2020_35a	Galactic Halo—Metal-poor giants (IR)	BOSS	345,721
openfibertargets_nov2020_35b	Galactic Halo—Metal-poor giants (SkyMapper)	BOSS	52,696
openfibertargets_nov2020_35c	Galactic Halo—Metal-poor giants (SAGES)	BOSS	7521
openfibertargets_nov2020_46	Binaries—LAMOST multi-epoch	BOSS	663,835
openfibertargets_nov2020_47a	SDSS-V Magellanic Genesis: RGB	BOSS	278,987
openfibertargets_nov2020_47b	SDSS-V Magellanic Genesis: AGB	APOGEE	27,731
openfibertargets_nov2020_47c	SDSS-V Magellanic Genesis: Massive	BOSS	1000
openfibertargets_nov2020_47d	SDSS-V Magellanic Genesis: Massive	APOGEE	1000
openfibertargets_nov2020_47e	SDSS-V Magellanic Genesis: Symbiotic	APOGEE	24
openfibertargets_nov2020_1000	Stellar Clusters	BOSS/APOGEE	102,172
openfibertargets_nov2020_1001a	Binaries—Wide Binaries—Merged 21/36a	BOSS/APOGEE	81,303
openfibertargets_nov2020_1001b	Binaries—Wide Binaries—Merged 36/36b	BOSS	10,545

Notes. AGB = asymptotic giant branch, BHB = blue horizontal branch, MS = main sequence, RRL = RR Lyrae.
[a] See the online documentation for expanded selection details: https://www.sdss.org/dr18/targeting/open_fiber_programs/.
[b] "Available Targets" is the number of targets that satisfy the carton selection function in the targeting database. The number of targets ultimately observed for each carton will be smaller than this value.

squared ($(S/N)_g^2$) of at least 7.5. However, most of the plates are significantly deeper than that, with 33 of the 37 eFEDS plates having $(S/N)_g^2 > 10$ (comparable to the typical exposure depth in BOSS/eBOSS; Dawson et al. 2016) and more than half the plates having $(S/N)_g^2 > 20$. The fiducial S/N^2 in the *i* band is typically twice that measured in the *g* band. An updated version of the BOSS `idlspec2d` data reduction pipeline (Bolton et al. 2012; see Section 10.1 for updates) was used to generate a set of spectral data products per `PLATE-MJD` combination, with individual 1D spectra for each combination of `PLATE-MJD-CATALOGID`.

Many science targets were observed on more than one `PLATE-MJD` combination. Therefore, a specialized coadding algorithm (within `idlspec2d`) was additionally implemented for these eFEDS plates, collating spectroscopic data across plates and MJDs, in order to increase the S/N in the 1D spectra (Section 10.1). This routine creates a single stacked spectrum per astrophysical object, using all suitable SDSS-V BOSS data. A total of 13,269 specially coadded spectra from eFEDS science targets are released in DR18, along with 2608 skies, 671 spectrophotometric standards, and several hundred unvetted spectra not intended for scientific use (Section 9.2).

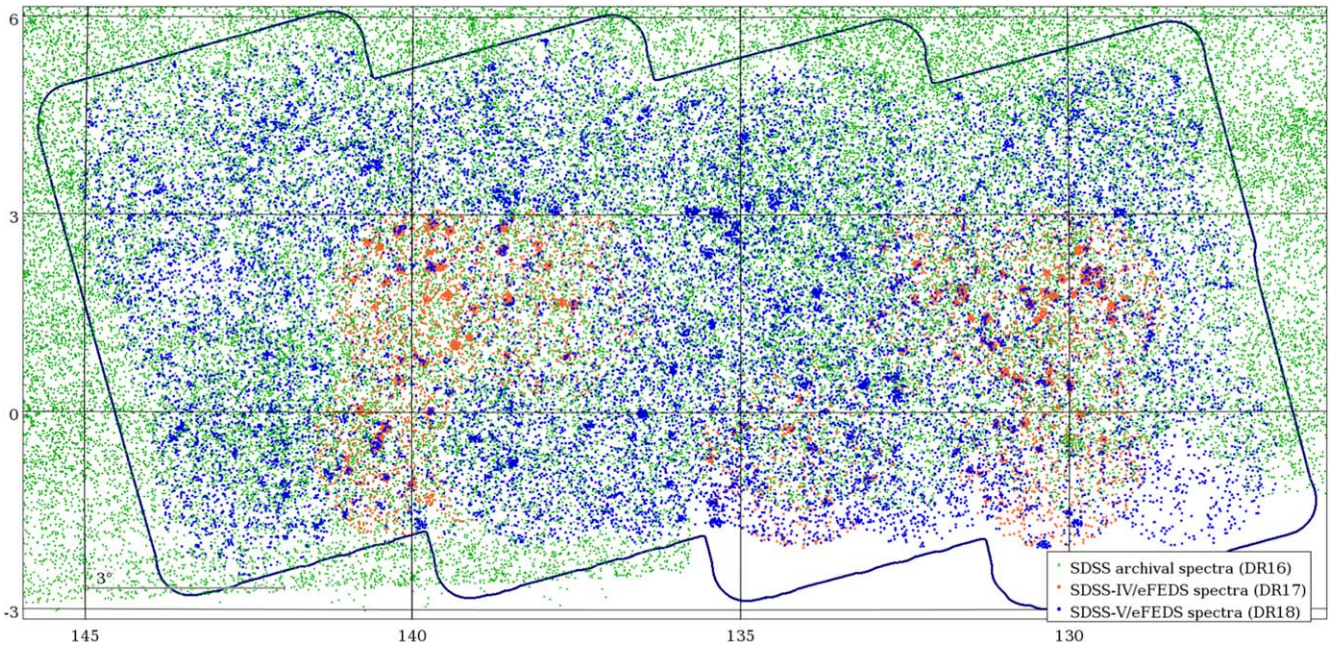

Figure 5. SDSS spectroscopic coverage in the eFEDS field (Section 9.1), color coded by the SDSS phase when the spectrum was taken. The green points show the locations of individual SDSS/BOSS spectra made available in DR16 or before; the orange points correspond to SDSS-IV/eFEDS BOSS spectroscopy released in DR17; and the blue points show the new optical BOSS spectroscopy being released in DR18. X-ray-selected galaxy clusters, specifically targeted in DR17 and DR18, are readily visible as compact concentrations of points. The approximate bound of the eROSITA X-ray data is shown with the thick black line. The southwest (lower right) corner is empty of DR16 spectroscopy because it lies outside the nominal SDSS imaging footprint. The map is shown on a tangential projection, in Equatorial coordinates, with units of degrees.

Redshifts, classifications, and quality flags were computed automatically on the specially coadded spectra using the `spec1d` template fitting pipeline (Bolton et al. 2012). A warning flag was set for 669/13,269 science spectra, indicating a problem with the data or the fit. Of the 12,600 science spectra without warnings, the main pipeline gives source classifications of "QSO" for 6204, "GALAXY" for 4782, and "STAR" for 1614 spectra. Pipeline redshifts for nonflagged "QSO"- and "GALAXY"-classified spectra span the range $0.0 < z < 4.5$, with 90% of these objects falling in the range $0.14 < z < 2.55$ (median 0.55).

Figure 6 shows the derived redshift distribution for good-quality (`ZWARNING`=0) spectra obtained from the SDSS-V/eFEDS plates, grouped by their primary target selection criteria. The observed redshift distributions are broadly in line with expectations. SPIDERS AGN targets span a wide range of redshifts ($0 < z < 4.5$; median 0.8), including a small fraction (10.0%) that are revealed by spectroscopy to be stellar in nature. SPIDERS galaxy cluster targets are found at relatively lower redshift ($0.1 < z < 0.6$; median 0.28).

In order to increase the completeness and reliability of the redshifts and classifications derived from these spectra, we carried out visual inspections of a large fraction of the SDSS-V/eFEDS spectra. Those inspections have been combined with earlier SDSS spectroscopic redshift information and with non-SDSS redshift information gathered from the literature. Please see A. Merloni et al. (2023, in preparation) and the associated VAC[102] (Section 11.2) for further details of the eFEDS spectroscopic compilation.

This data set has enabled in-depth study of the clustering of X-ray-selected AGNs, resulting in new constraints on the AGN halo occupation distribution (Comparat et al. 2023).

[102] https://www.sdss.org/dr18/data_access/value-added-catalogs/

9.1.3. Accessing eFEDS Data

To download the eFEDS spectra, go to https://dr18.sdss.org/sas/dr18/spectro/boss/redux/eFEDS/; the associated data models are at https://data.sdss.org/datamodel/files/BOSS_SPECTRO_REDUX/RUN2D/ and subdirectories. Note that these spectra were generated using the specialized coadding scheme described in Section 9.1.2. The "standard" coadds can be found at https://dr18.sdss.org/sas/dr18/spectro/boss/redux/v6_0_4/. To download the eFEDS VAC of improved redshifts (Section 11.2), visit the DR18 VAC website at https://www.sdss.org/dr18/data_access/value-added-catalogs/.

9.2. Other Spectra

Users of DR18 may come across science spectra (i.e., not standard stars or sky targets) that were included in the eFEDS plates (Section 9.1), but that are not associated with eROSITA/eFEDS target cartons. These data are included in DR18 for logistical reasons, but are not intended for scientific exploitation (e.g., they have not undergone any quality assurance testing). They can be identified by one of the following `FirstCarton` labels in the database:

1. `mwm_cb_cvcandidates`
2. `mwm_cb_gaiagalex`
3. `mwm_cb_uvex1`
4. `mwm_cb_uvex2`
5. `mwm_cb_uvex3`
6. `mwm_cb_uvex4`
7. `mwm_cb_uvex5`
8. `mwm_halo_bb`
9. `mwm_halo_sm`
10. `mwm_snc_100pc`
11. `mwm_wd`

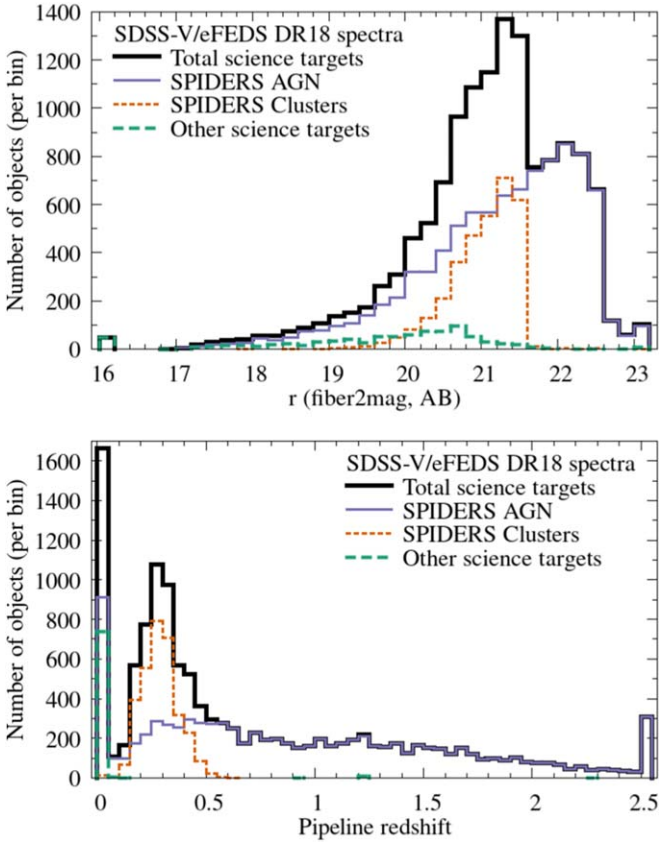

Figure 6. Upper panel: optical magnitude distribution of BOSS science targets in the SDSS-V/eFEDS plates (Section 9.1). Note that target magnitudes in SDSS-V are synthesized from a range of input photometric systems; in this case, we show the equivalent of an *r*-band "fiber2mag" (i.e., the light falling into a 2″ diameter fiber under nominal APO seeing conditions). Lower panel: distribution of pipeline-determined redshifts for science targets in the SDSS-V/eFEDS plate reductions (Section 9.1.2). Spectra with redshift fitting warnings have been removed. Redshifts outside the range of the plots are included in the extremal bins. The target selection for SPIDERS AGNs and Clusters is described in Section 7.3.2 and for other targets in Section 9.2.

Users can expect improved and vetted versions of these spectra in DR19.

10. Software

SDSS operations, data processing, and analysis rely on a large suite of software components. A limited number of these, new or updated for SDSS-V, have already been released or are being released as part of DR18.

10.1. Updates to the BOSS Spectral Reduction Algorithms

The optical BOSS data released in DR18 (Section 9.1) are processed with version `v6_0_4` of the BOSS pipeline software `idlspec2d` (Bolton et al. 2012; Dawson et al. 2013; S. Morrison et al. 2023, in preparation). This is the first official version of `idlspec2d` to be used for SDSS-V, with a few changes since the last full public release (`v5_13_2`) of SDSS-IV/eBOSS. All SDSS-V versions of `idlspec2d` are available for download from the SDSS GitHub, with the version described here available at https://github.com/sdss/idlspec2d/releases/tag/v6_0_4.

One of the most significant operational changes to the pipeline is a modification to reduce 500 fibers from a single BOSS spectrograph, rather then a combined reduction of 1000 fibers from the twin BOSS spectrographs. This change was made to support the move of the second BOSS spectrograph to LCO.

A number of smaller changes were implemented into the pipeline to both improve the ongoing reductions and facilitate future reductions of FPS/BOSS data. First, to improve the radial velocity precision of the extracted spectra, a refined arc lamp linelist (developed for the SDSS-IV MANGA project; Bundy et al. 2015) replaced the list from SDSS-IV, and skylines are utilized as a second-level calibrator. This second step required an adjustment to the outlier exclusion algorithm (designed to exclude cosmic rays) to preserve the peaks of the skylines by increasing the outlier rejection from 4σ to 50σ. This change, in some rare cases, might leave the remnant of a cosmic ray in the extracted spectra.

Second, we modified the coadding scheme of targets between exposure frames and the red/blue cameras; individual spectra are now grouped according to the R.A., decl. coordinates of the fiber(s) (or the SDSS-V CatalogID, if one exists), rather than on the combination of BOSS `PLATE-MJD-FIBERID`. The coadding scheme was also split into a two-step process, in which the red and blue data for each exposure are combined, and then the all-exposures red and blue data are combined to produce coadds for the full observation epoch. These changes were implemented to improve the S/N of the final reduced spectra.

Third, `v6_0_4` was modified to produce a special version of the DR18 SDSS-V/eFEDS spectra (Section 9.1.2), in addition to the existing standard pipeline results. This new combination includes every exposure of each target, regardless of the plate on which it was observed, to produce a set of spectra with maximum S/N. Both the standard pipeline, `v6_0_4`, and the `eFEDS` special coadds are available through the SAS[103] and the CAS, using SkyServer.[104] Future data releases will include variations of this special coadding routine, with the spectra included in each coadd chosen to fulfill the science requirements of the individual SDSS-V science programs.

Fourth, in addition to the changes in the reduction and coadding schemes, some modifications were made to the `spec1d` analysis part of `idlspec2d`. Utilizing 849 SDSS-IV RM quasars (Shen et al. 2019) and the weighted `empca` package (Bailey 2012, 2016), a new set of QSO principal component analysis (PCA) templates are used for PCA reconstruction and the redshift estimation of SDSS-V quasars. These new PCA templates are implemented with 10 eigenvectors instead of the four used in SDSS-I through SDSS-IV. To further support the MWM targets on the reduced eFEDs plates, on the observed MWM plates (not released in DR18, but documented here for completeness), and in future FPS observations, the Schlegel et al. (1998) model for dust extinction (see also Schlafly & Finkbeiner 2011) for MWM plates was replaced by the 3D Bayestar2015 dust map (Green et al. 2015) to properly account for differential dust extinction within the Milky Way. The package `pyXCSAO` (Kounkel 2022), a Python replication of the `xcsao` package (Tonry & Davis 1979; Kurtz et al. 1992; Mink & Kurtz 1998), was added as part of the `spec1d` analysis pipeline for cross-correlating a spectrum against template spectra of known

[103] https://dr18.sdss.org/sas/dr18/spectro/boss/redux
[104] http://casjobs.sdss.org/casjobs/

velocities. While this step is run for all targets, the results are only valid for stellar targets.

Finally, `idlspec2d`'s internal Python dependencies were updated to Python3, with the deprecation of Python 2.7. All of the changes described here improve either the data quality or spectroscopic classification success rates, or support the changes to the BOSS spectrograph for the SDSS-V plate program and FPS observations.

10.2. Migration to GitHub

For SDSS-V, all of the SDSS software has been moved to a GitHub organization,[105] from the previous Subversion private repository. With the exception of a few repositories containing proprietary code or credentials, all the code is publicly available under a BSD 3-Clause license. This includes most of the operational software, telescope and instrument control software, and data reduction pipelines.

10.3. MOS Software for DR19

The migration from plug plates to robotic fiber positioners in SDSS-V required the development of a suite of new software for targeting and operations. Although this software was not used for the acquisition of DR18 spectra (Section 9.1), it is currently in use for FPS operations and will become relevant for DR19 and future data releases. Here, we provide a short summary of FPS targeting and operations as a preview for those data releases. Further details are given in Sánchez-Gallego et al. (2020).

Combining the complex set of observing constraints and epoch cadences defined by the various target selection cartons into a set to observable FPS configurations requires the use of a specialized algorithm. `robostrategy` is the pipeline that takes the outputs of `target selection` and determines how the targets should be observed. It determines the cadence with which each field will be observed, which includes the number of epochs, the number of observations ("designs") per epoch, and the desired observing conditions for each design (including, e.g., the sky brightness conditions and hour angle). At the beginning of each night of observations, the software `roboscheduler` selects the optimal list of designs to be observed, based on cadence requirements and observing conditions, as well as on previous observations and achieved completions.

One major challenge of the SDSS robotic fiber positioner system derives from the fact that the patrol radius of each positioner overlaps with its neighboring ones. For a given set of target-to-positioner assignments defined in a `robostrategy` design, an algorithm named `Kaiju` (Sayres et al. 2021) provides a deterministic trajectory for each robotic positioner from a starting "folded" state, in which all robots are identically oriented, to the desired FPS configuration. `Kaiju` works following a reverse-solve method, in which it is considered simpler to calculate collision-free trajectories for each robot from a complex, deployed state to a lattice-like folded configuration. To create a path between two observable configurations, `Kaiju` calculates the reverse trajectories from each configuration to the folded state, and then applies the reverse trajectory. Following this approach, `Kaiju` is able to determine deadlock-free trajectories between any two physically reachable robot configurations in over 99% of cases (Sayres et al. 2021).

[105] https://github.com/sdss

Table 6
New or Updated VACs

Name	Reference(s)
SDSS-IV APOGEE-2	
BACCHUS Analysis of Weak Lines in APOGEE Spectra	Masseron et al. (2016); Hayes et al. (2022)
SDSS-IV MaNGA	
MaNGA Dwarf Galaxy Sample (MaNDala)	Cano-Díaz et al. (2022)
MaNGA Visual Morphology	Vázquez-Mata et al. (2022)
SDSS-V Black Hole Mapper	
eFEDS Spectral Compilation VAC	Section 11.2, A. Merloni et al. (2023, in preparation)

11. VACs

In addition to its fundamental data products, SDSS regularly includes "Value-added Catalogs" as part of its data releases.[106] These catalogs contain curated quantities from the data, usually to enable a specific scientific project, but are recognized as having value above and beyond the particular project for which the catalog was initially constructed.

11.1. SDSS-IV VACs

Table 6 includes the following VACs that rely on SDSS-IV data but have been updated or published for the first time after DR17:

BACCHUS Analysis of Weak Lines in APOGEE Spectra (BAWLAS). Weak-lined species in APOGEE spectra are challenging to measure and, in some cases, cannot be done with the standard ASPCAP pipeline. This VAC contains approximately 120,000 high-S/N giants from APOGEE DR17, for which Na, P, S, V, Cu, Ce, and Nd abundances and $^{12}C/^{13}C$ isotopic ratios have been derived with a specialized analysis (Hayes et al. 2022). An updated version of the Brussels Automatic Code for Characterizing High accUracy Spectra (BACCHUS; Masseron et al. 2016) was used in the derivation, along with ASPCAP fundamental stellar parameters, but also a dedicated set of individual line quality flags and a new prescription for identifying upper limits. Hayes et al. (2022) show how these newly derived abundances compare with literature values and provide examples of scientific projects that can be done with APOGEE and the new catalog, ranging from nuclear physics to Galactic chemical evolution and Milky Way population studies.

MaNGA Dwarf Galaxy Sample (MaNDala). This VAC presents properties for a sample of 125 dwarf galaxies ($M_\star < 10^9 M_\odot$) observed with MaNGA (Cano-Díaz et al. 2022), including newly derived photometric results, such as surface brightness, color, and position angle. Also measured are photometric profiles, along with Sérsic fits and new estimations of effective radii, for all of the galaxies, using DECaLS DR9 g, r, z images (Dey et al. 2019). Analysis of the MaNGA data provides estimates of $M_\star$, star formation rates, metallicities, ages, and other properties, using MaNGA Pipe3D data products (Sánchez et al. 2016, 2018). Details of the

[106] https://www.sdss.org/dr18/data_access/value-added-catalogs/

MaNDala sample and analysis are given in Cano-Díaz et al. (2022).

MaNGA Visual Morphology. This is an update of a VAC, originally released in DR17 (Section 5.5.2 in Abdurro'uf et al. 2022), which contains visual morphological classifications for MaNGA galaxies based on SDSS and DECaLs (Dey et al. 2019) images. See Vázquez-Mata et al. (2022) for details.

11.2. SDSS-V VACs

The only VAC in DR18 derived from SDSS-V data is that providing supplementary properties for the eFEDS spectroscopic data set (Section 7.3).

This VAC provides updated redshift and classification information for optical counterparts to X-ray sources detected in the eFEDS field (Brunner et al. 2022; Salvato et al. 2022). We update the spectroscopic redshifts and classifications (with respect to Salvato et al. 2022) using a large spectroscopic compilation dominated by SDSS optical spectroscopy. Most importantly, we include new information from the 37 dedicated SDSS-V/eFEDS plates, described in detail in Section 9.1. We combine automated redshifts and classifications, derived from the BOSS `idlspec1d` pipeline (Section 10.1), with an extensive set of visual inspections, which together increase the reliability and completeness of the spectroscopic coverage.

The VAC includes three separate catalogs:

1. `eFEDS_Main_speccomp`—an update of redshift and classification information for the eFEDS Main (0.2–2.3 keV selection) source counterparts catalog;
2. `eFEDS_Hard_speccomp`—an update of redshift and classification information for the eFEDS Hard-band (2.3–5 keV selection) source counterparts catalog; and
3. `eFEDS_SDSSV_spec_results`—a catalog of spectroscopic redshifts and classifications derived solely from the SDSS-V/eFEDS plate data set, supplemented by the results of an extensive visual inspection process.

A full description of this VAC will be provided in A. Merloni et al. (2023, in preparation).

12. Summary and DR19 Preview

In this paper, we have described the contents of the first data release of SDSS-V, which is also the eighteenth data release of the SDSS family of surveys. DR18 contains extensive targeting information for the MWM (Section 6) and BHM (Section 7), both compiled target catalogs, and the selection algorithms for their numerous scientific programs. Nearly ∼25,000 new spectra for X-ray sources in the eROSITA eFEDS field are also made available, along with substantial supplementary information, including improved redshifts and classifications based on visual inspections. Significant improvements to the BOSS data spectral reduction pipelines were also made, in support of these and other optical spectra.

The next SDSS-V data release will be DR19, anticipated in 2024. This will contain the first MWM spectra and derived stellar parameters and abundances, and the first spectra and derived properties from the primary BHM programs. Updates to the targeting catalogs presented in this paper will also be made available, along with updated simulations that predict the number of candidate targets in a carton that are likely be to observed. Additional tools for accessing and exploring all of the data are also anticipated to be released.

The capabilities and flexibility of SDSS-V make it unique among recent, ongoing, or imminent surveys, with well-vetted hardware, software, and collaboration infrastructure serving as the foundation for new innovations in all three areas. SDSS-V looks forward to expanding the SDSS legacy with high-quality, optical IFU data of 1000 $\deg^2$ and optical + IR spectra of millions of sources across the entire sky.

Acknowledgments

The documentation workshop for DR18 ("DocuLlama") was held virtually in 2022 September, organized by Anne-Marie Weijmans and Gail Zasowski. This event was the main venue for the documentation of DR18, including significant progress on this paper and the website, and it was attended by Scott Anderson, Joel Brownstein, Joleen Carlberg, Niall Deacon, Nathan De Lee, John Donor, Tom Dwelly, Keith Hawkins, Jennifer Johnson, Sean Morrison, Jordan Raddick, José Sánchez-Gallego, Diogo Souto, Taylor Spoo, Ani Thakar, Nick Troup, Anne-Marie Weijmans, Gail Zasowski, William Zhang, three llamas, and an elderly goat named Nibblets.

Funding for the Sloan Digital Sky Survey V has been provided by the Alfred P. Sloan Foundation, the Heising-Simons Foundation, the National Science Foundation, and the Participating Institutions. SDSS acknowledges support and resources from the Center for High-Performance Computing at the University of Utah. The SDSS website is www.sdss.org.

SDSS is managed by the Astrophysical Research Consortium for the Participating Institutions of the SDSS Collaboration, including the Carnegie Institution for Science, Chilean National Time Allocation Committee (CNTAC) ratified researchers, the Gotham Participation Group, Harvard University, The Johns Hopkins University, L'Ecole polytechnique fédérale de Lausanne (EPFL), Leibniz-Institut für Astrophysik Potsdam (AIP), Max-Planck-Institut für Astronomie (MPIA Heidelberg), Max-Planck-Institut für Extraterrestrische Physik (MPE), Nanjing University, National Astronomical Observatories of China (NAOC), New Mexico State University, The Ohio State University, Pennsylvania State University, Smithsonian Astrophysical Observatory, Space Telescope Science Institute (STScI), the Stellar Astrophysics Participation Group, Universidad Nacional Autónoma de México, University of Arizona, University of Colorado Boulder, University of Illinois at Urbana-Champaign, University of Toronto, University of Utah, University of Virginia, and Yale University.

The Pan-STARRS1 Surveys (PS1) and the PS1 public science archive have been made possible through contributions by the Institute for Astronomy, the University of Hawaii, the Pan-STARRS Project Office, the Max Planck Society and its participating institutes, the Max Planck Institute for Astronomy, Heidelberg and the Max Planck Institute for Extraterrestrial Physics, Garching, The Johns Hopkins University, Durham University, the University of Edinburgh, the Queen's University Belfast, the Harvard–Smithsonian Center for Astrophysics, the Las Cumbres Observatory Global Telescope Network Incorporated, the National Central University of Taiwan, the Space Telescope Science Institute, the National Aeronautics and Space Administration under grant No. NNX08AR22G, issued through the Planetary Science Division of the NASA Science Mission Directorate, the National Science Foundation grant No. AST-1238877, the University of Maryland, Eotvos Lorand University (ELTE), the Los

Alamos National Laboratory, and the Gordon and Betty Moore Foundation.

This publication makes use of data products from the Two Micron All Sky Survey, which is a joint project of the University of Massachusetts and the Infrared Processing and Analysis Center/California Institute of Technology, funded by the National Aeronautics and Space Administration and the National Science Foundation.

This work is based in part on observations made with the Spitzer Space Telescope, which was operated by the Jet Propulsion Laboratory, California Institute of Technology, under a contract with NASA.

This publication makes use of data products from the Wide-field Infrared Survey Explorer, which is a joint project of the University of California, Los Angeles, and the Jet Propulsion Laboratory/California Institute of Technology, funded by the National Aeronautics and Space Administration.

This work presents results from the European Space Agency (ESA) space mission Gaia. Gaia data are being processed by the Gaia Data Processing and Analysis Consortium (DPAC). Funding for the DPAC is provided by national institutions, in particular the institutions participating in the Gaia MultiLateral Agreement (MLA). The Gaia mission website is https://www.cosmos.esa.int/gaia. The Gaia archive website is https://archives.esac.esa.int/gaia.

The Legacy Surveys consist of three individual and complementary projects: the Dark Energy Camera Legacy Survey (DECaLS; Proposal ID #2014B-0404; PIs: David Schlegel and Arjun Dey), the Beijing-Arizona Sky Survey (BASS; NOAO Prop. ID #2015A-0801; PIs: Zhou Xu and Xiaohui Fan), and the Mayall *z*-band Legacy Survey (MzLS; Prop. ID #2016A-0453; PI: Arjun Dey). DECaLS, BASS, and MzLS together include data obtained, respectively, at the Blanco telescope, Cerro Tololo Inter-American Observatory, NSF's NOIRLab; the Bok telescope, Steward Observatory, University of Arizona; and the Mayall telescope, Kitt Peak National Observatory, NOIRLab. Pipeline processing and analyses of the data were supported by NOIRLab and the Lawrence Berkeley National Laboratory (LBNL). The Legacy Surveys project is honored to be permitted to conduct astronomical research on Iolkam Duâag (Kitt Peak), a mountain with particular significance to the Tohono Oâodham Nation.

NOIRLab is operated by the Association of Universities for Research in Astronomy (AURA) under a cooperative agreement with the National Science Foundation. LBNL is managed by the Regents of the University of California under contract to the U.S. Department of Energy.

This project used data obtained with the Dark Energy Camera (DECam), which was constructed by the Dark Energy Survey (DES) collaboration. Funding for the DES Projects has been provided by the U.S. Department of Energy, the U.S. National Science Foundation, the Ministry of Science and Education of Spain, the Science and Technology Facilities Council of the United Kingdom, the Higher Education Funding Council for England, the National Center for Supercomputing Applications at the University of Illinois at Urbana-Champaign, the Kavli Institute of Cosmological Physics at the University of Chicago, the Center for Cosmology and Astro-Particle Physics at the Ohio State University, the Mitchell Institute for Fundamental Physics and Astronomy at Texas A&M University, Financiadora de Estudos e Projetos, Fundacao Carlos Chagas Filho de Amparo, Financiadora de Estudos e Projetos, Fundacao Carlos Chagas Filho de Amparo a Pesquisa do Estado do Rio de Janeiro, Conselho Nacional de Desenvolvimento Cientifico e Tecnologico and the Ministerio da Ciencia, Tecnologia e Inovacao, the Deutsche Forschungsgemeinschaft, and the Collaborating Institutions in the Dark Energy Survey. The Collaborating Institutions are Argonne National Laboratory, the University of California at Santa Cruz, the University of Cambridge, Centro de Investigaciones Energeticas, Medioambientales y Tecnologicas-Madrid, the University of Chicago, University College London, the DES-Brazil Consortium, the University of Edinburgh, the Eidgenossische Technische Hochschule (ETH) Zurich, Fermi National Accelerator Laboratory, the University of Illinois at Urbana-Champaign, the Institut de Ciencies de l'Espai (IEEC/CSIC), the Institut de Fisica d'Altes Energies, Lawrence Berkeley National Laboratory, the Ludwig Maximilians Universitat Munchen and the associated Excellence Cluster Universe, the University of Michigan, NSF's NOIRLab, the University of Nottingham, the Ohio State University, the University of Pennsylvania, the University of Portsmouth, SLAC National Accelerator Laboratory, Stanford University, the University of Sussex, and Texas A&M University.

BASS is a key project of the Telescope Access Program (TAP), which has been funded by the National Astronomical Observatories of China, the Chinese Academy of Sciences (the Strategic Priority Research Program "The Emergence of Cosmological Structures," grant #XDB09000000), and the Special Fund for Astronomy from the Ministry of Finance. BASS is also supported by the External Cooperation Program of Chinese Academy of Sciences (grant #114A11KYSB20160057) and the Chinese National Natural Science Foundation (grants #12120101003 and #11433005).

The Legacy Survey team makes use of data products from the Near-Earth Object Wide-field Infrared Survey Explorer (NEOWISE), which is a project of the Jet Propulsion Laboratory/California Institute of Technology. NEOWISE is funded by the National Aeronautics and Space Administration.

The Legacy Surveys imaging of the DESI footprint is supported by the Director, Office of Science, Office of High Energy Physics of the U.S. Department of Energy, under Contract No. DE-AC02-05CH1123; by the National Energy Research Scientific Computing Center, a DOE Office of Science User Facility under the same contract; and by the U.S. National Science Foundation, Division of Astronomical Sciences, under Contract No. AST-0950945 to NOAO.

The national facility capability for SkyMapper has been funded through ARC LIEF grant LE130100104 from the Australian Research Council, awarded to the University of Sydney, the Australian National University, Swinburne University of Technology, the University of Queensland, the University of Western Australia, the University of Melbourne, Curtin University of Technology, Monash University, and the Australian Astronomical Observatory. SkyMapper is owned and operated by The Australian National University's Research School of Astronomy and Astrophysics. The survey data were processed and provided by the SkyMapper Team at ANU. The SkyMapper node of the All-Sky Virtual Observatory (ASVO) is hosted at the National Computational Infrastructure (NCI). The development and support of the SkyMapper node of the ASVO has been funded in part by Astronomy Australia Limited (AAL) and the Australian Government through the Commonwealth's Education Investment Fund (EIF) and

National Collaborative Research Infrastructure Strategy (NCRIS), particularly the National eResearch Collaboration Tools and Resources (NeCTAR) and the Australian National Data Service (ANDS) Projects.

This paper includes data collected by the TESS mission. Funding for the TESS mission is provided by NASA's Science Mission Directorate.

We acknowledge the use of public data from the Swift data archive.

Based on observations obtained with XMM-Newton, an ESA science mission with instruments and contributions directly funded by ESA Member States and NASA.

This research has made use of NASA's Astrophysics Data System Bibliographic Services.

Facilities: Du Pont (APOGEE), Sloan, Spitzer, WISE, CTIO:2MASS, Gaia, GALEX, PS1, TESS, Swift, CXO, XMM, eROSITA.

Appendix A
Details of MWM `v0.5.3` Target Cartons

In this appendix, we provide the detailed criteria used to select the MWM target cartons that are being released as part of SDSS DR18. We remind the reader that inclusion in a carton means that the target fits the carton selection criteria, not that it is guaranteed to be observed.

For each target carton, we provide the following information: the "Description of selection criteria" provides a short summary of the carton selection in human-readable terms. It also includes a list of the limits in color, magnitude, parallax, and other quantities applied to the carton's target candidates.[107] "Data sources" gives the catalogs from which these quantities are drawn. In "Target priority options," we indicate which priority is given to targets in this carton for observing; smaller priorities are more likely to be assigned fibers. The "Cadence options" describe which exposure time requirement(s) are assigned to sources in the carton. See Table 3 for each carton's instrument (BOSS or APOGEE) and the number of candidate targets that meet the carton's selection criteria.

A.1. manual_mwm_tess_ob

Description of selection criteria: a system selected from the Ijspeert et al. (2021) catalog of massive EBs in TESS. The systems chosen were in the TESS continuous viewing zones (CVZs) and had TESS lightcurves that show pronounced eclipses and intrinsic variability.
Data sources: Ijspeert et al. (2021).
Target priority options: 2200.
Cadence options: bright_8x1, bright_8x2, bright_8x4.

A.2. manual_nsbh_apogee

Description of selection criteria: list of targets drawn from public and private catalogs of binary systems with known or suspected black holes or neutron stars, such as X-ray binaries and pulsars. Must have a valid 2MASS H magnitude.
Data sources: 2MASS PSC (H), Gaia DR2 *(G).*
Target priority options: 1400.
Cadence options: bright_1x1.

A.3. manual_nsbh_boss

Description of selection criteria: list of targets drawn from public and private catalogs of binary systems with known or suspected black holes or neutron stars, such as X-ray binaries and pulsars. Must have a valid Gaia DR2 G magnitude.
Data sources: 2MASS PSC (H), Gaia DR2 *(G).*
Target priority options: 1400.
Cadence options: bright_1x1, dark_1x2.

A.4. mwm_cb_300pc_apogee

Description of selection criteria: bright compact binary candidates within 300 pc.
1. $(FUV - 5\log_{10}(r_{\rm est}/10)) > 14(FUV - NUV) - 46$;
2. $r_{\rm est} < 300$ pc;
3. $H < 11$.

Data sources: Bailer-Jones et al. (2018) distance catalog ($r_{\rm est}$), 2MASS PSC (H), GALEX (FUV, NUV).
Target priority options: 1400.
Cadence options: bright_1x1.

A.5. mwm_cb_300pc_boss

Description of selection criteria: faint compact binary candidates within 300 pc.
1. $(FUV - 5\log_{10}(r_{\rm est}/10)) > 14(FUV - NUV) - 46$;
2. $r_{\rm est} < 300$ pc.

Data sources: Bailer-Jones et al. (2018) distance catalog ($r_{\rm est}$), GALEX (FUV, NUV).
Target priority options: 1400.
Cadence options: bright_2x1, dark_2x1.

A.6. mwm_cb_cvcandidates_apogee

Description of selection criteria: bright AAVSO cataclysmic variables.
1. Target in `mos_cataclysmic_variables` table;
2. $H < 11$.

Data sources: 2MASS PSC (H).
Target priority options: 1400.
Cadence options: bright_1x1.

A.7. mwm_cb_cvcandidates_boss

Description of selection criteria: faint AAVSO cataclysmic variables.
1. Target in `mos_cataclysmic_variables` table;
2. $H \geqslant 11$.

Data sources: 2MASS PSC (H).
Target priority options: 1400.
Cadence options: bright_2x1, dark_2x1.

A.8. mwm_cb_gaiagalex_apogee

Description of selection criteria: bright compact binary candidates using Gaia G and GALEX FUV color cut.

[107] We note that the selection descriptions here describe the cuts made by the SDSS team. In some cases, targets were drawn from external catalogs, which may have undergone additional selection criteria prior to inclusion in the MWM survey. We refer the reader to the cited papers for more details on those selections.

1. $\varpi/\sigma_{\varpi} > 3$;
2. $G < 20$;
3. $FUV + 5\log_{10}(\varpi/1000) + 5 > 1.5 + 1.28(FUV - G)$;
4. $H < 11$.

Data sources: Gaia DR2 (G, ϖ, σ_{ϖ}), 2MASS PSC (H), GALEX (FUV).
Target priority options: 1400.
Cadence options: bright_1x1.

A.9. mwm_cb_gaiagalex_boss

Description of selection criteria: faint compact binary candidates using Gaia G and GALEX FUV color cut.

1. $\varpi/\sigma_{\varpi} > 3$;
2. $G < 20$;
3. $FUV + 5\log_{10}(\varpi/1000) + 5 > 1.5 + 1.28(FUV - G)$;
4. $H \geqslant 11$.

Data sources: Gaia DR2 (G, ϖ, σ_{ϖ}), 2MASS PSC (H), GALEX (FUV).
Target priority options: 1400.
Cadence options: bright_2x1, dark_2x1.

A.10. mwm_cb_uvex1

Description of selection criteria: Gaia and GALEX cross-match, keeping the nearest match within 5″ and removing objects with small proper motion and parallax. Color cuts utilize both FUV and NUV magnitudes. "AB" indicates magnitudes transformed to AB magnitudes, and M_G is the Gaia absolute magnitude calculated with $r_{\rm est}$.

1. $r_{\rm lo} \leqslant 1500$;
2. g_vis_per >5;
3. Neither of the following two conditions are met:
   (a) $(\log_{10}(\mu/\sigma_{\mu}) < 0.301)$ AND $(\varpi/\sigma_{\varpi} > -1.4996\log_{10}(\mu/\sigma_{\mu}) - 4.05)$ AND $(\varpi/\sigma_{\varpi} < 1.4995\log_{10}(\mu/\sigma_{\mu}) + 4.05)$;
   (b) $(\log_{10}(\mu/\sigma_{\mu}) - 0.301)^2/0.39794^2 + (\varpi/\sigma_{\varpi})^2/4.5^2 \leqslant 1$;
4. $NUV > -100$;
5. $FUV > -100$;
6. $\sigma_{\rm NUV} < 0.2$;
7. $\sigma_{\rm FUV} < 0.2$;
8. $M_G > 4.09$ OR $M_G > 4.5457(G_{\rm BP} - G_{\rm RP}) + 4.0457$;
9. $M_G > -1.11749253 \times 10^{-3}(FUV - NUV)^3 + 1.53748615 \times 10^{-2}(FUV - NUV)^2 + 3.66419895 \times 10^{-1}(FUV - NUV) + 2.20026639)$;
10. $(FUV - G_{\rm AB}) < 6.08$ OR $[(FUV - G_{\rm AB}) < 11.82(G_{\rm BP,AB} - G_{\rm RP,AB}) + 2.58$ AND $(FUV - G_{\rm AB}) < -0.79(G_{\rm BP,AB} - G_{\rm RP,AB} + 9.21)]$.

Data sources: Gaia DR2 (M_G, $G_{\rm BP}$, $G_{\rm RP}$, μ, $\sigma_m u$, ϖ, σ_{ϖ}, $r_{\rm lo}$, g_vis_per), Bailer-Jones et al. (2018) distance catalog ($r_{\rm est}$), GALEX (NUV, FUV, $\sigma_{\rm NUV}$, $\sigma_{\rm FUV}$).
Target priority options: 1400.
Cadence options: bright_1x1, dark_1x2, dark_1x3.

A.11. mwm_cb_uvex2

Description of selection criteria: Gaia and GALEX cross-match, keeping the nearest match within 5″ and removing objects with small proper motion and parallax. Color cuts utilize only NUV magnitudes. "AB" indicates magnitudes transformed to AB magnitudes, and M_G is Gaia absolute magnitude calculated with $r_{\rm est}$.

1. $r_{\rm lo} \leqslant 1500$;
2. g_vis_per >5;
3. Neither of the following two conditions are met:
   (a) $(\log_{10}(\mu/\sigma_{\mu}) < 0.301)$ AND $(\varpi/\sigma_{\varpi} > -1.4996\log_{10}(\mu/\sigma_{\mu}) - 4.05)$ AND $(\varpi/\sigma_{\varpi} < 1.4995\log_{10}(\mu/\sigma_{\mu}) + 4.05)$;
   (b) $(\log_{10}(\mu/\sigma_{\mu}) - 0.301)^2/0.39794^2 + (\varpi/\sigma_{\varpi})^2/4.5^2 \leqslant 1$;
4. $NUV > -100$;
5. $\sigma_{\rm NUV} < 0.2$;
6. $M_G > 4.09$ OR $M_G > 4.5457(G_{\rm BP} - G_{\rm RP}) + 4.0457$;
7. $(NUV - G_{\rm AB} < 2.25)$ OR $[(NUV - G_{\rm AB} < 6.725(G_{\rm BP,AB} - G_{\rm RP,AB}) - 1.735)$ AND $(NUV - G_{\rm AB} < -0.983(G_{\rm BP,AB} - G_{\rm RP,AB} + 8.24)]$.

Data sources: Gaia DR2 (M_G, $G_{\rm AB}$, $G_{\rm BP}$, $G_{\rm BP,AB}$, $G_{\rm RP}$, $G_{\rm RP,AB}$, μ, $\sigma_m u$, ϖ, σ_{ϖ}, g_vis_per), Bailer-Jones et al. (2018) distance catalog ($r_{\rm lo}$, $r_{\rm est}$), GALEX (NUV, $\sigma_{\rm NUV}$).
Target priority options: 1400.
Cadence options: bright_1x1, dark_1x2, dark_1x3.

A.12. mwm_cb_uvex3

Description of selection criteria: Gaia and XMM-Newton Optical Monitor SUSS Catalog crossmatch, keeping the nearest match within 3″ and removing objects with small proper motion and parallax. Color and quality cuts utilize the XMM UVM2 band.

1. $r_{\rm lo} \leqslant 1500$;
2. g_vis_per >5;
3. Neither of the following two conditions are met:
   (a) $(\log_{10}(\mu/\sigma_{\mu}) < 0.301)$ AND $(\varpi/\sigma_{\varpi} > -1.4996\log_{10}(\mu/\sigma_{\mu}) - 4.05)$ AND $(\varpi/\sigma_{\varpi} < 1.4995\log_{10}(\mu/\sigma_{\mu}) + 4.05)$;
   (b) $(\log_{10}(\mu/\sigma_{\mu}) - 0.301)^2/0.39794^2 + (\varpi/\sigma_{\varpi})^2/4.5^2 \leqslant 1$;
4. The following conditions are all NOT met:
   (a) qflag bit 1, 7, 8, or 9 is set;
   (b) qflag bit 2 or 3 is set AND UVM2 $_{\rm signif} < 10$;
5. $M_G > 4.09$ OR $M_G > 4.5457(G_{\rm BP} - G_{\rm RP}) + 4.0457$;
6. $\rm UVM2_{AB} - G_{AB} < 2.25$ OR $[(\rm UVM2_{AB} - G_{AB} < 6)$ AND $(\rm UVM2_{AB} - G_{AB} < 5.57377(G_{BP,AB} - G_{RP,AB}) + 0.2049)]$.

Data sources: Gaia DR2 (M_G, $G_{\rm AB}$, $G_{\rm BP}$, $G_{\rm BP,AB}$, $G_{\rm RP}$, $G_{\rm RP,AB}$, μ, $\sigma_m u$, ϖ, σ_{ϖ}, g_vis_per), Bailer-Jones et al. (2018) distance catalog ($r_{\rm lo}$, $r_{\rm est}$), XMM OM SUSS v4.1($\rm UVM2_{AB}$, UVM2 $_{\rm signif}$, qflag).
Target priority options: 1400.
Cadence options: bright_1x1, dark_1x2, dark_1x3.

A.13. mwm_cb_uvex4

Description of selection criteria: Gaia and Swift UVOT Catalog crossmatch, keeping the nearest match within 3″ and removing objects with small proper motion and parallax. Color cuts utilize the UVW2 band, and quality cuts utilize both UVW2 and UVW1.

1. $r_{\rm lo} \leqslant 1500$;
2. g_vis_per >5;
3. $\rm UVW1_{AB} > -100$;
4. $\rm UVW2_{AB} > -100$;

5. Neither of the following two conditions are met:
   (a) $(\log_{10}(\mu/\sigma_\mu) < 0.301)$ AND $(\varpi/\sigma_\varpi > -1.4996 \log_{10}(\mu/\sigma_\mu) - 4.05)$ AND $(\varpi/\sigma_\varpi < 1.4995 \log_{10}(\mu/\sigma_\mu) + 4.05)$;
   (b) $(\log_{10}(\mu/\sigma_\mu) - 0.301)^2/0.39794^2 + (\varpi/\sigma_\varpi)^2/4.5^2 \leqslant 1$;
6. The following conditions are all NOT met:
   (a) qflag bit 0 or 6 is set;
   (b) qflag bit 1, 2, or 5 is set AND UVW2 $_{\rm signif} < 10$;
7. $M_G > 4.09$ OR $M_G > 4.5457(G_{\rm BP} - G_{\rm RP}) + 4.0457$;
8. $\rm UVW2_{AB} - G_{AB} < 2.25$ OR [$(\rm UVW2_{AB} - G_{AB} < 6)$ AND $(\rm UVW2_{AB} - G_{AB} < 5.57377((G_{BP,AB} - G_{RP,AB}) + 0.2049)$].

Data sources: Gaia DR2 (M_G, $G_{\rm AB}$, $G_{\rm BP}$, $G_{\rm BP,AB}$, $G_{\rm RP}$, $G_{\rm RP,AB}$, μ, σ_μ, ϖ, σ_ϖ, g_vis_per), Bailer-Jones et al. (2018) distance catalog ($r_{\rm lo}$, $r_{\rm est}$), Swift UVOT($\rm UVW1_{AB}$, $\rm UVW2_{AB}$, UVW2 $_{\rm signif}$, qflag2).
Target priority options: 1400.
Cadence options: bright_1x1, dark_1x2, dark_1x3.

A.14. mwm_cb_uvex5

Description of selection criteria: Gaia and GALEX cross-match, keeping the nearest match within 5″ and removing objects with small proper motion and parallax. Only objects with FUV and NUV detections are kept, but the color cuts utilize only optical colors and magnitudes. Here, the expected Gaia Main Sequence (GMS) locus is defined by $\rm GMS = 0.00206868742x^6 + 0.0401594518x^5 - 0.842512410x^4 + 4.89384979x^3 - 12.3826637x^2 + 17.0197205x - 3.19987835$, where $x = G - G_{\rm RP}$. M_G is the Gaia absolute magnitude calculated with $r_{\rm est}$.

1. $r_{\rm lo} \leqslant 1500$;
2. g_vis_per >5;
3. Neither of the following two conditions are met:
   (a) $(\log_{10}(\mu/\sigma_\mu) < 0.301)$ AND $(\varpi/\sigma_\varpi > -1.4996 \log_{10}(\mu/\sigma_\mu) - 4.05)$ AND $(\varpi/\sigma_\varpi < 1.4995 \log_{10}(\mu/\sigma_\mu) + 4.05)$;
   (b) $(\log_{10}(\mu/\sigma_\mu) - 0.301)^2/0.39794^2 + (\varpi/\sigma_\varpi)^2/4.5^2 \leqslant 1$;
4. $NUV > -100$;
5. $FUV > -100$;
6. $\sigma_{\rm NUV} < 0.2$;
7. $\sigma_{\rm FUV} < 0.2$;
8. $M_G > 4.0866$;
9. $H < 15$;
10. $|\rm GMS - M_G| \leqslant 0.5$;
11. $r_{\rm est} < 0.51 \times 10^{0.2291\,G}$.

Data sources: Gaia DR2 (M_G, $G_{\rm RP}$, μ, σ_μ, ϖ, σ_ϖ, $r_{\rm lo}$, g_vis_per), Bailer-Jones et al. (2018) distance catalog ($r_{\rm est}$), GALEX (NUV, FUV, $\sigma_{\rm NUV}$, $\sigma_{\rm FUV}$), 2MASS PSC (H).
Target priority options: 1400.
Cadence options: bright_1x1, dark_1x2, dark_1x3.

A.15. mwm_dust_core

Description of selection criteria: the dust carton selects bright, nearby, midplane giants with the same quality cuts as GG to supplement GG targets in regions of high reddening. The galaxy within 5 kpc and with $|z| < 0.2$ kpc is divided into 100 $\rm pc^3$ regions ("voxels"), and the number of GG targets in each voxel are counted. In voxels with fewer than 10 GG stars, $10 - n_{\rm GG}$ stars are selected for inclusion in this carton.

1. $\sigma_\varpi/\varpi < 0.2$;
2. $1/\varpi < 5$ kpc;
3. $|z| < 0.2$ kpc (using ϖ-based distances);
4. $M_K < 2.6$, adopting $A_K = 0.918(H - 4.5)$;
5. $(J - K)_0 > 0.5$, where $E(J - K) = 1.5A_K$;
6. $H < 11.2$;
7. gal_contam==0;
8. cc_flg==0;
9. 0 < rd_flag < = 3;
10. ph_qual flag is A or B.

Data sources: Gaia DR2 (ϖ, σ_ϖ), 2MASS PSC (J, H, K, gal_contam, cc_flag, rd_flag, ph_qual).
Target priority options: 2720.
Cadence options: bright_1x1.

A.16. mwm_erosita_compact_gen

Description of selection criteria: optical counterpart in Gaia DR2 to a candidate compact binary detected by eROSITA, chosen as the possible counterpart with the smallest angular separation.

1. $G > 16$;
2. $L > 8$ in at least one of the three eROSITA energy bands;
3. Detections in three eROSITA energy bands;
4. $\log(f_x/f_{\rm opt}) < 2.7$;
5. radec_err > 0 and s/radec_err < 2.1, where s is the separation between the Gaia and eROSITA sources;
6. Neither of the following two conditions are met:
   (a) $(\log_{10}(\mu/\sigma_\mu) < 0.301)$ AND $(\varpi/\sigma_\varpi > -1.4996 \log_{10}(\mu/\sigma_\mu) - 4.05)$ AND $(\varpi/\sigma_\varpi < 1.4995 \log_{10}(\mu/\sigma_\mu) + 4.05)$;
   (b) $(\log_{10}(\mu/\sigma_\mu) - 0.301)^2/0.39794^2 + (\varpi/\sigma_\varpi)^2/4.5^2 \leqslant 1$;
7. Is the optical source that meets the above criteria with the smallest separation s.

Data sources: eROSITA (f_x, L, radec_err), Gaia DR2 (G, μ, σ_μ, ϖ, σ_ϖ, f_{opt} (from G)).
Target priority options: 1910, 2400.
Cadence options: bright_1x1, dark_1x2, dark_1x3.

A.17. mwm_erosita_compact_var

Description of selection criteria: optical counterpart to a candidate compact binary detected by eROSITA, chosen as the possible counterpart with the largest variability in Gaia DR2.

1. $G > 16$;
2. $L > 8$ in at least one of the three eROSITA energy bands;
3. Detections in three eROSITA energy bands;
4. $\log(f_x/f_{\rm opt}) < 2.7$;
5. radec_err > 0 and s/radec_err < 2.1, where s is the separation between the Gaia and eROSITA sources;
6. Neither of the following two conditions are met:
   (a) $(\log_{10}(\mu/\sigma_\mu) < 0.301)$ AND $(\varpi/\sigma_\varpi > -1.4996 \log_{10}(\mu/\sigma_\mu) - 4.05)$ AND $(\varpi/\sigma_\varpi < 1.4995 \log_{10}(\mu/\sigma_\mu) + 4.05)$;
   (b) $(\log_{10}(\mu/\sigma_\mu) - 0.301)^2/0.39794^2 + (\varpi/\sigma_\varpi)^2/4.5^2 \leqslant 1$;

7. Is the optical source that meets the above criteria with the largest variability $\log_{10}\left(\left(\frac{\text{phot\_g\_n\_obs}}{\text{phot\_g\_mean\_flux\_over\_error}}\right)^{1/2}\right)$.

Data sources: eROSITA (f_x, L, radec_err), Gaia DR2 (G, μ, $\sigma_m u$, ϖ, σ_ϖ, $f_{\rm opt}$ (from G), phot_g_n_obs, phot_g_mean_flux_over_error).
Target priority options: 1900, 2400.
Cadence options: bright_1x1, dark_1x2, dark_1x3.

A.18. mwm_erosita_stars

Description of selection criteria: optical or IR counterpart to a candidate stellar source detected by eROSITA. Counterpart identified using the techniques and data described in Freund et al. (2022).
Data sources: eROSITA, Gaia DR2, 2MASS PSC.
Target priority options: 1920, 2400.
Cadence options: bright_1x1, dark_1x2, dark_1x3.

A.19. mwm_galactic_core

Description of selection criteria: a simple color–magnitude cut effectively targets luminous cool giant stars (median($\log g$) $\sim$ 1.0–1.5) with little (<6%) contamination from dwarf stars.
1. $H < 11$;
2. $G - H > 3.5$ or Gaia nondetection;
3. gal_contam==0;
4. cc_flg==0;
5. $0 <$ rd_flag $<= 3$;
6. ph_qual flag is A or B.

Data sources: Gaia DR2 (G), 2MASS PSC (H, gal_contam, cc_flg, rd_flag, ph_qual).
Target priority options: 2710.
Cadence options: bright_1x1.

A.20. mwm_legacy_ir2opt

Description of selection criteria: this carton selects all bright Gaia objects that are in APOGEE DR16 (in particular, the `sdss_apogeeallstarmerge_r13` file) to be observed with BOSS.
1. $3 < G < 18$;
2. $G_{\rm BP} > 13$;
3. $G_{\rm RP} > 13$.

Data sources: Gaia DR2 (G, $G_{\rm BP}$, $G_{\rm RP}$), APOGEE DR16.
Target priority options: 6100.
Cadence options: bright_1x1.

A.21. mwm_ob_cepheids

Description of selection criteria: catalog of cepheids compiled by Inno et al. (2021).
Data sources: Inno et al. (2021).
Target priority options: 2910.
Cadence options: bright_3x1.

A.22. mwm_ob_core

Description of selection criteria: this carton uses color and magnitude cuts to select hot, young stars.
1. $\varpi < 10^{(10-K-0.61)/5)}$;
2. $G < 16$;
3. $J - K - 0.25(G - K) < 0.10$;
4. $J - K - 0.25(G - K) > -0.30$;
5. $J - H < 0.15(G - K) + 0.05$;
6. $J - H > 0.15(G - K) - 0.15$;
7. $J - K < 0.23(G - K) + 0.03$;
8. $G > 2(G - K) + 3.0$;
9. Crossmatch separation $1''$;
10. RUWE < 1.4.

Data sources: Gaia DR2 (G, ϖ, RUWE), 2MASS PSC (*J, H, K*).
Target priority options: 2910.
Cadence options: bright_3x1.

A.23. mwm_rv_long_fps

Description of selection criteria: this carton selects stars previously observed at least three times with the APOGEE instrument if it was targeted as part of the main APOGEE sample or the APOGEE-2 binary program.
1. Presence in `sdss_apogeeallstarmerge_r13` file (previously observed with APOGEE-1 and/or APOGEE-2);
2. APOGEE number of visits $\geqslant$3;
3. $H < 11.5$;
4. APOGEE TARGFLAGS includes one of the following: APOGEE_SHORT, APOGEE_INTERMEDIATE, APOGEE_LONG, APOGEE2_BIN;
5. Gaia-based distance.

Data sources: APOGEE, 2MASS PSC (H), Gaia DR 2.
Target priority options: 2510, 2520, 2530, 2540.
*Cadence options:*bright_6x1 bright_6x2, bright_9x1, bright_9x2, bright_12x1, bright_12x2, bright_15x1, bright_15x2.

A.24. mwm_rv_short_fps

Description of selection criteria: this carton selects stars that were never previously observed with APOGEE and applies the same color and quality cuts as the main APOGEE surveys.
1. $H < 10.8$;
2. $J - K_s - (1.5 \cdot 0.918(H - W2 - 0.05)) >= 0.05$;
3. $J\_msigcom$, $H\_msigcom$, $K_s\_msigcom \leqslant 0.1$;
4. $W2\_sigmpro \leqslant 0.1$;
5. 2MASS ph_qual any of the following: AAA, AAB, ABA, BAA, ABB, BAB, BBA, BBB;
6. 2MASS gal_contam=0;
7. 2MASS cc_flg=0;
8. 2MASS rd_flg any of the following: 111, 112, 121, 211, 122, 212, 221, 222;
9. 2MASS prox $\geqslant$ 6;
10. Gaia DR2 parallax exists;
11. Does not match a source in the 2MASS extended catalog.

Data sources: 2MASS PSC (J, H, K_s, J_msigcom, H_msigcom, K_s_msigcom, ph_qual, gal_contam, cc_flg, rd_flg, prox), Gaia DR 2, AllWise (W2).
Target priority options: 2515, 2525, 2535, 2545.
Cadence options: bright_18x1.

A.25. mwm_snc_100pc_apogee

Description of selection criteria: IR bright targets in the 100 pc volume-limited region.

1. $\varpi - \sigma_{\varpi} > 10$;
2. $H < 11$;
3. astrometric_excess_noise <2 if in one of the following regions:
   (a) $l \leqslant 180$ AND $b < -0.139\,l + 25$ AND $b > 0.139\,l - 25$;
   (b) $l > 180$ AND $b > -0.139\,l + 25$ AND $b < 0.139\,l - 25$;
   (c) $\sqrt{(l - 303.2)^2 + 2^*(b + 44.4)^2} < 5$;
   (d) $\sqrt{(l - 280.3)^2 + 2^*(b + 33.0)^2} < 8$.

Data sources: Gaia DR2 (ϖ, σ_{ϖ}, astrometric_excess_noise, l, b), 2MASS PSC (H).
Target priority options: 1805.
Cadence options: bright_1x1.

A.26. mwm_snc_100pc_boss

Description of selection criteria: optically bright targets in the 100 pc volume-limited region.
1. $\varpi - \sigma_{\varpi} > 10$;
2. astrometric_excess_noise <2 if in one of the following regions:
   (a) $l \leqslant 180$ AND $b < -0.139\,l + 25$ AND $b > 0.139\,l - 25$;
   (b) $l > 180$ AND $b > -0.139\,l + 25$ AND $b < 0.139\,l - 25$;
   (c) $\sqrt{(l - 303.2)^2 + 2^*(b + 44.4)^2} < 5$;
   (d) $\sqrt{(l - 280.3)^2 + 2^*(b + 33.0)^2} < 8$.

Data sources: Gaia DR2 (ϖ, σ_{ϖ}, astrometric_excess_noise, l, b, G).
Target priority options: 1800.
Cadence options: bright_2x1, dark_2x1.

A.27. mwm_snc_250pc_apogee

Description of selection criteria: IR bright targets in the 250 pc volume-limited region.
1. $G + 5\log_{10}(\varpi/1000) + 5 < 6$;
2. $\varpi - \sigma_{\varpi} > 4$;
3. $H < 11$;
4. astrometric_excess_noise <2 if in one of the following regions:
   (a) $l \leqslant 180$ AND $b < -0.139\,l + 25$ AND $b > 0.139\,l - 25$;
   (b) $l > 180$ AND $b > -0.139\,l + 25$ AND $b < 0.139\,l - 25$;
   (c) $\sqrt{(l - 303.2)^2 + 2^*(b + 44.4)^2} < 5$;
   (d) $\sqrt{(l - 280.3)^2 + 2^*(b + 33.0)^2} < 8$.

Data sources: Gaia DR2 (ϖ, σ_{ϖ}, astrometric_excess_noise, l, b, G), 2MASS PSC (H).
Target priority options: 1815.
Cadence options: bright_1x1.

A.28. mwm_snc_250pc_boss

Description of selection criteria: optically bright targets in the 250 pc volume-limited region.
1. $G + 5\log_{10}(\varpi/1000) + 5 < 6$;
2. $\varpi - \sigma_{\varpi} > 4$;
3. astrometric_excess_noise <2 if in one of the following regions:
   (a) $l \leqslant 180$ AND $b < -0.139\,l + 25$ AND $b > 0.139\,l - 25$;
   (b) $l > 180$ AND $b > -0.139\,l + 25$ AND $b < 0.139\,l - 25$;
   (c) $\sqrt{(l - 303.2)^2 + 2^*(b + 44.4)^2} < 5$;
   (d) $\sqrt{(l - 280.3)^2 + 2^*(b + 33.0)^2} < 8$.

Data sources: Gaia DR2 (ϖ, σ_{ϖ}, astrometric_excess_noise, l, b, G), 2MASS PSC (H).
Target priority options: 1810.
Cadence options: bright_2x1, dark_2x1.

A.29. mwm_tess_planet

Description of selection criteria: stars with TESS 2 minute cadence data taken during the nominal 2 year mission, prioritizing those that are either TOIs or community TOIs.
1. $7 < H < 12$.

Data sources: 2MASS PSC (H), TESS.
Target priority options: 2600, 2605, 2610.
Cadence options: bright_1x1, bright_1x2, bright_1x3, bright_1x4, bright_1x5, bright_1x6.

A.30. mwm_tessrgb_core

Description of selection criteria: this carton selects red giant candidates with a color cut and uses a magnitude cut to limit stars likely to have stellar oscillations detectable in TESS lightcurve data.
1. $J - K > 0.5$;
2. $H < 12$;
3. $T < 13$;
4. $H - 10 + 5\log_{10}\varpi < 1$;
5. $|b| > 20$.

Data sources: Gaia DR2 (ϖ), 2MASS PSC (J, H, K), TESS (T).
Target priority options: 2800.
Cadence options: bright_1x1, bright_1x2, bright_1x3, bright_1x4, bright_1x5, bright_1x6.

A.31. mwm_wd_core

Description of selection criteria: all sufficiently bright WD candidates, where $P_{\rm WD}$ is the probability a target is a WD.
1. $G < 20$;
2. $P_{\rm WD} > 0.5$.

Data sources: Gaia DR2 (G), Gentile Fusillo et al. (2019, $P_{\rm WD}$).
Target priority options: 1400.
Cadence options: dark_2x1.

A.32. mwm_yso_cluster_apogee

Description of selection criteria: IR bright YSO candidates associated with young moving groups, as identified by Kounkel et al. (2020).
1. $H < 13$;
2. age $<10^{7.5}$ yr.

Data sources: 2MASS PSC (H), Kounkel et al. (2020, age).
Target priority options: 2705.
Cadence options: bright_3x1.

A.33. mwm_yso_cluster_boss

Description of selection criteria: optically bright YSO candidates associated with young moving groups, as identified by Kounkel et al. (2020).
1. $G_{RP} < 15.5$;
2. age $< 10^{7.5}$ yr.

Data sources: Gaia DR2 (G_{RP}), Kounkel et al. (2020, age).
Target priority options: 2705.
Cadence options: bright_3x1, bright_4x1, bright_5x1, bright_6x1.

A.34. mwm_yso_cmz_apogee

Description of selection criteria: YSOs in the central molecular zone, the most extreme star-forming environment in the Milky Way.
1. $H < 13$;
2. $[8.0] - [24] > 2.5$, in the Gutermuth & Heyer (2015) catalog;
3. $\varpi < 0.2$ or not measured.

Data sources: Gaia DR2 (ϖ), 2MASS PSC (H), Spitzer ([8.0], [24]).
Target priority options: 2700.
Cadence options: bright_3x1.

A.35. mwm_yso_disk_apogee

Description of selection criteria: YSOs expected to have protoplanetary disks, as identified by larger IR excesses.
1. $H < 13$;
2. $W1 - W2 > 0.25$;
3. $W2 - W3 > 0.50$;
4. $W3 - W4 > 1.50$;
5. $\varpi > 0.3$ mas.

Data sources: Gaia DR2 (ϖ), 2MASS PSC (H), AllWise (W1, W2, W3, W4).
Target priority options: 2705.
Cadence options: bright_3x1.

A.36. mwm_yso_disk_boss

Description of selection criteria: optically bright YSOs expected to have protoplanetary disks, as identified by larger IR excesses.
1. $G_{RP} < 8.5$;
2. $W1 - W2 > 0.25$;
3. $W2 - W3 > 0.50$;
4. $W3 - W4 > 1.50$;
5. $\varpi > 0.3$ mas.

Data sources: Gaia DR2 (G_{RP}, ϖ), AllWise (W1, W2, W3, W4).
Target priority options: 2705.
Cadence options: bright_3x1, bright_4x1, bright_5x1, bright_6x1.

A.37. mwm_yso_embedded_apogee

Description of selection criteria: deeply embedded YSO candidates too optically faint for parallax measurements have more stringent IR color cuts to avoid contamination with reddened field stars.
1. $H < 13$;
2. $G > 18.5$ or undetected;
3. $J - H > 1$;
4. $H - K > 0.5$;
5. W1–W2 > 0.5;
6. W2–W3 > 1;
7. W3–W4 > 1.5;
8. W3–W4 $> 0.8(W1 - W2) + 1.1$.

Data sources: Gaia DR2 (G), 2MASS PSC (*J, H, K*), AllWise (W1, W2, W3, W4).
Target priority options: 2705.
Cadence options: bright_3x1.

A.38. mwm_yso_nebula_apogee

Description of selection criteria: YSOs with strong nebular emission should saturate in the long AllWise bands and are identified with short-wavelength color cuts.
1. $H < 13$;
2. (no W4 AND $W2 - W3 > 4$) OR (no W3, W4 AND $J - H > 1.1$);
3. $b < 5°$;
4. $b > -5°$ OR $l > 180°$.

Data sources: 2MASS PSC (J, H), AllWise (W1, W2, W3, W4).
Target priority options: 2705.
Cadence options: bright_3x1.

A.39. mwm_yso_pms_apogee

Description of selection criteria: IR bright YSO candidates based on their location above the main sequence, as identified by Zari et al. (2018) or McBride et al. (2021).
1. $H < 13$.

Data sources: 2MASS PSC (H).
Target priority options: 2700.
Cadence options: bright_3x1.

A.40. mwm_yso_pms_boss

Description of selection criteria: optically bright YSO candidates based on their location above the main sequence, as identified by Zari et al. (2018) or McBride et al. (2021).
1. $G_{RP} < 15.5$.

Data sources: Gaia DR2 (G_{RP}).
Target priority options: 2700.
Cadence options: bright_3x1, bright_4x1, bright_5x1, bright_6x1.

A.41. mwm_yso_variable_apogee

Description of selection criteria: YSO candidates that are variable in the Gaia bands, to be observed with APOGEE. Variability in a given band X is defined by $V_X = \sqrt{N_{obs}\sigma_{\overline{I_X}}/(\overline{I_X})}$, where $\overline{I_X}$ is the mean flux and $\sigma_{\overline{I_X}}$ its associated error. Below, $M_X = G_X - 5(\log_{10}(1000/\varpi) - 1)$.
1. $H < 13$;
2. $G < 18.5$;
3. $\varpi > 0.3$;
4. $V_G > 0.02$;

5. $V_{BP} > 0.02$;
6. $V_{RP} > 0.02$;
7. $V_G^{0.75} < V_{BP} < V_G$;
8. $0.75V_G < V_{RP} < V_G^{0.95}$;
9. $G_{BP} - G_{RP} > 1.3$.
10. $M_{BP} > 5\log_{10} V_{BP} + 11$;
11. $2.5(G_{BP} - G_{RP}) - 1 < M_G < 2.5^*(G_{BP} - G_{RP}) + 2.5$.

Data sources: Gaia DR2 (G, G_{RP}, G_{BP}, ϖ, $\overline{I_X}$, $\sigma_{\overline{I_X}}$), 2MASS PSC (H).
Target priority options: 2705.
Cadence options: bright_3x1.

A.42. mwm_yso_variable_boss

Description of selection criteria: YSO candidates that are variable in the Gaia bands, to be observed with BOSS. Variability in a given band X is defined by $V_X = \sqrt{N_{obs}\sigma_{\overline{I_X}}/(\overline{I_X})}$, where $\overline{I_X}$ is the mean flux and $\sigma_{\overline{I_X}}$ its associated error. Below, $M_X = G_X - 5(\log_{10}(1000/\varpi) - 1)$.

1. $H < 13$;
2. $G < 18.5$;
3. $\varpi > 0.3$;
4. $V_G > 0.02$;
5. $V_{BP} > 0.02$;
6. $V_{RP} > 0.02$;
7. $V_G^{0.75} < V_{BP} < V_G$;
8. $0.75V_G < V_{RP} < V_G^{0.95}$;
9. $G_{BP} - G_{RP} > 1.3$;
10. $M_{BP} > 5\log_{10} V_{BP} + 11$;
11. $2.5(G_{BP} - G_{RP}) - 1 < M_G < 2.5^*(G_{BP} - G_{RP}) + 2.5$.

Data sources: Gaia DR2 (G, G_{RP}, G_{BP}, ϖ, $\overline{I_X}$, $\sigma_{\overline{I_X}}$), 2MASS PSC (H).
Target priority options: 2705.
Cadence options: bright_3x1, bright_4x1, bright_5x1, bright_6x1.

Appendix B
Details of BHM `v0.5.3` Target Cartons

In this appendix, we provide a more detailed description of the full set of BHM target cartons that are being released as part of SDSS DR18. We describe not only the "core" BHM cartons in Table 4, but also all ancillary/supplementary BHM cartons, which collectively expand the scope, footprint, and depth of the project beyond the core science goals. We remind the reader that inclusion in a carton means that the target fits the carton selection criteria, not that it is guaranteed to be observed.

For each target carton, we provide the following information: the *target_selection plan* and *target_selection tag* codes give the software and configuration versions of the `target_selection` code that were used in this carton instance. In the "Summary," we provide a short synopsis of the content of the target carton, followed by a "Simplified description of selection criteria" with a human-readable description of the specific selection criteria that have been applied to build the carton, including quantitative limits on colors, magnitudes, and other quantities. The "Target priority options" and "Cadence options" indicate which "priority" and "cadence" option(s) have been allocated to the targets in this carton. Targets with numerically smaller priority are more likely to be assigned fibers; the cadence describes a target's exposure time requirement. Under "Implementation," we point to the specific section of the `target_selection` Python code that implements this carton.[108] Finally, the "Number of targets" lists the number of targets that pass all of the carton selection criteria. Note that targets are often shared between two or more cartons.

B.1. bhm_aqmes_med

target_selection plan: 0.5.0.
target_selection tag: 0.3.0.
Summary: spectroscopically confirmed optically bright SDSS QSOs, selected from the SDSS QSO catalog (DR16Q; Lyke et al. 2020). Located in 36 mostly disjoint fields within the SDSS QSO footprint that were preselected to contain higher than average numbers of bright QSOs and CSC targets. The list of field centers can be found within the target_selection repository.
Simplified description of selection criteria: select all objects from the SDSS DR16 QSO catalog that have SDSS $16.0 < i_{psf} < 19.1$ AB and that lie within 1°.49 of at least one AQMES-medium field location.
Target priority options: 1100.
Cadence options: dark_10x4_4yr.
Implementation: bhm_aqmes.py.
Number of targets: 2663.

B.2. bhm_aqmes_med_faint

target_selection plan: 0.5.0.
target_selection tag: 0.3.0.
Summary: spectroscopically confirmed optically faint SDSS QSOs, selected from the SDSS QSO catalog (DR16Q; Lyke et al. 2020). Located in 36 mostly disjoint fields within the SDSS QSO footprint that were preselected to contain higher than average numbers of bright QSOs and CSC targets. The list of field centers can be found within the target_selection repository.
Simplified description of selection criteria: select all objects from the SDSS DR16 QSO catalog that have SDSS $19.1 < i_{psf} < 21.0$ AB and that lie within 1°.49 of at least one AQMES-medium field location.
Target priority options: 3100.
Cadence options: dark_10x4_4yr.
Implementation: bhm_aqmes.py.
Number of targets: 16,853.

B.3. bhm_aqmes_wide2

target_selection plan: 0.5.4.
target_selection tag: 0.3.5.
Summary: spectroscopically confirmed optically bright SDSS QSOs, selected from the SDSS QSO catalog (DR16Q; Lyke et al. 2020). Located in 425 fields within the SDSS QSO footprint, where the choice of survey are a prioritized fields that overlapped with the SPIDERS footprint (approximately $180° < l < 360°$) and/or had higher than average numbers of bright QSOs and CSC targets. The list of field centers can be found within the target_selection repository.

[108] These can be found at URLs like https://github.com/sdss/target_selection/blob/0.3.0/python/target_selection/cartons/bhm_aqmes.py, where "0.3.0" is the `target_selection` git tag in this example.

Simplified description of selection criteria: select all objects from the SDSS DR16 QSO catalog that have SDSS $16.0 < i_{\rm psf} < 19.1$ AB and that lie within 1.°49 of at least one AQMES wide-field location.
Target priority options: 1210, 1211.
Cadence options: dark_2x4.
Implementation: bhm_aqmes.py.
Number of targets: 24,142.

B.4. bhm_aqmes_wide2_faint

target_selection plan: 0.5.4.
target_selection tag: 0.3.5.
Summary: spectroscopically confirmed optically faint SDSS QSOs, selected from the SDSS QSO catalog (DR16Q; Lyke et al. 2020). Located in 425 fields within the SDSS QSO footprint, where the choice of survey area prioritized fields that overlapped with the SPIDERS footprint (approximately $180° < l < 360°$) and/or had higher than average numbers of bright QSOs and CSC targets. The list of field centers can be found within the target_selection repository.
Simplified description of selection criteria: select all objects from the SDSS DR16 QSO catalog that have SDSS $19.1 < i_{\rm psf} < 21.0$ AB and that lie within 1.°49 of at least one AQMES wide-field location.
Target priority options: 3210, 3211.
Cadence options: dark_2x4.
Implementation: bhm_aqmes.py.
Number of targets: 99,586.

B.5. bhm_aqmes_bonus_core

target_selection plan: 0.5.4.
target_selection tag: 0.3.5.
Summary: spectroscopically confirmed optically bright SDSS QSOs, selected from the SDSS QSO catalog (DR16Q; Lyke et al. 2020). Located anywhere within the SDSS DR16Q footprint.
Simplified description of selection criteria: select all objects from the SDSS DR16 QSO catalog that have SDSS $16.0 < i_{\rm psf} < 19.1$ AB.
Target priority options: 3300, 3301.
Cadence options: dark_1x4.
Implementation: bhm_aqmes.py.
Number of targets: 83,163.

B.6. bhm_aqmes_bonus_faint

target_selection plan: 0.5.4.
target_selection tag: 0.3.5.
Summary: spectroscopically confirmed optically faint SDSS QSOs, selected from the SDSS QSO catalog (DR16Q; Lyke et al. 2020). Located anywhere within the SDSS DR16Q footprint.
Simplified description of selection criteria: select all objects from the SDSS DR16 QSO catalog that have SDSS $19.1 < i_{\rm psf} < 21.0$ AB.
Target priority options: 3302, 3303.
Cadence options: dark_1x4.
Implementation: bhm_aqmes.py.
Number of targets: 424,163.

B.7. bhm_aqmes_bonus_bright

target_selection plan: 0.5.4.
target_selection tag: 0.3.5.
Summary: spectroscopically confirmed, extremely optically bright SDSS QSOs, selected from the SDSS QSO catalog (DR16Q; Lyke et al. 2020). Located anywhere within the SDSS DR16Q footprint.
Simplified description of selection criteria: select all objects from the SDSS DR16 QSO catalog that have SDSS $14.0 < i_{\rm psf} < 18.0$ AB.
Target priority options: 4040, 4041.
Cadence options: bright_3x1.
Implementation: bhm_aqmes.py.
Number of targets: 10,848.

B.8. bhm_rm_ancillary

target_selection plan: 0.5.0.
target_selection tag: 0.3.0.
Summary: a supporting sample of candidate QSOs that have been selected by the Gaia–unWISE AGN catalog (Shu et al. 2019) and/or the SDSS XDQSO catalog (Bovy et al. 2011). These targets are located within five (plus one backup) well-known survey fields (SDSS-RM, COSMOS, XMM-LSS, ECDFS, CVZ-S/SEP, and ELIAS-S1).
Simplified description of selection criteria: starting from a parent catalog of optically selected objects in the RM fields (as presented by Yang & Shen 2023), select candidate QSOs that satisfy all of the following: (i) are identified via external ancillary methods (photo_bitmask & 3 !=0); (ii) have $15 < i_{\rm psf} < 21.5$ AB (or $16 < G < 21.7$ Vega in the CVZ-S/SEP field; photometry taken from Yang & Shen 2023); (iii) do not have significant detections ($>3\sigma$) of parallax and/or proper motion in Gaia DR2; (iv) are not vetoed due to results of visual inspections of recent spectroscopy; and (v) do not lie in the SDSS-RM field.
Target priority options: 900–1050.
Cadence options: dark_174x8, dark_100x8.
Implementation: bhm_rm.py.
Number of targets: 943.

B.9. bhm_rm_core

target_selection plan: 0.5.0.
target_selection tag: 0.3.0.
Summary: a sample of candidate QSOs selected via the methods presented by Yang & Shen (2023). These targets are located within five (plus one backup) well-known survey fields (SDSS-RM, COSMOS, XMM-LSS, ECDFS, CVZ-S/SEP, and ELIAS-S1).
Simplified description of selection criteria: starting from a parent catalog of optically selected objects in the RM fields (as presented by Yang & Shen 2023), select candidate QSOs that satisfy all of the following: (i) are identified via the Skew-T algorithm (skewt_qso==1); (ii) have $17 < i_{\rm psf} < 21.5$ AB (or $16 < G < 21.7$ Vega in the CVZ-S/SEP field; photometry taken from Yang & Shen 2023); (iii) do not have significant detections ($>3\sigma$) of parallax and/or proper motion in Gaia DR2; (iv) are not vetoed due to results of visual inspections of recent spectroscopy; (v) have detections in all of the *gri* bands (a Gaia detection is sufficient in the CVZ-S/SEP field); and (vi) do not lie in the SDSS-RM field.

Target priority options: 900–1050.
Cadence options: dark_174x8, dark_100x8.
Implementation: bhm_rm.py.
Number of targets: 3721.

B.10. bhm_rm_var

target_selection plan: 0.5.0.
target_selection tag: 0.3.0.
Summary: a sample of candidate QSOs selected via their optical variability properties, as presented by Yang & Shen (2023). These targets are located within five (plus one backup) well-known survey fields (SDSS-RM, COSMOS, XMM-LSS, ECDFS, CVZ-S/SEP, and ELIAS-S1).
Simplified description of selection criteria: starting from a parent catalog of optically selected objects in the RM fields (as presented by Yang & Shen 2023), select candidate QSOs that satisfy all of the following: (i) have significant variability in the Dark Energy Survey or Pan-STARRS1 multi-epoch photometry (var_sn$[g] > 3$ and var_rms$[g] > 0.05$); (ii) have $17 < i_{\rm psf} < 20.5$ AB (or $16 < G < 21.7$ Vega in the CVZ-S/SEP field; photometry taken from Yang & Shen 2023); (iii) do not have significant detections ($>3\sigma$) of parallax and/or proper motion in Gaia DR2; (iv) are not vetoed due to results of visual inspections of recent spectroscopy; and (v) do not lie in the SDSS-RM field.
Target priority options: 900–1050.
Cadence options: dark_174x8, dark_100x8.
Implementation: bhm_rm.py.
Number of targets: 934.

B.11. bhm_rm_known_spec

target_selection plan: 0.5.0.
target_selection tag: 0.3.0.
Summary: a sample of known QSOs identified through optical spectroscopy from various projects, as collated by Yang & Shen (2023). These targets are located within five (plus one backup) well-known survey fields (SDSS-RM, COSMOS, XMM-LSS, ECDFS, CVZ-S/SEP, and ELIAS-S1).
Simplified description of selection criteria: starting from a parent catalog of optically selected objects in the RM fields (as presented by Yang & Shen 2023), select targets that satisfy all of the following: (i) are flagged as having a spectroscopic identification (in the parent catalog or in the bhm_rm_tweaks table); (ii) have $15 < i_{\rm psf} < 21.7$ AB (SDSS-RM, CDFS, and ELIAS-S1 fields), $15 < i_{\rm psf} < 21.5$ AB (COSMOS and XMM-LSS fields), $16 < G < 21.7$ Vega in the CVZ-S/SEP field (photometry taken from Yang & Shen 2023); (iii) have a spectroscopic redshift in the range $0.005 < z < 7$; and (iv) are not vetoed due to results of visual inspections of recent spectroscopy.
Target priority options: 900–1050.
Cadence options: dark_174x8, dark_100x8.
Implementation: bhm_rm.py.
Number of targets: 3022.

B.12. bhm_csc_apogee

target_selection plan: 0.5.15.
target_selection tag: 0.3.14.
Summary: X-ray sources from the CSC2.0 source catalog with near-IR counterparts in 2MASS PSC
Simplified description of selection criteria: starting from the parent catalog of CSC2.0 sources associated with optical/IR counterparts (`bhm_csc_v2`), select entries satisfying the following criteria: (i) near-IR counterpart is from the 2MASS catalog; and (ii) 2MASS H-band magnitude measurement is not null and in the accepted range for SDSS-V: $7.0 < H < 14.0$. Allocate cadence (exposure time) requests based on H magnitude.
Target priority options: 2930–2939.
Cadence options: bright_1x1,bright_3x1.
Implementation: bhm_csc.py.
Number of targets: 48,928.

B.13. bhm_csc_boss

target_selection plan: 0.5.15.
target_selection tag: 0.3.14.
Summary: X-ray sources from the CSC2.0 source catalog with counterparts in Pan-STARRS1 DR1 or Gaia DR2.
Simplified description of selection criteria: starting from the parent catalog of CSC2.0 sources associated with optical/IR counterparts (`bhm_csc_v2`), select entries satisfying the following criteria: (i) optical counterpart is from the Pan-STARRS1 or Gaia DR2 catalogs; and (ii) optical flux/magnitude is in the accepted range for SDSS-V: Pan-STARRS1 $g_{\rm psf}$, $r_{\rm psf}$, $i_{\rm psf}$, $z_{\rm psf} > 13.5$ AB and non-Null $i_{\rm psf}$ (objects with Pan-STARRS1 counterparts); G, $G_{\rm RP} > 13.0$ Vega (Gaia DR2 counterparts). Deprioritize targets that already have good-quality SDSS spectroscopy. Allocate cadence (exposure time) requests based on optical brightness (Pan-STARRS1 $i_{\rm psf}$ or Gaia G).
Target priority options: 1920–1939, 2920–2939.
Cadence options: bright_1x1,dark_1x2,dark_1x4.
Implementation: bhm_csc.py.
Number of targets: 122,731.

B.14. bhm_gua_bright

target_selection plan: 0.5.0.
target_selection tag: 0.3.0.
Summary: a sample of optically bright candidate AGNs lacking spectroscopic confirmations, derived from the parent sample presented by Shu et al. (2019), who applied a machine-learning approach to select QSO candidates from a combination of the Gaia DR2 and unWISE catalogs.
Simplified description of selection criteria: starting with the Shu et al. (2019) catalog, select targets that satisfy the following criteria: (i) have a Random Forest probability of being a QSO of >0.8; (ii) are in the magnitude range suitable for BOSS spectroscopy in bright time ($G_{\rm dered} > 13.0$ and $G_{\rm RP,dered} > 13.5$, as well as $G_{\rm dered} < 18.5$ or $G_{\rm RP,dered} < 18.5$ Vega); and (iii) do not have good optical spectroscopic measurements from a previous iteration of SDSS.
Target priority options: 4040.
Cadence options: bright_2x1.
Implementation: bhm_gua.py.
Number of targets: 254,601.

B.15. bhm_gua_dark

target_selection plan: 0.5.0.
target_selection tag: 0.3.0.
Summary: a sample of optically faint candidate AGNs lacking spectroscopic confirmations, derived from the parent sample presented by Shu et al. (2019), who applied a machine-learning approach to select QSO candidates from a combination of the Gaia DR2 and unWISE catalogs.
Simplified description of selection criteria: starting with the Shu et al. (2019) catalog, select targets that satisfy the following criteria: (i) have a Random Forest probability of being a QSO of >0.8; (ii) are in the magnitude range suitable for BOSS spectroscopy in dark time ($G_{\rm dered} > 16.5$ and $G_{\rm RP,dered} > 16.5$, as well as $G_{\rm dered} < 21.2$ or $G_{\rm RP,dered} < 21.0$ Vega); and (iii) do not have good optical spectroscopic measurements from a previous iteration of SDSS.
Target priority options: 3400.
Cadence options: dark_1x4.
Implementation: bhm_gua.py.
Number of targets: 2,156,582.

B.16. bhm_colr_galaxies_lsdr8

target_selection plan: 0.5.16.
target_selection tag: 0.3.13.
Summary: a supplementary magnitude-limited sample of optically bright galaxies selected from the DESI Legacy Survey DR8 optical/IR imaging catalog. Selection is based on optical morphology, lack of Gaia DR2 parallax, and several magnitude cuts.
Simplified description of selection criteria: starting from the DESI Legacy Survey DR8 catalog (lsdr8), select entries satisfying all of the following criteria: (i) lsdr8 morphological type !="PSF"; (ii) zero or Null parallax in Gaia DR2; and (iii) $z_{\rm model,dered} < 19.0$ AB and $z_{\rm fiber,dered} < 19.5$ AB and $z_{\rm fiber} < 19.0$ AB and $r_{\rm fiber} > 16.0$ AB and $G > 15.0$ Vega and $G_{\rm RP} > 15.0$ Vega (photometry from lsdr8).
Target priority options: 7100.
Cadence options: bright_1x1, dark_1x1, dark_1x4.
Implementation: bhm_galaxies.py.
Number of targets: 7,320,203.

B.17. bhm_spiders_agn_lsdr8

target_selection plan: 0.5.0.
target_selection tag: 0.3.0.
Summary: This is the highest-priority carton for SPIDERS AGN wide-area follow-up. The carton provides optical counterparts to pointlike (unresolved) X-ray sources detected in early reductions of the first six months of the eROSITA all-sky survey data (eRASS:1). The sample is expected to contain a mixture of QSOs, AGNs, stars, and compact objects. The X-ray sources have been crossmatched by the eROSITA-DE team to DESI Legacy Survey DR8 (lsdr8) optical/IR counterparts. All targets are located in the sky hemisphere where Max-Planck-Institut für Extraterrestrische Physik (MPE) controls the data rights (approximately $180° < l < 360°$). Due to the footprint of lsdr8, nearly all targets in this carton are located at high Galactic latitudes ($|b| > 15°$).
Simplified description of selection criteria: starting from a parent catalog of eRASS:1 point source → legacysurvey.org/dr8 associations (method: NWAY assisted by optical/IR priors computed via a pretrained random forest, building on Salvato et al. 2022), select targets that meet all of the following criteria: (i) have eROSITA detection likelihood >6.0; (ii) have an X-ray → optical/IR crossmatch probability (NWAY) of p_any >0.1; (iii) have $13.5 < r_{\rm fibertot} < 22.5$ or $13.5 < z_{\rm fibertot} < 21.0$ AB; (iv) are not saturated in Legacy Survey imaging; (v) have at least one observation in r band and at least one observation in g or z band; and (vi) if detected by Gaia DR2, then have $G > 13.5$ and $G_{\rm RP} > 13.5$ Vega (photometry from lsdr8). We deprioritize targets if any of the following criteria are met: (i) the target already has existing good-quality SDSS spectroscopy; (ii) the X-ray detection likelihood is < 8.0; or (iii) the target is a secondary X-ray → optical/IR association. We assign cadences (exposure time requests) based on optical brightness.
Target priority options: 1520–1523, 1720–1723.
Cadence options: bright_2x1, dark_1x2, dark_1x4.
Implementation: bhm_spiders_agn.py.
Number of targets: 235,745.

B.18. bhm_spiders_agn_ps1dr2

target_selection plan: 0.5.0.
target_selection tag: 0.3.0.
Summary: This is the second-highest-priority carton for SPIDERS AGN wide-area follow-up, included to expand the survey footprint beyond Legacy Survey DR8. The carton provides optical counterparts to pointlike (unresolved) X-ray sources detected in early reductions of the first six months of eROSITA all-sky survey data (eRASS:1). The sample is expected to contain a mixture of QSOs, AGNs, stars, and compact objects. The X-ray sources have been crossmatched by the eROSITA-DE team, first to CatWISE2020 mid-IR sources (Marocco et al. 2021) and then to optical counterparts from the Pan-STARRS1 DR2 catalog. All targets are located in the sky hemisphere where MPE controls the data rights (approximately $180° < l < 360°$) and at decl. $> -30°$, spanning a wide range of Galactic latitudes. Targets at low Galactic latitudes ($|b| < 15°$) do not drive survey strategy.
Simplified description of selection criteria: starting from a parent catalog of eRASS:1 point source → CatWISE2020 → Pan-STARRS1 associations (method: NWAY assisted by IR priors computed via a pretrained random forest, building on Salvato et al. 2022), select targets that meet all of the following criteria: (i) have eROSITA detection likelihood >6.0; (ii) have an X-ray → IR crossmatch probability of p_any >0.1; (iii) have Pan-STARRS1 $g_{\rm psf}$, $r_{\rm psf}$, $i_{\rm psf}$, $z_{\rm psf} > 13.5$ AB and at least one of Pan-STARRS1 $g_{\rm psf} < 22.5$, $r_{\rm psf} < 22.0$, $i_{\rm psf} < 21.5$, or $z_{\rm psf} < 20.5$ AB; (iv) are not associated with a bad Pan-STARRS1 image stack; (v) have non-null measurements of $g_{\rm psf}$, $r_{\rm psf}$, and $i_{\rm psf}$; and (vi) if detected by Gaia DR2, then have $G > 13.5$ and $G_{\rm RP} > 13.5$ Vega. We deprioritize targets if any of the following criteria are met: (i) the target already has existing good-quality SDSS spectroscopy; (ii) the X-ray detection likelihood is < 8.0; or (iii) the target is a secondary X-ray → IR association. We assign cadences (exposure time requests) based on optical brightness.
Target priority options: 1530–1533, 1730–1733, 3530–3533, 3730–3732.

Cadence options: bright_2x1, dark_1x2, dark_1x4.
Implementation: bhm_spiders_agn.py.
Number of targets: 200,681.

B.19. bhm_spiders_agn_gaiadr2

target_selection plan: 0.5.0.
target_selection tag: 0.3.0.
Summary: This is the third-highest-priority carton for SPIDERS AGN wide-area follow-up, included to expand the survey footprint to the full hemisphere where X-ray sources are available (beyond Legacy Survey DR8 and Pan-STARRS1). The carton provides optical counterparts to pointlike (unresolved) X-ray sources detected in early reductions of the first six months of eROSITA all-sky survey data (eRASS:1). The sample is expected to contain a mixture of QSOs, AGNs, stars, and compact objects. The X-ray sources have been crossmatched by the eROSITA-DE team, first to CatWISE2020 mid-IR sources (Marocco et al. 2021) and then to optical counterparts from the Gaia DR2 catalog. All targets are located in the sky hemisphere where MPE controls the data rights (approximately $180° < l < 360°$). The targets in this carton are distributed over a wide range of Galactic latitudes, but targets at low Galactic latitudes ($|b| < 15°$) do not drive survey strategy.
Simplified description of selection criteria: starting from a parent catalog of eRASS:1 point source → CatWISE2020 → Gaia DR2 associations (method: NWAY assisted by IR priors computed via a pretrained random forest, building on Salvato et al. 2022), select targets that meet all of the following criteria: (i) have eROSITA detection likelihood >6.0; (ii) have an X-ray → IR crossmatch probability of p_any >0.1; and (iii) have $G > 13.5$ and $G_{RP} > 13.5$ Vega. We deprioritize targets if any of the following criteria are met: (i) the target already has existing good-quality SDSS spectroscopy; (ii) the X-ray detection likelihood is < 8.0; or (iii) the target is a secondary X-ray → IR association. We assign cadences (exposure time requests) based on optical brightness.
Target priority options: 1540–1543, 1740–1743, 3540–3543, 3740–3742.
Cadence options: bright_2x1, dark_1x2, dark_1x4.
Implementation: bhm_spiders_agn.py.
Number of targets: 324,576.

B.20. bhm_spiders_agn_skymapperdr2

target_selection plan: 0.5.0.
target_selection tag: 0.3.0.
Summary: This is a lower-ranked carton for SPIDERS AGN wide-area follow-up, which supplements the survey in areas that rely on Gaia DR2 (beyond Legacy Survey DR8 and Pan-STARRS1) by recovering extended targets (galaxies) that are missed by Gaia. The carton provides optical counterparts to pointlike (unresolved) X-ray sources detected in early reductions of the first six months of eROSITA all-sky survey data (eRASS:1). The sample is expected to contain a mixture of QSOs, AGNs, stars, and compact objects. The X-ray sources have been crossmatched by the eROSITA-DE team, first to CatWISE2020 mid-IR sources (Marocco et al. 2021) and then to optical counterparts from the SkyMapper DR2 catalog (Onken et al. 2019). All targets are located in the sky hemisphere where MPE controls the data rights (approximately $180° < l < 360°$) and at decl. $< 0°$, spanning a wide range of Galactic latitudes. Targets at low Galactic latitudes ($|b| < 15°$) do not drive survey strategy.
Simplified description of selection criteria: starting from a parent catalog of eRASS:1 point source → CatWISE2020 → SkyMapper DR2 associations (method: NWAY assisted by IR priors computed via a pretrained random forest, building on Salvato et al. 2022), select targets that meet all of the following criteria: (i) have eROSITA detection likelihood >6.0; (ii) have an X-ray → IR crossmatch probability of p_any >0.1; (iii) have SkyMapper g_{psf}, r_{psf}, i_{psf}, $z_{psf} > 13.5$ AB and at least one of SkyMapper $g_{psf} < 22.5$, $r_{psf} < 22.0$, $i_{psf} < 21.5$, or $z_{psf} < 20.5$ AB; (iv) are not associated with a bad SkyMapper source detection (flags < 4); (v) have non-null measurements of g_{psf}, r_{psf}, and i_{psf}; and (vi) if detected by Gaia DR2, then have $G > 13.5$ and $G_{RP} > 13.5$ Vega. We deprioritize targets if any of the following criteria are met: (i) the target already has existing good-quality SDSS spectroscopy; (ii) the X-ray detection likelihood is < 8.0; or (iii) the target is a secondary X-ray → IR association. We assign cadences (exposure time requests) based on optical brightness.
Target priority options: 1550–1553, 1750–1753, 3550–3553, 3750–3752.
Cadence options: bright_2x1, dark_1x2, dark_1x4.
Implementation: bhm_spiders_agn.py.
Number of targets: 82,683.

B.21. bhm_spiders_agn_supercosmos

target_selection plan: 0.5.0.
target_selection tag: 0.3.0.
Summary: This is a lower-ranked carton for SPIDERS AGN wide-area follow-up, which supplements the survey in areas that rely on Gaia DR2 (beyond DESI Legacy Survey DR8 and Pan-STARRS1) by recovering extended targets (galaxies) that are missed by Gaia. The carton provides optical counterparts to pointlike (unresolved) X-ray sources detected in early reductions of the first six months of eROSITA all-sky survey data (eRASS:1). The sample is expected to contain a mixture of QSOs, AGNs, stars, and compact objects. The X-ray sources have been crossmatched by the eROSITA-DE team, first to CatWISE2020 mid-IR sources (Marocco et al. 2021) and then to optical counterparts from the SuperCosmos Sky Surveys catalog[109] (derived from scans of photographic plates). All targets are located in the sky hemisphere where MPE controls the data rights (approximately $180° < l < 360°$), spanning a wide range of Galactic latitudes. Targets at low Galactic latitudes ($|b| < 15°$) do not drive survey strategy.
Simplified description of selection criteria: starting from a parent catalog of eRASS:1 point source → CatWISE2020 → SuperCosmos associations (method: NWAY assisted by IR priors computed via a pretrained random forest, building on Salvato et al. 2022), select targets that meet all of the following criteria: (i) have eROSITA detection likelihood >6.0; (ii) have an X-ray → IR crossmatch probability of p_any >0.1; (iii) have $B_{J,psf}$, R_{psf}, $I_{psf} > 13.5$ Vega and at least one of $B_{J,psf} < 22.5$, $R_{psf} < 22.0$, or $I_{psf} < 21.5$ Vega

[109] https://www-wfau.roe.ac.uk/sss/intro.html

(photometry from SuperCosmos); and (iv) if detected by Gaia DR2, then have $G > 13.5$ and $G_{RP} > 13.5$ Vega. We deprioritize targets if any of the following criteria are met: (i) the target already has existing good-quality SDSS spectroscopy; (ii) the X-ray detection likelihood is < 8.0; or (iii) the target is a secondary X-ray → IR association. We assign cadences (exposure time requests) based on optical brightness.
Target priority options: 1560–1563, 1760–1763, 3560–3563, 3760–3763.
Cadence options: bright_2x1, dark_1x2, dark_1x4.
Implementation: bhm_spiders_agn.py.
Number of targets: 430,780.

B.22. bhm_spiders_agn_efeds_stragglers

target_selection plan: 0.5.0.
target_selection tag: 0.3.0.
Summary: This is an opportunistic supplementary carton for SPIDERS AGN follow-up, aiming, where fiber resources allow, to gather a small additional number of spectra for targets in the eFEDS field (which has been repeatedly surveyed in earlier iterations of SDSS). This carton provides optical counterparts to pointlike (unresolved) X-ray sources detected in early reductions of the eROSITA/eFEDS performance validation field. The sample is expected to contain a mixture of QSOs, AGNs, stars, and compact objects. The X-ray sources have been crossmatched by the eROSITA-DE team to DESI Legacy Survey DR8 optical/IR counterparts. All targets in this carton are located within the eFEDS field (approximately $126° < \text{R.A.} < 146°$, $-3° < \text{decl.} < +6°$). These targets do not drive survey strategy.
Simplified description of selection criteria: starting from a parent catalog of eFEDS point source → legacysurvey.org/dr8 associations (method: NWAY assisted by optical/IR priors computed via a pretrained random forest; see Salvato et al. 2022), select targets that meet all of the following criteria: (i) have eROSITA detection likelihood >6.0; (ii) have an X-ray → optical/IR crossmatch probability (NWAY) of p_any >0.1; (iii) have $13.5 < r_{\text{fibertot}} < 22.5$ or $13.5 < z_{\text{fibertot}} < 21.0$ AB; (iv) are not saturated in Legacy Survey imaging; (v) have at least one observation in r band and at least one observation in g or z band; and (vi) if detected by Gaia DR2, then have $G > 13.5$ and $G_{RP} > 13.5$ Vega. We deprioritize targets if any of the following criteria are met: (i) the target already has existing good-quality SDSS spectroscopy; (ii) the X-ray detection likelihood is < 8.0; or (iii) the target is a secondary X-ray → optical/IR association. We assign cadences (exposure time requests) based on optical brightness.
Target priority options: 1510–1514, 1710–1714.
Cadence options: bright_2x1, dark_1x2, dark_1x4.
Implementation: bhm_spiders_agn.py.
Number of targets: 15,926.

B.23. bhm_spiders_agn_sep

target_selection plan: 0.5.0.
target_selection tag: 0.3.0.
Summary: This special carton is dedicated to SPIDERS AGN follow-up in the CVZ-S/SEP field. The carton provides optical counterparts to pointlike (unresolved) X-ray sources detected in a dedicated analysis of the first six months of eROSITA scanning data near the South Ecliptic Pole. The X-ray sources have been crossmatched by the eROSITA-DE team, first to CatWISE2020 mid-IR sources (Marocco et al. 2021) and then to optical counterparts from the Gaia DR2 catalog, using additional filtering (including Gaia EDR3 astrometric information) to reduce the contamination from foreground stars located in the LMC. All targets are located within 1.5° of the South Ecliptic Pole (R.A., decl. = 90.°0−66.°56).
Simplified description of selection criteria: starting from a parent catalog of eRASS:1/SEP point source → CatWISE2020 → Gaia DR2 associations (method: NWAY assisted by IR priors computed via a pretrained random forest, building on Salvato et al. 2022), select targets that meet all of the following criteria: (i) have eROSITA detection likelihood >6.0; (ii) have an X-ray → IR crossmatch probability of p_any >0.1; and (iii) have Gaia $G > 13.5$ and $G_{RP} > 13.5$ Vega. We deprioritize targets if any of the following criteria are met: (i) the X-ray detection likelihood is < 8.0; or (ii) the target is a secondary X-ray → IR association. We assign cadences (exposure time requests) based on optical brightness.
Target priority options: 1510, 1512.
Cadence options: bright_2x1, dark_1x2, dark_1x4.
Implementation: bhm_spiders_agn.py.
Number of targets: 697.

B.24. bhm_spiders_clusters_lsdr8

target_selection plan: 0.5.0.
target_selection tag: 0.3.0.
Summary: This is the highest-priority carton for SPIDERS Clusters wide-area follow-up. The carton provides a list of galaxies that are candidate members of clusters selected from early reductions of the first six months of eROSITA all-sky survey data (eRASS:1). The X-ray clusters have been associated by the eROSITA-DE team to DESI Legacy Survey DR8 (lsdr8) optical/IR counterparts using the eROMaPPeR red-sequence finder algorithm (Rykoff et al. 2014; Ider Chitham et al. 2020). All targets are located in the sky hemisphere where MPE controls the data rights (approximately $180° < l° < 360°$). Due to the footprint of lsdr8, nearly all targets in this carton are located at high Galactic latitudes ($|b| > 15°$).
Simplified description of selection criteria: starting from a parent catalog of eRASS:1 → lsdr8 eROMaPPeR cluster associations, select targets that meet all of the following criteria: (i) have $13.5 < r_{\text{fibertot}} < 21.0$ or $13.5 < z_{\text{fibertot}} < 20.0$ AB; (ii) if detected by Gaia DR2, then have $G > 13.5$ and $G_{RP} > 13.5$ Vega (photometry from lsdr8); and (iii) do not have existing good-quality SDSS spectroscopy. We assign a range of priorities to targets in this carton, with brightest cluster galaxies (BCGs) being top ranked, followed by candidate member galaxies, according to their probability of membership. We assign cadences (exposure time requests) based on optical brightness.
Target priority options: 1501, 1630–1659.
Cadence options: bright_2x1, dark_1x2, dark_1x4.
Implementation: bhm_spiders_clusters.py.
Number of targets: 87,490.

B.25. bhm_spiders_clusters_ps1dr2

target_selection plan: 0.5.0.
target_selection tag: 0.3.0.

Summary: This is the second-highest-priority carton for SPIDERS Clusters wide-area follow-up, designed to expand the survey area beyond the Legacy Survey DR8 footprint. The carton provides a list of galaxies that are candidate members of clusters selected from early reductions of the first six months of eROSITA all-sky survey data (eRASS:1). The X-ray clusters have been associated by the eROSITA-DE team to the Pan-STARRS1 DR2 catalog using the eROMaPPeR red-sequence finder algorithm (Rykoff et al. 2014; Ider Chitham et al. 2020). All targets are located in the sky hemisphere where MPE controls the data rights (approximately $180° < l < 360°$). Nearly all targets in this carton are located at high Galactic latitudes ($|b| > 15°$).
Simplified description of selection criteria: starting from a parent catalog of eRASS:1 → Pan-STARRS1 DR2 eROMaPPeR cluster associations, select targets that meet all of the following criteria: (i) have Pan-STARRS1 r_{psf}, i_{psf}, $z_{psf} > 13.5$ AB and at least one of $r_{psf} < 21.5$, $i_{psf} < 21.0$, or $z_{psf} < 20.5$ AB; and (ii) do not have existing good-quality SDSS spectroscopy. We assign a range of priorities to targets in this carton, with BCGs being top ranked, followed by candidate member galaxies, according to their probability of membership. We assign cadences (exposure time requests) based on optical brightness.
Target priority options: 1502, 1660–1689.
Cadence options: bright_2x1, dark_1x2, dark_1x4.
Implementation: bhm_spiders_clusters.py.
Number of targets: 86,179.

B.26. bhm_spiders_clusters_efeds_stragglers

target_selection plan: 0.5.0.
target_selection tag: 0.3.0.
Summary: This is an opportunistic supplementary carton for SPIDERS Clusters follow-up, aiming, where fiber resources allow, to gather a small additional number of spectra for targets in the eFEDS field (which has been repeatedly surveyed in earlier iterations of SDSS). The carton provides a list of galaxies that are candidate members of clusters selected from early reductions of the eROSITA performance verification survey in the eFEDS field. The X-ray clusters have been associated by the eROSITA-DE team to DESI Legacy Survey DR8 (lsdr8) optical/IR counterparts. All targets in this carton are located within the eFEDS field (approximately $126° < \text{R.A.} < 146°$, $-3° < \text{decl.} < +6°$).
Simplified description of selection criteria: starting from a parent catalog of eFEDS → legacysurvey.org/dr8 cluster associations (eROMaPPeR; Rykoff et al. 2014; Ider Chitham et al. 2020; Liu et al. 2022), select targets that meet all of the following criteria: have $13.5 < r_{fibertot} < 21.0$ or $13.5 < z_{fibertot} < 20.0$ AB; (ii) if detected by Gaia DR2, then have $G > 13.5$ and $G_{RP} > 13.5$ Vega (photometry from lsdr8); and (iii) do not have existing good-quality SDSS spectroscopy. We assign a range of priorities to targets in this carton, with BCGs being top ranked, followed by candidate member galaxies, according to their probability of membership. We assign cadences (exposure time requests) based on optical brightness.
Target priority options: 1500, 1600–1629.
Cadence options: dark_1x2, dark_1x4.
Implementation: bhm_spiders_clusters.py.
Number of targets: 3060.

B.27. bhm_spiders_agn-efeds

target_selection plan: 0.1.0.
target_selection tag: 0.1.0.
Summary: A carton used during SDSS-V plate-mode observations that contains candidate AGN targets found in the eROSITA/eFEDS X-ray survey field. This carton provides optical counterparts to pointlike (unresolved) X-ray sources detected in early reductions ("c940/V2T") of the eROSITA/eFEDS performance validation field. The sample is expected to contain a mixture of QSOs, AGNs, stars, and compact objects. The X-ray sources have been crossmatched by the eROSITA-DE team to DESI Legacy Survey DR8 (lsdr8) optical/IR counterparts. All targets in this carton are located within the eFEDS field (approximately $126° < \text{R.A.} < 146°$, $-3° < \text{decl.} < +6°$).
Simplified description of selection criteria: starting from a parent catalog of eFEDS point source → lsdr8 associations (primarily via NWAY assisted by optical/IR priors computed via a pretrained random forest—see Salvato et al. 2022—supplemented by counterparts selected via a likelihood ratio, or LR, using *r*-band magnitudes), select targets that meet all of the following criteria: (i) have eROSITA detection likelihood >6.0; (ii) have an X-ray → optical/IR crossmatch probability of either p_any >0.1 (NWAY associations) or LR >0.2 (LR associations); (iii) have $r_{fiber} > 16.5$ and either $r_{fiber} < 22.0$ or $z_{fiber} < 21.0$ AB (photometry from lsdr8); and (iv) did not receive high-quality spectroscopy during the SDSS-IV observations of the eFEDS field (Abdurro'uf et al. 2022). We deprioritize targets if any of the following criteria are met: (i) the target already has existing good-quality SDSS spectroscopy in SDSS DR16; (ii) the X-ray detection likelihood is < 8.0; (iii) the target is a secondary X-ray → optical/IR association; or (iv) the optical/IR counterpart was only chosen by the LR method. All targets were assigned a nominal cadence of: bhm_spiders_1x8 (8 x 15 minutes in dark time).
Target priority options: 1510–1519.
Cadence options: bhm_spiders_1x8.
Implementation: bhm_spiders_agn.py.
Number of targets: 12,459.

B.28. bhm_spiders_clusters-efeds-ls-redmapper

target_selection plan: 0.1.0.
target_selection tag: 0.1.0.
Summary: A carton used during SDSS-V plate-mode observations that contains galaxy cluster targets found in the eROSITA/eFEDS X-ray survey field. The carton provides a list of galaxies that are candidate members of clusters selected from early reductions ("c940") of the eROSITA performance verification survey in the eFEDS field. The parent sample of galaxy clusters and their member galaxies has been selected via a joint analysis of X-ray and (several) optical/IR data sets using the eROMaPPeR red-sequence finder algorithm (Rykoff et al. 2014; Ider Chitham et al. 2020). This particular carton relies on optical/IR data from DESI Legacy Survey DR8 (lsdr8). All targets in this carton are located within the eFEDS field (approximately $126° < \text{R.A.} < 146°$, $-3° < \text{decl.} < +6°$).
Simplified description of selection criteria: starting from a parent catalog of eFEDS → optical/IR cluster associations, select targets that meet all of the following criteria: (i) are

selected by eROMaPPeR applied to lsdr8 photometric data; (ii) have eROSITA X-ray detection likelihood >8.0; (iii) have $r_{\rm fiber} > 16.5$ and either $r_{\rm fiber} < 21.0$ or $z_{\rm fiber} < 20.0$ AB (photometry from lsdr8); and (iv) do not have existing good-quality (SDSS or external) spectroscopy. We assign a range of priorities to targets in this carton, with BCGs being top ranked, followed by candidate member galaxies, according to their probability of membership. All targets were assigned a nominal cadence of: bhm_spiders_1x8 (8 x 15 minutes in dark time).
Target priority options: 1500, 1511–1610.
Cadence options: dark_1x8.
Implementation: bhm_spiders_clusters.py.
Number of targets: 4432.

B.29. bhm_spiders_clusters-efeds-sdss-redmapper

target_selection plan: 0.1.0.
target_selection tag: 0.1.0.
Summary: A carton used during SDSS-V plate-mode observations that contains galaxy cluster targets found in the eROSITA/eFEDS X-ray survey field. The carton provides a list of galaxies that are candidate members of clusters selected from early reductions ("c940") of the eROSITA performance verification survey in the eFEDS field. The parent sample of galaxy clusters and their member galaxies has been selected via a joint analysis of X-ray and (several) optical/IR data sets using the eROMaPPeR red-sequence finder algorithm (Rykoff et al. 2014; Ider Chitham et al. 2020). This particular carton relies on optical photometric data from SDSS DR13. All targets in this carton are located within the eFEDS field (approximately $126° <$ R.A. $< 146°$, $-3° <$ decl. $< +6°$).
Simplified description of selection criteria: starting from a parent catalog of eFEDS → optical/IR cluster associations, select targets that meet all of the following criteria: (i) are selected by eROMaPPeR applied to SDSS dr13 photometric data; (ii) have eROSITA X-ray detection likelihood >8.0; (iii) have $r_{\rm fiber} > 16.5$ and either $r_{\rm fiber} < 21.0$ or $z_{\rm fiber} < 20.0$ AB (photometry from DESI Legacy Survey DR8); and (iv) do not have existing good-quality (SDSS or external) spectroscopy. We assign a range of priorities to targets in this carton, with BCGs being top ranked, followed by candidate member galaxies, according to their probability of membership. All targets were assigned a nominal cadence of: bhm_spiders_1x8 (8 x 15 minutes in dark time).
Target priority options: 1500, 1511–1610.
Cadence options: dark_1x8.
Implementation: bhm_spiders_clusters.py.
Number of targets: 4304.

B.30. bhm_spiders_clusters-efeds-hsc-redmapper

target_selection plan: 0.1.0.
target_selection tag: 0.1.0.
Summary: A carton used during SDSS-V plate-mode observations that contains galaxy cluster targets found in the eROSITA/eFEDS X-ray survey field. The carton provides a list of galaxies that are candidate members of clusters selected from early reductions ("c940") of the eROSITA performance verification survey in the eFEDS field. The parent sample of galaxy clusters and their member galaxies has been selected via a joint analysis of X-ray and (several) optical/IR data sets using the eROMaPPeR red-sequence finder algorithm (Rykoff et al. 2014; Ider Chitham et al. 2020). This particular carton relies on optical/IR data from the Hyper Suprime-Cam Subaru Strategic Program (HSC-SSP).[110] All targets in this carton are located within the eFEDS field (approximately $126° <$ R.A. $< 146°$, $-3° <$ decl. $< +6°$).
Simplified description of selection criteria: starting from a parent catalog of eFEDS → optical/IR cluster associations, select targets that meet all of the following criteria: (i) are selected by eROMaPPeR applied to HSC-SSP photometric data; (ii) have eROSITA X-ray detection likelihood >8.0; (iii) have $r_{\rm fiber} > 16.5$ and either $r_{\rm fiber} < 21.0$ or $z_{\rm fiber} < 20.0$ AB (photometry from DESI Legacy Survey DR8); and (iv) do not have existing good-quality (SDSS or external) spectroscopy. We assign a range of priorities to targets in this carton, with BCGs being top ranked, followed by candidate member galaxies, according to their probability of membership. All targets were assigned a nominal cadence of: bhm_spiders_1x8 (8 x 15 minutes in dark time).
Target priority options: 1500, 1511–1610.
Cadence options: dark_1x8.
Implementation: bhm_spiders_clusters.py.
Number of targets: 924.

B.31. bhm_spiders_clusters-efeds-erosita

target_selection plan: 0.1.0.
target_selection tag: 0.1.0.
Summary: A carton used during SDSS-V plate-mode observations that contains galaxy cluster targets found in the eROSITA/eFEDS X-ray survey field. The carton provides a list of galaxies that are candidate members of clusters selected from early reductions ("c940") of the eROSITA performance verification survey in the eFEDS field. The parent sample of galaxy clusters and their member galaxies has been selected via a joint analysis of X-ray and (several) optical/IR data sets. This particular carton includes counterparts to X-ray extended sources that were not selected by the eROMaPPeR red-sequence finder algorithm when applied to any of the DESI Legacy Survey DR8, SDSS DR13, or HSC-SSP data sets (i.e., complementary to the cartons bhm_spiders_clusters-efeds-ls-redmapper, bhm_spiders_clusters-efeds-sdss-redmapper, and bhm_spiders_clusters-efeds-hsc-redmapper). All targets in this carton are located within the eFEDS field (approximately $126° <$ R.A. $< 146°$, $-3° <$ decl. $< +6°$).
Simplified description of selection criteria: starting from a parent catalog of eFEDS → optical/IR cluster associations, select targets that meet all of the following criteria: (i) are identified as being X-ray extended, but not selected via the eROMaPPeR algorithm; (ii) have eROSITA X-ray detection likelihood >8.0; (iii) have $r_{\rm fiber} > 16.5$ and either $r_{\rm fiber} < 21.0$ or $z_{\rm fiber} < 20.0$ AB (photometry from DESI Legacy Survey DR8); and (iv) do not have existing good-quality (SDSS or external) spectroscopy. We assign a range of priorities to targets in this carton, with BCGs being top ranked, followed by candidate member galaxies, according to their probability of membership. All targets were assigned a nominal cadence of: bhm_spiders_1x8 (8 x 15 minutes in dark time).

[110] https://hsc.mtk.nao.ac.jp/ssp/

Target priority options: 1500, 1511–1535.
Cadence options: dark_1x8.
Implementation: bhm_spiders_clusters.py.
Number of targets: 15.

ORCID iDs

Carles Badenes https://orcid.org/0000-0003-3494-343X
Kat Barger https://orcid.org/0000-0001-5817-0932
Jorge K. Barrera-Ballesteros https://orcid.org/0000-0003-2405-7258
Chad F. Bender https://orcid.org/0000-0003-4384-7220
Erika Benitez https://orcid.org/0000-0003-1018-2613
Jonathan C. Bird https://orcid.org/0000-0001-5838-5212
Dmitry Bizyaev https://orcid.org/0000-0002-3601-133X
Michael R. Blanton https://orcid.org/0000-0003-1641-6222
John Bochanski https://orcid.org/0000-0001-7096-425X
Jo Bovy https://orcid.org/0000-0001-6855-442X
Joel R. Brownstein https://orcid.org/0000-0002-8725-1069
Johannes Buchner https://orcid.org/0000-0003-0426-6634
Joseph N. Burchett https://orcid.org/0000-0002-1979-2197
Mariana Cano Díaz https://orcid.org/0000-0001-9553-8230
Joleen K. Carlberg https://orcid.org/0000-0001-5926-4471
Andrew R. Casey https://orcid.org/0000-0003-0174-0564
Vedant Chandra https://orcid.org/0000-0002-0572-8012
Brian Cherinka https://orcid.org/0000-0002-4289-7923
Abigail A. Coker https://orcid.org/0000-0003-2710-0338
Johan Comparat https://orcid.org/0000-0001-9200-1497
Charlie Conroy https://orcid.org/0000-0002-1590-8551
Kevin Covey https://orcid.org/0000-0001-6914-7797
Jeffrey D. Crane https://orcid.org/0000-0002-5226-787X
Katia Cunha https://orcid.org/0000-0001-6476-0576
Megan C. Davis https://orcid.org/0000-0001-9776-9227
Nathan De Lee https://orcid.org/0000-0002-3657-0705
José Eduardo Méndez Delgado https://orcid.org/0000-0002-6972-6411
Sebastian Demasi https://orcid.org/0009-0006-8478-7163
Mike Eracleous https://orcid.org/0000-0002-3719-940X
Xiaohui Fan https://orcid.org/0000-0003-3310-0131
Sara Frederick https://orcid.org/0000-0001-9676-730X
Logan Fries https://orcid.org/0000-0001-8032-2971
Peter Frinchaboy https://orcid.org/0000-0002-0740-8346
Boris T. Gänsicke https://orcid.org/0000-0002-2761-3005
Catherine Grier https://orcid.org/0000-0001-9920-6057
Patrick Hall https://orcid.org/0000-0002-1763-5825
Christian R. Hayes https://orcid.org/0000-0003-2969-2445
J. J. Hermes https://orcid.org/0000-0001-5941-2286
Lorena Hernández-García https://orcid.org/0000-0002-8606-6961
David W. Hogg https://orcid.org/0000-0003-2866-9403
Jon A. Holtzman https://orcid.org/0000-0002-9771-9622
Hector Javier Ibarra-Medel https://orcid.org/0000-0002-9790-6313
Alexander Ji https://orcid.org/0000-0002-4863-8842
Jennifer A. Johnson https://orcid.org/0000-0001-7258-1834
Karen Kinemuchi https://orcid.org/0000-0001-7908-7724
Matthias Kluge https://orcid.org/0000-0002-9618-2552
Anton Koekemoer https://orcid.org/0000-0002-6610-2048
Marina Kounkel https://orcid.org/0000-0002-5365-1267
Dhanesh Krishnarao https://orcid.org/0000-0002-7955-7359
Chao Liu https://orcid.org/0000-0002-1802-6917
Xin Liu https://orcid.org/0000-0003-0049-5210
Alexandre Roman Lopes https://orcid.org/0000-0002-1379-4204
Matin Macktoobian https://orcid.org/0000-0002-4964-8962
Steven R. Majewski https://orcid.org/0000-0003-2025-3147
Dan Maoz https://orcid.org/0000-0002-6579-0483
Thomas Masseron https://orcid.org/0000-0002-6939-0831
Karen L. Masters https://orcid.org/0000-0003-0846-9578
Aidan McBride https://orcid.org/0000-0003-2401-0097
Andrea Merloni https://orcid.org/0000-0002-0761-0130
Natalie Myers https://orcid.org/0000-0001-9738-4829
C. Alenka Negrete https://orcid.org/0000-0002-1656-827X
David L. Nidever https://orcid.org/0000-0002-1793-3689
Christian Nitschelm https://orcid.org/0000-0003-4752-4365
Kaike Pan https://orcid.org/0000-0002-2835-2556
Marc H. Pinsonneault https://orcid.org/0000-0002-7549-7766
Rick Pogge https://orcid.org/0000-0003-1435-3053
Hans-Walter Rix https://orcid.org/0000-0003-4996-9069
Jessie Runnoe https://orcid.org/0000-0001-8557-2822
Mara Salvato https://orcid.org/0000-0001-7116-9303
Sebastian F. Sanchez https://orcid.org/0000-0001-6444-9307
Felipe A. Santana https://orcid.org/0000-0002-4023-7649
Andrew Saydjari https://orcid.org/0000-0002-6561-9002
Conor Sayres https://orcid.org/0000-0002-4454-1920
Kevin C. Schlaufman https://orcid.org/0000-0001-5761-6779
Donald P. Schneider https://orcid.org/0000-0001-7240-7449
Axel Schwope https://orcid.org/0000-0003-3441-9355
Javier Serna https://orcid.org/0000-0001-7351-6540
Yue Shen https://orcid.org/0000-0003-1659-7035
Jennifer Sobeck https://orcid.org/0000-0002-4989-0353
Diogo Souto https://orcid.org/0000-0002-7883-5425
Keivan G. Stassun https://orcid.org/0000-0002-3481-9052
Matthias Steinmetz https://orcid.org/0000-0001-6516-7459
Ilya Straumit https://orcid.org/0000-0002-2812-2259
Guy Stringfellow https://orcid.org/0000-0003-1479-3059
Jamie Tayar https://orcid.org/0000-0002-4818-7885
Patricia B. Tissera https://orcid.org/0000-0001-5242-2844
Benny Trakhtenbrot https://orcid.org/0000-0002-3683-7297
Nicholas Troup https://orcid.org/0000-0003-3248-3097
Jonathan R. Trump https://orcid.org/0000-0002-1410-0470
Sarah Tuttle https://orcid.org/0000-0002-7327-565X
Jose Antonio Vazquez-Mata https://orcid.org/0000-0001-8694-1204
Sandro Villanova https://orcid.org/0000-0001-6205-1493
John Wilson https://orcid.org/0000-0001-7828-7257
Leigh Wojno https://orcid.org/0000-0002-3233-3032
Xiang-Xiang Xue https://orcid.org/0000-0002-0642-5689
Gail Zasowski https://orcid.org/0000-0001-6761-9359

References

Abazajian, K. N., Adelman-McCarthy, J. K., Agüeros, M. A., et al. 2009, ApJS, 182, 543
Abdurro'uf, Accetta, K., Aerts, C., et al. 2022, ApJS, 259, 35
Ahumada, R., Prieto, C. A., Almeida, A., et al. 2020, ApJS, 249, 3
Aihara, H., AlSayyad, Y., Ando, M., et al. 2019, PASJ, 71, 114
Albareti, F. D., Allende Prieto, C., Almeida, A., et al. 2017, ApJS, 233, 25

Bailer-Jones, C. A. L., Rybizki, J., Fouesneau, M., Mantelet, G., & Andrae, R. 2018, AJ, 156, 58
Bailey, S. 2012, PASP, 124, 1015
Bailey, S. 2016, Weighted EMPCA: Weighted Expectation Maximization Principal Component Analysis, Astrophysics Source Code Library, ascl:1609.007
Barkhouser, R. H., Smee, S. A., Hammond, R. P., et al. 2022, Proc. SPIE, 12182, 121823O
Bianchi, L., Shiao, B., & Thilker, D. 2017, ApJS, 230, 24
Blanton, M. R., Bershady, M. A., Abolfathi, B., et al. 2017, AJ, 154, 28
Bolton, A. S., Schlegel, D. J., Aubourg, É., et al. 2012, AJ, 144, 144
Bovy, J., Hennawi, J. F., Hogg, D. W., et al. 2011, ApJ, 729, 141
Bowen, I. S., & Vaughan, A. H., Jr 1973, ApOpt, 12, 1430
Brunner, H., Liu, T., Lamer, G., et al. 2022, A&A, 661, A1
Bulbul, E., Liu, A., Pasini, T., et al. 2022, A&A, 661, A10
Bundy, K., Bershady, M. A., Law, D. R., et al. 2015, ApJ, 798, 7
Cano-Díaz, M., Hernández-Toledo, H. M., Rodríguez-Puebla, A., et al. 2022, AJ, 164, 127
Chandra, V., Hwang, H.-C., Zakamska, N. L., et al. 2021, ApJ, 921, 160
Churchwell, E., Babler, B. L., Meade, M. R., et al. 2009, PASP, 121, 213
Clerc, N., Kirkpatrick, C. C., Finoguenov, A., et al. 2020, MNRAS, 497, 3976
Clerc, N., Merloni, A., Zhang, Y. Y., et al. 2016, MNRAS, 463, 4490
Comparat, J., Luo, W., Merloni, A., et al. 2023, A&A, 673, A122
Comparat, J., Merloni, A., Dwelly, T., et al. 2020, A&A, 636, A97
Cutri, R. M., Wright, E. L., Conrow, T., et al. 2013, Explanatory Supplement to the AllWISE Data Release Products
Dawson, K. S., Kneib, J.-P., Percival, W. J., et al. 2016, AJ, 151, 44
Dawson, K. S., Schlegel, D. J., Ahn, C. P., et al. 2013, AJ, 145, 10
Dey, A., Schlegel, D. J., Lang, D., et al. 2019, AJ, 157, 168
Driver, S. P., Norberg, P., Baldry, I. K., et al. 2009, A&G, 50, 5.12
Dwelly, T., Salvato, M., Merloni, A., et al. 2017, MNRAS, 469, 1065
Eisenstein, D. J., Weinberg, D. H., Agol, E., et al. 2011, AJ, 142, 72
Evans, I. N., Primini, F. A., Glotfelty, K. J., et al. 2010, ApJS, 189, 37
Flewelling, H. A., Magnier, E. A., Chambers, K. C., et al. 2020, ApJS, 251, 7
Freund, S., Czesla, S., Robrade, J., Schneider, P. C., & Schmitt, J. H. M. M. 2022, A&A, 664, A105
Frieman, J. A., Bassett, B., Becker, A., et al. 2008, AJ, 135, 338
Gaia Collaboration, Brown, A. G. A., Vallenari, A., et al. 2018, A&A, 616, A1
Ge, J., Mahadevan, S., Lee, B., et al. 2008, in ASP Conf. Ser. 398, Extreme Solar Systems, ed. D. Fischer et al. (San Francisco, CA: ASP), 449
Gentile Fusillo, N. P., Tremblay, P.-E., Gänsicke, B. T., et al. 2019, MNRAS, 482, 4570
Górski, K. M., Hivon, E., Banday, A. J., et al. 2005, ApJ, 622, 759
Green, G. M., Schlafly, E. F., Finkbeiner, D. P., et al. 2015, ApJ, 810, 25
Gunn, J. E., Siegmund, W. A., Mannery, E. J., et al. 2006, AJ, 131, 2332
Gutermuth, R. A., & Heyer, M. 2015, AJ, 149, 64
Hambly, N. C., MacGillivray, H. T., Read, M. A., et al. 2001, MNRAS, 326, 1279
Hayes, C. R., Masseron, T., Sobeck, J., et al. 2022, ApJS, 262, 34
Herbst, T. M., Bilgi, P., Bizenberger, P., et al. 2020, Proc. SPIE, 11445, 114450J
Høg, E., Fabricius, C., Makarov, V. V., et al. 2000, A&A, 355, L27
Ider Chitham, J., Comparat, J., Finoguenov, A., et al. 2020, MNRAS, 499, 4768
Ijspeert, L. W., Tkachenko, A., Johnston, C., et al. 2021, A&A, 652, A120
Inno, L., Rix, H.-W., Stanek, K. Z., et al. 2021, ApJ, 914, 127
Jarrett, T. H., Chester, T., Cutri, R., et al. 2000, AJ, 119, 2498
Klein, M., Oguri, M., Mohr, J. J., et al. 2022, A&A, 661, A4
Kollmeier, J. A., Zasowski, G., Rix, H.-W., et al. 2017, arXiv:1711.03234
Kounkel, M. 2022, PyXCSAO, v0.2, Zenodo, doi:10.5281/zenodo.6998993
Kounkel, M., Covey, K., & Stassun, K. G. 2020, AJ, 160, 279
Kurtz, M. J., Mink, D. J., Wyatt, W. F., et al. 1992, in ASP Conf. Ser. 25, Astronomical Data Analysis Software and Systems I, ed. D. M. Worrall, C. Biemesderfer, & J. Barnes (San Francisco, CA: ASP), 432
LaMassa, S. M., Georgakakis, A., Vivek, M., et al. 2019, ApJ, 876, 50
Liu, A., Bulbul, E., Ghirardini, V., et al. 2022, A&A, 661, A2
Lyke, B. W., Higley, A. N., McLane, J. N., et al. 2020, ApJS, 250, 8
MacLeod, C. L., Green, P. J., Anderson, S. F., et al. 2018, AJ, 155, 6
Magnier, E. A., Chambers, K. C., Flewelling, H. A., et al. 2020, ApJS, 251, 3
Majewski, S. R., Schiavon, R. P., Frinchaboy, P. M., et al. 2017, AJ, 154, 94
Marocco, F., Eisenhardt, P. R. M., Fowler, J. W., et al. 2021, ApJS, 253, 8
Masseron, T., Merle, T., & Hawkins, K. 2016, BACCHUS: Brussels Automatic Code for Characterizing High accUracy Spectra, Astrophysics Source Code Library, ascl:1605.004
Mazzola, C. N., Badenes, C., Moe, M., et al. 2020, MNRAS, 499, 1607
McBride, A., Lingg, R., Kounkel, M., Covey, K., & Hutchinson, B. 2021, AJ, 162, 282
Menzel, M. L., Merloni, A., Georgakakis, A., et al. 2016, MNRAS, 457, 110
Merloni, A., Predehl, P., Becker, W., et al. 2012, arXiv:1209.3114
Mink, D. J., & Kurtz, M. J. 1998, in ASP Conf. Ser. 145, Astronomical Data Analysis Software and Systems VII, ed. R. Albrecht, R. N. Hook, & H. A. Bushouse (San Francisco, CA: ASP), 93
Onken, C. A., Wolf, C., Bessell, M. S., et al. 2019, PASA, 36, e033
Padmanabhan, N., Schlegel, D. J., Finkbeiner, D. P., et al. 2008, ApJ, 674, 1217
Page, M. J., Brindle, C., Talavera, A., et al. 2012, MNRAS, 426, 903
Perruchot, S., Guy, J., Le Guillou, L., et al. 2018, Proc. SPIE, 10702, 107027K
Pogge, R. W., Derwent, M. A., O'Brien, T. P., et al. 2020, Proc. SPIE, 11447, 1144781
Predehl, P., Andritschke, R., Arefiev, V., et al. 2021, A&A, 647, A1
Price-Whelan, A. M., Hogg, D. W., Rix, H.-W., et al. 2020, ApJ, 895, 2
Rix, H.-W., Hogg, D. W., Boubert, D., et al. 2021, AJ, 162, 142
Rockosi, C. M., Lee, Y. S., Morrison, H. L., et al. 2022, ApJS, 259, 60
Rykoff, E. S., Rozo, E., Busha, M. T., et al. 2014, ApJ, 785, 104
Salvato, M., Wolf, J., Dwelly, T., et al. 2022, A&A, 661, A3
Sánchez, S. F., Avila-Reese, V., Hernandez-Toledo, H., et al. 2018, RMxAA, 54, 217
Sánchez, S. F., Pérez, E., Sánchez-Blázquez, P., et al. 2016, RMxAA, 52, 171
Sánchez-Gallego, J. R., Sayres, C., Donor, J., et al. 2020, Proc. SPIE, 11449, 114490O
Sayres, C., Sánchez-Gallego, J. R., Blanton, M. R., et al. 2021, AJ, 161, 92
Schlafly, E. F., & Finkbeiner, D. P. 2011, ApJ, 737, 103
Schlafly, E. F., Meisner, A. M., Stutz, A. M., et al. 2016, ApJ, 821, 78
Schlegel, D. J., Finkbeiner, D. P., & Davis, M. 1998, ApJ, 500, 525
Shen, Y., Brandt, W. N., Dawson, K. S., et al. 2015, ApJS, 216, 4
Shen, Y., Hall, P. B., Horne, K., et al. 2019, ApJS, 241, 34
Shu, Y., Koposov, S. E., Evans, N. W., et al. 2019, MNRAS, 489, 4741
Skrutskie, M. F., Cutri, R. M., Stiening, R., et al. 2006, AJ, 131, 1163
Smee, S. A., Gunn, J. E., Uomoto, A., et al. 2013, AJ, 146, 32
Stalzer, M., & Mentzel, C. 2016, SpringerPlus, 5, 1266
Stassun, K. G., Oelkers, R. J., Paegert, M., et al. 2019, AJ, 158, 138
Stoughton, C., Lupton, R. H., Bernardi, M., et al. 2002, AJ, 123, 485
Tonry, J., & Davis, M. 1979, AJ, 84, 1511
Vázquez-Mata, J. A., Hernández-Toledo, H. M., Avila-Reese, V., et al. 2022, MNRAS, 512, 2222
Washington, J. E., Lewis, H. M., Anguiano, B., et al. 2021, ApJ, 918, 19
Weijmans, A.-M., Blanton, M., Bolton, A. S., et al. 2019, in ASP Conf. Ser. 521, Astronomical Data Analysis Software and Systems XXVI, ed. M. Molinaro, K. Shortridge, & F. Pasian (San Francisco, CA: ASP), 177
Wilson, J. C., Hearty, F. R., Skrutskie, M. F., et al. 2019, PASP, 131, 055001
Yang, Q., & Shen, Y. 2023, ApJS, 264, 9
Yanny, B., Rockosi, C., Newberg, H. J., et al. 2009, AJ, 137, 4377
Yershov, V. N. 2014, Ap&SS, 354, 97
York, D. G., Adelman, J., Anderson, J. E., Jr, et al. 2000, AJ, 120, 1579
Zari, E., Hashemi, H., Brown, A. G. A., Jardine, K., & de Zeeuw, P. T. 2018, A&A, 620, A172
Zari, E., Rix, H. W., Frankel, N., et al. 2021, A&A, 650, A112
Zasowski, G., Cohen, R. E., Chojnowski, S. D., et al. 2017, AJ, 154, 198
Zasowski, G., Finkbeiner, D. P., Green, G. M., et al. 2019, BAAS, 51, 314
Zasowski, G., Johnson, J. A., Frinchaboy, P. M., et al. 2013, AJ, 146, 81